MONITORING, MODELING, DYNAMICS AND CONTROL OF LEAFHOPPER PESTS IN TEA PLANTATIONS

PEI YUAN

A DISSERTATION SUBMITTED TO
THE FACULTY OF GRADUATE STUDIES
IN PARTIAL FULFILMENT OF THE REQUIREMENTS
FOR THE DEGREE OF
DOCTOR OF PHILOSOPHY

GRADUATE PROGRAM IN MATHEMATICS AND STATISTICS
YORK UNIVERSITY
TORONTO, ONTARIO

August 2021

Abstract

The tea green leafhopper *Empoasca onukii* is one kind of insect pests threatening the tea production. To reduce economic losses, pesticides are commonly used yet it causes the pest resistance, pest resurgence and the undesirable pesticide residues. Therefore, biological control has received increasing attention in recent years with the predatory mite *Anystis baccarum* as a potential agent. In this study, we aim to investigate the correlation and dynamics of *E. onukii* and *A. baccarum* and the mechanism for informing biological control.

Through the statistical modeling and analysis, we find intercropping treatments help to enhance the densities of the predatory mite, *A. baccarum*, and may reduce the populations of the leafhopper pest, *E. onukii*. Then, we analyze a predator-prey type of model with generalist predator and aim to understand the dynamics of *E. onukii* and *A. baccarum* for a purpose to develop a biological control strategy. We find that the nilpotent singularities are associated with a cubic Liénard system, and the nilpotent bifurcations are three-parameter bifurcations of a codimension 4 nilpotent focus, and the degenerate

nilpotent focus serves as an organizing center to connect all the codimension 3 bifurcations in the system. One interesting observation is that we show numerically the existence of three limit cycles in the system. Finally, we incorporate the stage structure into our generalist predator prey model to better explore the complex dynamics and to find the window of time to promote the use of *A. baccarum* to control *E. onukii*. The complex dynamics are also observed. Moreover, the hatching rate of *E. onukii* eggs is associated with the classification of the nilpotent singularity, which impacts the dynamics of the system significantly. Our results suggest that extending the incubation time of *E. onukii* eggs can be beneficial for pest control.

We present bifurcation diagrams and numerical simulations from numerical tools are presented to illustrate and support our findings. Furthermore, we also find that the higher codimension bifurcations involving nilpotent singularities in the system are associated to the well-known Hilbert's 16th problem. The existence of three limit cycles and associated bifurcations supplies an interesting angle to understand the dynamics of planar systems when we consider them as a two-dimensional central manifold of the higher dimensional systems.

Keywords: leafhopper pest *Empoasca onukii*, generalist predator *Anystic baccarum*, biological control of pest, bifurcation analysis, bifurcation diagrams, nilpotent singularities, nilpotent focus, nilpotent elliptic point, limit cycles, saddle-node bifurcation, Hopf bifurcation, Bogdanov-Takens bifurcation, nilpotent bifurcations.

To my beloved family

Acknowledgements

First of all, I would like to express my deepest gratitude towards my supervisor, Professor Huaiping Zhu, for his encouragement and patient supervision. Professor Zhu is a role model in my life. I have been greatly inspired by his brilliant insights and way of thinking. His enthusiasm and dedication to academics and his understanding of life have had a significant impact on me. He always answers questions for me when I encounter problems, and patiently teaches me, so that I gradually understand the beauty and meaning of mathematical models from a layman who has no knowledge of dynamical systems. Moreover, Professor Zhu is very attentive and considerable. He cares for every member of our Lamps laboratory like a loving father. He is very good at cooking and discovering the subtle beauty in life. He not only cares about our academic development but also care about our lives. He led us to explore the joys of academics and at the same time experience the beautiful natural scenery. I am so grateful for having such a kind supervisor in my doctoral studies. I have learned so much from him for the past years, which will benefit me in my whole life.

My sincere thanks also go to Professor Xin Gao and Professor Neal Madras for accepting to be my supervisory committee members and for their patient academic guidance within these years.

I also would like to thank my collaborator, Professor Mingsheng You, Dr. Lilin Chen from Fujian Agriculture and Forestry University. Dr. Lilin Chen gave me a deeper understanding of species in tea plantations. Thanks for her kindness and patience.

My special thanks go to our Lamps and CCDM group members, Elena Aruffo, Yi Tan, Juan Li, Jun Li, Tingting Zheng, Qi Li, Steven Chen, Ziwang Deng, Xiaolan Zhou, Xianghong Zhang, Haitao Song, Guihong Fan, Xinmiao Rong, Liping Wang, Mengyun Wang, Qigang Yuan, Junbo Jia, Dawei Zhang, Liu Yang, Bing Hu, Luana Bassani, Hamed Babazadeh, Jummy David for their help. I have learned a lot while working with them.

I also would like to thank the sponsor from the China Scholarship Council, who gave me the support. I am very grateful for having this opportunity.

I am also heartily thankful to my parents for their love. Their selfless love nourishes me and makes me become the person I want to be. My mother, Putao Zhou, dedicated her life to me and my old sister. She is the driving force for my continuous progress in life. She taught me to be diligent and strong. The deepest appreciation goes to my father, my old sister, my beloved for caring for me, understanding and supporting my studies.

I would like to express my special thanks to my friends, Shengwen Yang, Shanshan

Qin, Xinjie Gao and Lisha Lin, who are always here, and willing to listen to me and encourage me. Also, I want to thank Xiao Hu, Hang Du, Guanlin Zhang, Mingfu (Morgan) Wang, Kaiyan Lin, Yuan Zhong for their help and for making our time at York enjoyable.

I am also grateful to the Department of Mathematics and Statistics, York University. The professors and staff are always nice and helpful.

Last but not least, thanks to all my friends in my life who have supported and encouraged me.

Table of Contents

List of Tables

List of Figures

1 Introduction

Tea is a popular drink around the world with an estimation of 25000 cups consumed every second, about 2.16 billion cups per day worldwide [1]. Tea consumption is seeing an annual growth of 2.8 percent and is expected to becoming higher in the future [1]. Hence, tea has been an important commercial crop which is planted in more than 48 countries and regions, and by 2018 the global gross production value reached 16.75 billion US dollars [2]. However, the tea production has been damaged by insects and mite pests, causing on average a 5% to 55% yield loss (approximately U.S. $500 million and $1 billion) [3].

To mitigate the damage of tea pests, various pest control techniques have been developed and applied, including cultural (like pruning and plucking, trap crop, resistance breeding) [4, 5], mechanical and physical (hand destruction, barriers, light traps, sticky trap) [5], chemical (insecticides) [5] and biological (natural enemies, biopesticides, and botanical pesticides) [3, 4]. Cultural and physical methods are simple and safe but require lots of manpower. Commonly used pesticides are effective, however it will cause

pest resistance, pest resurgence, and the undesirable pesticide residues on brewed tea [6]. The use of natural enemies to control pests is effective, safe, and economical. Therefore, the biological control methods have received much attention in recent years [4, 7], especially by improving the influence of natural enemies on pest population via conservation biological control method [8]. Understanding the basis of interactions of tea pests and natural enemies is essential not only for an eco-friendly tea production system [3, 7], but help to control the tea pests while reduce or even eliminate the use of pesticide.

1.1 The tea green leafhopper *Empoasca onukii*

There are different kinds of tea pests, including mirids (*Helopeltis scboutedeni* Reuter (Hemiptera: Miridae) and *Helopeltis tbeivora* Waterhouse (Hemiptera: Miridae) in Africa and Asia), tea tortricids (*Adoxopbyes bonmai* Yasuda (Lepidoptera: Tortricidae) in central and south Japan, *Homona magnanima* Diakonoff (Lepidoptera: Tortricidae) in south Japan), scolytids (*Xyleborus fornicatus* Eichhoff (Coleoptera: Scolytidae) in Sri Lanka) and mites (*Tetranycbus kanzawai* Kishida (Acarina: Tetranychidae) in China, Japan and the Philippines, *Acapbylla tbeae* (Watt) (Acarina: Eriophyidae) in Asia and Africa) [3]. Among those pests, the tea green leafhopper (TGL) *Empoasca onukii* (Hemiptera: Cicadellidae) is one of the most predominant threatening the tea production in China, Vietnam, Japan, Indonesia and other countries in Asia [9, 10, 11, 12]. It is also a severe pest of vineyards in Europe that causes serious economic damage [13, 14, 15]. Owing to

the short generation cycle, serious overlapping of generations, and strong reproductive ability, it is one of the most difficult pests to control in tea gardens.

The *E. onukii* grow up through several processes, including the stages of egg, nymph and adult. The egg is crescent-shaped, about 0.8 mm in length and 0.15 mm in width, with milky white colour initially and gradually turning light green. The nymph stage is composed of five instars. Above the third instar nymphs are lively, good at crawling and jumping, but afraid of wet and light. Nymphs often gather on the backs of leaves or stems where their peeling shells easily can be found and rarely migrate if they are not disturbed. The *E. onukii* adult is 3.1 - 3.8mm in length, with yellow-green or pale yellow-green colour [16] and the adult females are larger than the males and live longer usually [17]. The average lifespan for the adults at 26-29°C is 19.7 days, from minimum 6 days to maximum 38 days [18]. Above third instar nymphs and adults are the main harmful state of *E. onukii* in tea plantations.

Eggs are usually laid beneath the phloem of tender tea shoots by female adults, which harm the growth of tea trees by hindering the transport of nutrient substances. Both nymphs and adults of *E. onukii* pierce the tea buds, leaves and shoots and suck the sap. The symptoms of damage can range from leaf curling, bronzing, shriveling to necrosis (hopperburn), or even severe to complete stand loss [19, 11]. Consequently, the quality of tea products can be severely affected by leaf damage caused by the TGL [11], resulting in a total annual economic loss of up to 15%–50% of the Chinese tea economy [11]. In tea

plantation areas, *E. onukii* has many overlapping generations (up to 10–17) in one year. The TGL remains active throughout the year but maximum population growth occurs from May to July and from September to November in tea plantations [20, 21, 22].

The main methods for preventing and controlling *E. onukii* are agricultural control, chemical control, physical control and biological control. Field cultivation is the basis of agricultural control, including the selection of insect-resistant varieties, timely batch picking, appropriate pruning at the peak period of TGL, covering the soil of the tea garden with weeds and closing the tea garden in winter [3, 16, 23]. Also, some physical control methods are effective in prevention and control by interfering with the growth, development and reproduction of *E. onukii* through the use of physical factors or mechanical effects, which mainly include the insect removing fan, yellow insect-attracting boards, lamp trap, and insect nets. However, the control against *E. onukii* mainly relies on chemical measures. The widespread use of pesticides in tea gardens has caused concern about the quality and safety of tea [3, 23]. For consumers, pesticide residue is the most concerning issue due to the risks of consumers exposed to pesticides through drinking tea. Although 0.2 - 24% of pesticide residues can be removed by rinsing tea leaves in boiled water before brewing, there is no effective way to reduce the level of pesticide residues completely [24]. While the biological control method is more conducive to maintaining ecological balance, including the utilization of botanical pesticides, microbial pesticides and natural enemies, such as predatory natural enemies, parasitic natural

enemies and pathogenic natural enemies [16, 23]. Considering the tea garden ecosystem as a whole and utilizing the principle of competition among species, the sustainable control of *E. onukii* may be achieved through increasing biodiversity and effectively use the role of natural control factors. In this study, we will explore the possible control effect of the predatory natural enemy, taking the generalist predator *Anystis baccarum* as an example.

1.2 Generalist predator *Anystis baccarum*

The *Anystis baccarum* was first found by Hooke in 1665 and first named by Linnaeus in 1758. This whirligig mite is moderately large (1.0-1.5mm in length), with long-legged and bright orange or red color. This species is parthenogenetic and has no males. The lifecycle of *A. baccarum* goes through the stage of egg, prelarva, larva, nymph and adult. Female adults lay eggs in 15-24 unit clusters under loose bark on the tree trunk and in the soil litter surrounding the tree base [25, 26]. After eggshells split, the eggs hatch with the emergence of the legs of the pre-larva. The pre-larva are small (0.2 mm), six-legged. They are immobile, do not eat and scarcely leave the split eggshells. Once they progress to the larvae stage, they become active and can feed on suitable prey. Successively, after three nymphal instars that are eight-legged, where they become adults [26]. The *A. baccarum* is cannibalistic. The larva may feed on egg and pre-larva and the active adults may feed on all other life stages. Under the temperature of 21 $\pm$ 0.5 °C, it takes 81-114

days for *A. baccarum* to complete a generation, with an average of 99.5 days [27]. It can be found all year around and the peak population occurs in spring or early summer (April - June) depending on local climate condition [25, 28] and it can have 2-3 generations in one year, which is observed in Guangzhou [27], and with a similar observation in apple orchards in Northern Ireland [29].

The *A. baccarum* is a predatory mite that has been cited as feeding on a range of invertebrate prey (Table 1.1). It causes no damage to fruit and can move rapidly over the branches and foliage of the trees. This mite has strong activity and predation ability and can readily feed upon any prey item it can over-power [25, 27]. Also, it has compatibility with several chemical fungicides (e.g., dithianon). The dry residues of some insecticides (e.g., methoxyfenozide, acetamiprid, imidacloprid and spinosad) are harmless to this whirligig mite [26]. Hence, it may be used in combination with other methods of pest suppression and have an additive effect on controlling. Moreover, it has been found that *A.baccarum* is beneficial to various agricultural systems, such as the tea plantations [30, 31], the solanaceous crop [32], the apple orchards [25, 28] and so on (Table 1.1). For tea ecosystem, *A.baccarum* can feed upon the *E.onukii* [30] and tea red mite *Oligonychus coffeae* [31]. Hence, the *A.baccarum* can be the potential bio-control agent of TGL *E. onukii*.

Table 1.1: *Anystis baccarum* is a potential biocontrol agent of various economically significant pest arthropods in agricultural systems

Agricultural systems	Biocontrol of pest arthropods	Taxa	References
Tea plantations	*E. vitis*	Hemiptera: Cicadellidae	Zeng et al. [33], Hong et al. [34]
	Empoasca pirisuga Matumura	Hemiptera: Cicadellidae	Liu [35]
	Oligonychus coffeae (Nietner)	Prostigmata: Tetranychidae	Liao et al. [36]
Apple orchards	*Aculus schlechtendali* (Nalepa)	Prostigmata: Eriophyidae	Cuthbertson and Murchie [25]
	Archips podana (Scopoli)	Lepidoptera: Tortricidae	Cuthbertson and Murchie [37]
	Panonychus ulmi (Koch)	Trombidiformes: Tetranychidae	Cuthbertson et al. [26]
	Epiphyas postvittana (Walker)	Lepidoptera: Tortricidae	Baker [38]
	Rhopalosiphum insertum (Walker)	Hemiptera: Aphididae	Cuthbertson et al. [39]
	Collembola	Collembola	Cuthbertson and Murchie [40]
Vineyards	*E. postvittana*	Lepidoptera: Tortricidae	Paull et al. [41]
Longan orchards	*Cornegenapsylla sinica* Yang and Li	Hemiptera: Phacopteronidae	Qiu et al. [42]
Vegetable crops	*Lipaphis erysimi* (Kaltenbach)	Hemiptera: Aphididae	Xiong et al. [43]
Tomato potato patch	*Bactericera cockerelli* (Sülc)	Hemiptera: Triozidae	Geary et al. [32]
Mulberry fields	*Pseudodendrothrips mori* (Niwa)	Thysanoptera: Thripidae	Jiang et al. [44]
	Tetranychus cinnabarinus (Boisduval)	Trombidiformes: Tetranychidae	
	Pealius mori (Takahashi)	Hemiptera: Aleyrodidae	
Pine forests	*Marchalina hellenica* (Gennadius)	Hemiptera: Margarodidae	Ülgentürk et al. [45]
	Hemiberlesia pitysoqilo Takagi	Hemiptera: Diaspididae	Wu [46]
	Matsucoccus matsumurae Kuwana	Hemiptera: Margarodidae	Ming et al. [47]

1.3 Current modeling and literature review

The use of mathematical models to study ecosystem populations has a long history [48, 49]. Although no models in the literature of population dynamics come remotely close to simulating the insect population considering all the features affecting its growth, a simplified mathematical model allows us to better understand the population dynamics of single species and interaction between different species. The mathematical model to study the dynamics of a single population can be traced back to 1838. Verhulst (1838) proposed the logistic growth to describe the dynamics of many single-species populations [50]. Then, Lotka first proposed the predator-prey model in 1925 and began to study the interaction between two species [51]. Afterwards Volterra adopted chemical principles of mass action in 1928 [52] and developed the following classical predator-prey model, the so-called Lotka-Volterra model.

$$\begin{cases} \dfrac{dN}{dt} &= aN - bNP, \\ \dfrac{dP}{dt} &= cNP - dP. \end{cases} \tag{1.1}$$

where N, P are the biomass densities of prey and predator, respectively. a is the per-capita growth rate of prey, and d is the death rate of predator. b, c are their respective change rates due to the interaction. In the Lotka-Volterra model, the prey grows infinitely in the absence of predator, hence, to correct this unreasonable assumption, the logistic growth of the prey population was added. Regarding the predators, in the absence of

prey they will become extinct . This is the most common assumption in many extended predator-prey models and it is reasonable for the specialist predator whose growth relies on the prey population. In 1948, Leslie was the first to consider the logistic growth of predator population [53], and proposed the following equations.

$$\begin{cases} \dfrac{dN}{dt} &= aN(1-\frac{N}{K}) - bNP, \\ \dfrac{dP}{dt} &= cP(1-e\frac{P}{N}). \end{cases} \tag{1.2}$$

where e is the density of prey required to maintain a single predator and to replace it with one offspring when it dies. $\frac{N}{e}$ is the carrying capacity of predators when provided with a constant supply of prey. K is the carrying capacity of prey population. The trophic relationship depends on the ratio of the predator and prey rather than their products. Then, the addition of a predator functional response into the predator-prey model further promotes the studies of population dynamics between predator and prey. Holling argued that the linear relationship between species as the number of prey that predator can only handle in a unit of time is limited [54], and proposed the nonlinear functional response ($b(N)$). Then, we obtained the general predator-prey model.

$$\begin{cases} \dfrac{dN}{dt} &= aN(1-\frac{N}{K}) - b(N)P, \\ \dfrac{dP}{dt} &= P[cb(N) - d]. \end{cases} \tag{1.3}$$

Afterwards, there are extensive works regarding the predator-prey model with different functional responses which describe how the predator species capture the prey. In addi-

tion, the life-cycle stages of prey and predator are also considered into the models. In general, there are two types of functional response, prey-dependent and predator dependent [55]. The prey-dependent type considers the density of prey, like Holling type-I (or Lotka–Volterra type) [56, 57], Holling type-II (or Michaelis-Menten type) [58], Holling type-III [59], Holling type-IV (or Monod-Haldane type) [60, 61] and Ivlev type [62]. And the predator dependent type is considering the effect of predator and prey density, like Beddington-DeAngelis type [63, 64], Hassel-Verley type [65], Crowley-Martin type [66], and ratio-dependence type [67]. Table 1.2 summarizes the formula of different functional responses.

As the predator-prey models are consistent with the idea of the biological control method using natural enemies to prevent and control pests, they are applied to inform pest controls. It is one of the dominant themes in mathematical ecology. Whereas the bifurcation theory can be a help to understand the overall dynamics of the system, and it is used to classify the different critical regimes and ascertain the conditions required for the realization of certain critical regimes [68], like the Hopf bifurcation is related to the periodic oscillation of predator and prey population. Using the carrying capacity of the environment as the bifurcation parameter, Wolkowicz (1988) found that the predator-prey system with group defence that predation is decreased as prey population increase undergoes homoclinic bifurcation and Hopf bifurcation. The group defence of prey combined with sufficient enrichment of the environment leads to the extinction of

Table 1.2: The summary of different functional response.

	Functional response	Formula	Note
Prey dependent	Holling type-I (or Lotka–Volterra type)	mx	$m > 0$, the linear predation rate.
	Holling type-II (or Michaelis-Menten type)	$\frac{mx}{a+x}$	$m, a > 0$, m is the maximal predation rate, a is the half saturation constant of the species.
	Holling type-III	$\frac{mx^2}{a+bx^2}$	$m, a, b > 0$.
	Holling type-IV (or Monod-Haldane type)	$\frac{mx}{a+bx+x^2}$ or $\frac{mx}{a+x^2}$	$m, a, b > 0$
	Ivlev type	$b(1-e^{-ax})$	$a, b > 0$.
Predator dependent	Beddington-DeAngelis type	$\frac{mx}{a+bx+cy}$	$m, a, b, c > 0$.
	Hassel-Verley type	$\frac{mx}{ay^\gamma+x}$	$m, a, b > 0$, $\gamma \in (0, 1)$. When $\gamma = 1$, it produces the ratio-dependence type; $\gamma = \frac{1}{2}$ or $\gamma = \frac{1}{3}$ for terrestrial or aquatic predators that form a fixed number of tight groups, respectively [65].
	Crowley-Martin type	$\frac{mx}{1+ax+by+abxy}$	$m, a, b > 0$, and describe the effects of capture rate, handling time and the magnitude of interference among predators, respectively[66].
	Ratio-dependence type	$\frac{mx}{ay+x}$	$m, a > 0$.

the predator [69]. Bazykin (1993) discussed the bifurcation approach to the predator-prey population models, then analyzed the population dynamics with the change of parameters [68]. Zhu et al. (2002) conducted a comprehensive bifurcation analysis of a predator-prey system with the nonmonotonic functional response and showed the existence of Bogdanov-Takens bifurcation point of codimension 3 served as an organizing center for the system [60]. Xiao and Zhu (2006) calculated the largest multiplicity of a multiple focus in the model of Zhu et al. (2002) and presented the existence of the two limit cycles bifurcated from the multiple focus [70]. There are many works related to the bifurcation analysis of the planar system, but just a few are conducted on bifurcation analysis of the high-dimensional model due to its complexity. Beay et al. (2020) consider a Rosenzweig-MacArthur predator-prey model with stage-structure in prey that can exhibit Hopf bifurcation [71].

In the model that we mentioned above (Zhu (2002), Xiao and Zhu (2006), Beay et al. (2020)), the predator is a specialist predator that will go extinct in the absence of the prey population. However, generalist predators are more common in ecosystems because they are more conducive to the survival of species. Other studies show that the generalist predator can reduce the pest number significantly [72, 73]. It is widely accepted that the Holling type II functional response is reasonable for the specialist predator while the Holling type III functional response is more appropriate for the generalist predators. This is because the sigmoidal shaped function can better reflect the ”prey switching”

phenomenon that the generalist predator will focus on other prey if one of the certain prey is at low density [74]. Hanski et al. (1991) considered a model including both specialist predator and generalist predators. The density of generalist predators is assumed to be constant. They assumed sigmoid (Holling type III) functional response for the generalist predators and demonstrated that the generalist predators have a stabilizing effect on a cycle driven by specialist predators [75]. However, if we only consider the Holling type III functional response in the general predator-prey model, then the generalist predator will die in the absence of prey, which maybe unrealistic. Erbach et al. (2013) constructed a two-dimensional predator-prey model considering the generalist predator with the Holling type III functional response and the reproduction of predator in the absence of focal prey [76]. They assumed that the generalist predator reproduces with a Beverton–Holt-like function that the per capita reproduction rate decreases with density. Then they analyzed the bistability and limit cycles in this predator-prey system. Magal et al. (2008) considered the control of invasive hosts by generalist parasitoids. In the model, they incorporated the carrying capacity of generalist parasitoids in the absence of leafminers and predation of leafminers by a generalist parasitoid with Holling Type II functional response [77]. Seo and Wolkowicz (2020) focused on the non-spatial model of leaf miner and parasitoid interaction which proposed in Magal et al. (2008) and adopted the bifurcation theory to discuss pest control by generalist parasitoids [78]. Huang (2020) also conducted the bifurcation analysis toward this host-generalist parasitoid model [79].

The pest insects monitoring or surveillance programs data can help to estimate the pest population density, dispersions and dynamics [3]. However, due to the scarcity of field monitoring data, there is little literature on modeling with the actual data to prevent and control pests. Although there are many theoretical studies on pest control using mathematical models, there is an unbridged gap between mathematicians and experimentalists [80]. Recently, there are a few studies that tried to incorporate the data into the mathematical model for pest control. Satake et al. (2008) [81] built a mathematical model in which individuals are categorized according to their life-cycle stages to predict the emergence timing of tea leaf roller, *Caloptilia theivora* and compared the model prediction with the field data of observed captures in pheromone traps at the experimental site of Kagoshima Tea Experiment Research Station in Japan. They also applied the logistic regression model to analyze the relationship between the timing of adult emergence and the leaf damage level. Yamanaka et al. (2012) analyzed 48 years of data of tea tortrix moths and constructed a stage-structured model including the intraspecific competition. Comparing the observed dynamics with the prediction from models, they found that even weak larval competition in the presence of seasonal temperature forcing predicts two cycles [82]. Kettle et al. (2019) developed a stage-structured mathematical model of host-parasitoid considering the biocontrol of the egg stages of hopper life cycle and applied the model to data from field experiments on rice hoppers. They found that the two-enemy system is more effective in controlling hopper eggs than a single enemy

(parasitoid or predator) [83].

1.4 Modeling

According to the biological process, we assume that the life cycle of predatory mite *A. baccarum* and the pest leafhopper *E. onukii* has three stages, including eggs, nymphs and adults. For *A. baccarum*, we use $M_1(t)$, $M_2(t)$ and $M_3(t)$ to denote their density of mite in eggs, nymphs and adults at any time t respectively, and use $E_1(t)$, $E_2(t)$ and $E_3(t)$ to denote the density of eggs, nymphs and adults of *E. onukii* at any time t respectively.

1.4.1 Stage-structured model of predatory mite *A. baccarum*

Firstly, we consider a single species population model of the predatory mite *A. baccarum*. For the growth of *A. baccarum* at different stages, we make the following assumptions:

(A1) The *A. baccarum* eggs population $M_1(t)$: the oviposition rate of *A. baccarum* is proportional to the existing *A. baccarum* adults population, with proportionality $r_2 > 0$. The *A. baccarum* eggs may not be successfully hatched due to the other biological factors, like the temperature. Hence, the death rate of *A. baccarum* eggs d_{m1} is also positive. β_1 is the hatchability of *A. baccarum* eggs.

(A2) The *A. baccarum* nymphs population $M_2(t)$: $c_1 > 0$ is the intra-specific competition rate of the *A. baccarum* nymphs population. $d_{m2} > 0$ is the death rate

of nymphs population. β_2 denotes the rate of *A. baccarum* nymphs becoming *A. baccarum* adults.

(A3) The *A. baccarum* adults population $M_3(t)$: $c_2 > 0$ is the intra-specific competition rate of the *A. baccarum* adults population. The death rate of adults population is proportional to the existing adults population, with proportionality $d_{m3} > 0$.

(A4) There is enough food for *A. baccarum* in the tea plantations, hence cannibalism is not considered in the model.

Then we have the following stage-structured model of *A. baccarum*:

$$\begin{cases} \dfrac{dM_1}{dt} &= r_2 M_3 - d_{m1} M_1 - \beta_1 M_1, \\ \dfrac{dM_2}{dt} &= \beta_1 M_1 - d_{m2} M_2 - c_1 M_2^2 - \beta_2 M_2, \\ \dfrac{dM_3}{dt} &= \beta_2 M_2 - d_{m3} M_3 - c_2 M_3^2. \end{cases} \tag{1.4}$$

1.4.2 Stage-structured model of pest leafhopper *E. onukii*

Similarly, we can obtain the stage structured model of the pest leafhopper *E. onukii* with the following assumptions:

(B1) The *E. onukii* eggs population $E_1(t)$: We denote $r_1 > 0$ as the per-capita intrinsic oviposition rate of the *E. onukii* adults. Not all eggs can be hatched, and the death

rate d_{e1} is proportional to the existing eggs population which is also positive. α_1 is the hatchability of *E. onukii* eggs.

(B2) The *E. onukii* nymphs population $E_2(t)$: $b_1 > 0$ is the intra-specific competition rate of the *E. onukii* nymphs population. $d_{e2} > 0$ is the death rate of nymphs population which is proportional to the existing nymphs population. α_2 denotes the conversion rate of *E. onukii* nymphs becoming *E. onukii* adults.

(B3) The *E. onukii* adults population $E_3(t)$: $b_2 > 0$ is the intra-specific competition rate of the *E. onukii* adults population; the death rate of adults population which is proportional to the existing adults population with proportionality $d_{e3} > 0$.

(B4) The competition between the nymphs and adults of *E. onukii* is ignored.

Hence, we have the following stage-structured model of *E. onukii*:

$$\begin{cases} \dfrac{dE_1}{dt} &= r_1 E_3 - d_{e1} E_1 - \alpha_1 E_1, \\ \dfrac{dE_2}{dt} &= \alpha_1 E_1 - d_{e2} E_2 - b_1 E_2^2 - \alpha_2 E_2, \\ \dfrac{dE_3}{dt} &= \alpha_2 E_2 - d_{e3} E_3 - b_2 E_3^2. \end{cases} \tag{1.5}$$

1.4.3 The predator-prey model with stage structure

Since the life cycle of both predator and prey includes different stages, we consider a more comprehensive Predatory-Prey model with stage structure both in predator and

prey. Most of the researchers consider models with stage structures for only one species, either prey [84, 85] or predator [86, 87]. Some have considered the stage structure for both predator and prey [88, 89, 90, 91], but only analyze the interaction between one stage of predator and prey. Here, we propose a more realistic model where the *A. baccarum* adults can feed on *E. onukii* nymphs and *E. onukii* adults. Also, the predatory mite nymphs can only feed on *E. onukii* nymphs. For simplicity, we only take the *A. baccarum* as enemy of *E. onukii* and neglect the influence of other factors which also can cause the death of the *E. onukii*.

Also, we assume the functional response of *A. baccarum* adults and *E. onukii* nymphs ($P_1(E_2)$) is Holling's type I, as the *A. baccarum* adults can easily capture *E. onukii* nymphs. The functional response of the *A. baccarum* nymphs and *E. onukii* nymphs ($P_2(E_2)$) and the *A. baccarum* adults and *E. onukii* adults ($P_3(E_3)$), are Holling's type II [30].

$$P_1(E_2) = \gamma_1 E_2,$$

$$P_2(E_2) = \frac{m_1 E_2}{a_1 + E_2},$$

$$P_3(E_3) = \frac{m_2 E_3}{a_2 + E_3}.$$

Figure 1.1 describes the flow chart of the model (1.6).

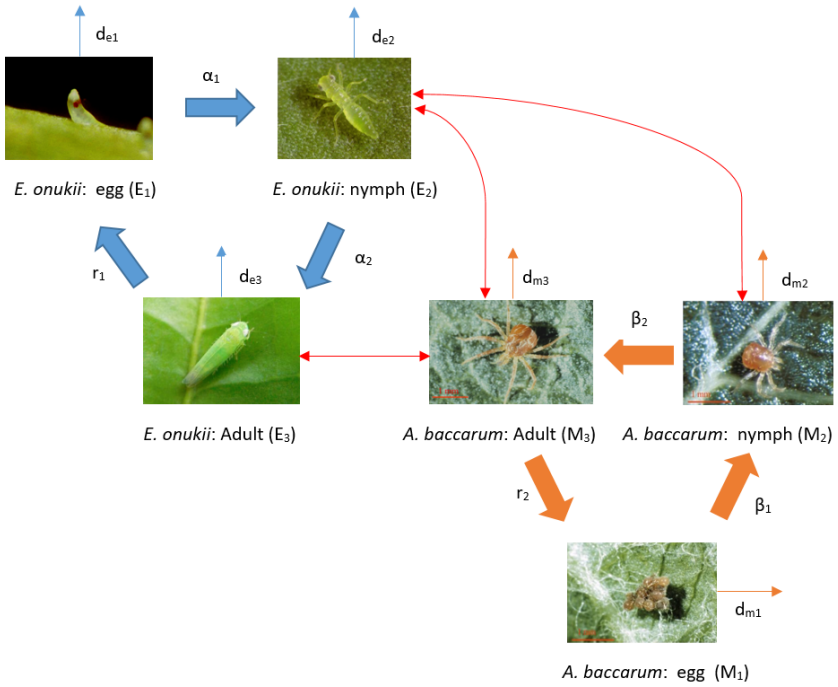

Figure 1.1: The flow chart of the model (1.6).

The system describing the dynamic of *A. baccarum* and *E. onukii* is given by

$$\begin{cases} \dfrac{dE_1}{dt} &= r_1E_3 - d_{e1}E_1 - \alpha_1E_1, \\ \dfrac{dE_2}{dt} &= \alpha_1E_1 - d_{e2}E_2 - \alpha_2E_2 - b_1E_2^2 - \dfrac{m_1E_2M_2}{a_1+E_2} - \gamma_1E_2M_3, \\ \dfrac{dE_3}{dt} &= \alpha_2E_2 - d_{e3}E_3 - b_2E_3^2 - \dfrac{m_2E_3M_3}{a_2+E_3}, \\ \dfrac{dM_1}{dt} &= r_2M_3 - d_{m1}M_1 - \beta_1M_1, \\ \dfrac{dM_2}{dt} &= \beta_1M_1 - d_{m2}M_2 - \beta_2M_2 - c_1M_2^2 + \dfrac{\theta_1m_1E_2M_2}{a_1+E_2}, \\ \dfrac{dM_3}{dt} &= \beta_2M_2 - d_{m3}M_3 - c_2M_3^2 + \gamma_2E_2M_3 + \dfrac{\theta_2m_2E_3M_3}{a_2+E_3}. \end{cases} \tag{1.6}$$

However, the system (1.6) is too complicated for theoretical analysis. In this study, we will firstly simplify the model and start to analyze the dynamics of *A. baccarum* and *E. onukii* in the tea plantation.

Table 1.3: Description of parameters of system (1.6)

Parameters	Description (day^{-1})
r_1	the oviposition rate of *E. onukii* adults
r_2	the oviposition rate of *A. baccarum* adults
α_1	hatching rate of *E. onukii* eggs
α_2	conversion rate of *E. onukii* nymphs into adults
β_1	hatching rate of *A. baccarum* eggs
β_2	conversion rate of *A. baccarum* nymphs into adults
d_{e1}	the mortality rate of *E. onukii* eggs
d_{e2}	the mortality rate of *E. onukii* nymphs
d_{e3}	the mortality rate of *E. onukii* adults
d_{m1}	the mortality rate of *A. baccarum* eggs
d_{m2}	the mortality rate of *A. baccarum* nymphs
d_{m3}	the mortality rate of *A. baccarum* adults
a_1	half saturation amount of *A. baccarum* nymphs
a_2	half saturation amount of *A. baccarum* adults
b_1	the intra-specific competition rate of the *E. onukii* nymphs
b_2	the intra-specific competition rate of the *E. onukii* adults
c_1	the intra-specific competition rate of the *A. baccarum* nymphs
c_2	the intra-specific competition rate of the *A. baccarum* adults
m_1	maximum amount of the *E. onukii* nymphs eaten by *A. baccarum* nymphs
m_2	maximum amount of the *E. onukii* adults eaten by *A. baccarum* adults
γ_1	the rate of *E. onukii* nymphs eaten by *A. baccarum* adults
$\frac{\gamma_2}{\gamma_1}$	the rate of conversing *E. onukii* nymphs into *A. baccarum* adults
θ_1	the rate of conversing *E. onukii* nymphs into *A. baccarum* nymphs
θ_2	the rate of conversing *E. onukii* adults into *A. baccarum* adults

1.5 Objectives of the research

The TGL *E. onukii* is one of the most common and predominant harmful pests in tea plantations, and its improper control is one of the main factors causing pesticide residues in tea. Therefore, the biological control of *E. onukii* should be strengthened. Increasing the biodiversity and making use of the control effect of natural enemies is crucial to achieve sustainable control of tea garden pests and then promote the sustainable development of the tea industry. The predatory mite *A. baccarum* is a potential biological control agent and it has been found that it can be beneficial to various agricultural systems. The overall goal of this dissertation is to investigate the relationship between the *E. onukii* and the *A. baccarum* populations using statistical models and dynamical analysis techniques, and finally to find the window of time to promote the use of *A. baccarum* to control *E. onukii* in tea plantations.

The dissertation is structured as follows:

In Chapter 1, we describe a general description of the problem, introduction to mathematical models, and literature review.

In Chapter 2, using the field experiment data, we investigate how the relationship of the abundance of the predatory mite *A. baccarum* and its leafhopper prey *E. onukii* is influenced by two different cover crops and a manually weeded inter-row treatment as a contrast to naturally growing vegetation in a tea plantation in China. We applied gen-

eralized linear mixed models (GLMMs) to examine the impact of cover crop treatments on the abundance of *A. baccarum* and *E. onukii*, and to explore the relationship between them over time. Results suggest that the abundance of *A. baccarum* in a tea plantation is influenced by intercropping and it can affect its leafhopper prey *E. onukii*, albeit, with varying levels of suppression.

In Chapter 3, we start our analysis from the two dimensional generalist predator prey model. Using the qualitative theory and bifurcation theory, we analyze the complex dynamic of the system, with the existence of saddle node bifurcation of codimension 1 and 2, Hopf bifurcation, Bogdanov-Takens bifurcation and nilpotent singularities of codimension 3 and 4. We also present the bifurcation diagrams near the nilpotent singularities of codimension 3.

In Chapter 4, to better understand the population dynamics between *A. baccarum* and *E. onukii*, we propose a generalist predator prey model with stage structure for prey *E. onukii*. We consider the *E. onukii* has two stages, the eggs and the nymph and adults. Then, we analyze the local complex dynamics in the two-dimensional center manifold of three-dimensional nonlinear system and compare our generalist predator prey model with and without stage structure. Moreover, we examine the effect of the successful hatching rate of *E. onukii* eggs.

In Chapter 5, we present our conclusions and future work.

2 The impact of cover crops on the predatory mite *Anystis baccarum* and the leafhopper pest *Empoasca onukii* in a tea plantation

This work has been conducted in collaboration with Dr. Chen, L. L., Dr. Pozsgai, G., Dr. Chen, P., Dr. Zhu, H., and Dr. You, M. S. I have collaborated in conducting the statistical analysis. Figure 2.3 and 2.4 were made by Dr. Chen based on the statistical analysis which I did.

2.1 Introduction

There have been extensive studies on the methods in controlling TGL, including biological, physical, and chemical controls. However, to date, a safe, timely, highly effective, and yet sustainable, strategy for prevention and control of the TGL is still to be developed [5, 6]. One such strategy may be intercropping the rows with beneficial plants, a common practice for ecological engineering. In theory, greater botanical diversity in

an intercropped tea plantation system, along with a higher number of available niches, can support greater diversity of invertebrate species than that with cleared rows [8, 92]. However, diverse, naturally grown, weedy vegetation between tea rows may compete with tea for resources and its growth may be difficult to control. An alternative solution is a planned modification of habitat structure in tea plantations, using cover crops [8, 22]. Crops are chosen so that the competition for nutrients with tea at a minimal level. The aim is that they reduce pest damage by attracting and sustaining natural enemies of the pest species. Furthermore, they can reduce weed growth. Whilst predation or parasitism from natural enemies serve as 'top-down controls' on pests, intercropping may also operate as a 'bottom-up effect' when cover species are preferred to crops for the pests to oviposit or feed upon [93], and this, in turn, reduces the feeding activity on the crop.

Recent studies on the effects of cover crops on leafhoppers in agricultural ecosystems have helped to improve our understanding of how habitat management can improve pest control [94, 95]. Intercropping treatments have been shown to have significantly lower abundance of TGL than bare ground treatments [94, 96] or traditional clearing tillage [20] in a tea plantation. However, Jiang et al. [97] found opposite results when compared to conventional clearing tillage in a tea plantation (Table 2.1). Costello and Daane [95] and Nicholls et al. [98] found that the abundance of grape leafhoppers (Erythroneura spp.) was lower in intercropping treatments than in monocultures in vineyard systems. However, English-Loeb et al. [99] did not find significant effects in intercropped grape

ecosystems (Table 2.1).

Apart from their effect on arthropod assemblages in crop ecosystems, intercropping with cover crops can have additional positive effects, such as decreasing soil erosion and preventing the leaching of nutrients [20]. The grass, *Paspalum notatum* Flüggé (Poales: Poaceae) has been used to mitigate water runoff and soil erosion, improve soil quality, increase plant quality and productivity, to enhance water and nutrition resource utilization by crop roots, and to control weeds [100, 101]. *Chamaecrista rotundifolia* (Pers.) Greene (Fabales: Fabaceae) has also been used for similar purposes, as well as for enhancing biological pest management [102, 103, 104, 105]. Whether or not these cover crops promote invertebrate biological control agents, and thus have an enhanced benefit in tea plantations, has not yet been studied in detail.

An important taxon for invertebrate biological control agents are whirligig mites (Acari: Anystidae), which are generalist predators, feeding on various invertebrate species [27, 106, 107]. One of the common species that may benefit from planting cover crops is *Anystis baccarum* (L.) (Acari: Anystidae) [35]. *A. baccarum* is a large-sized (1.0–1.5 mm), red-orange, long-legged, soft-bodied mite that moves rapidly over the foliage and branches of the trees. Parthenogenetic females lay eggs under loose bark on the trunk or in soil litter surrounding the tree base [29, 108]. *A. baccarum* abundances peak from March to April, from October to November, and from December to January, without any apparent overwinter dormancy period in tea plantations in Guangdong and Guangxi

Table 2.1: Effects of cover crops on leafhoppers in agricultural ecosystems

Agricultural systems	Intercropping cover crop	Comment	References
Tea plantations	*Lavandula pinnata* Lundmark (Lamiales: Lamiaceae), *Corymbia citriodora* (Hook.) Hill & Johnson (Myrtales: Myrtaceae), *Catsia tora* L. (Fabales: Fabaceae), *Hedyotis uncinella* Hook. & Arn. (Gentianales: Rubiaceae), or *Trifolium repens* L. (Fabales: Fabaceae) *T. repens* or *Vigna sinensis* (L.) (Fabales: Fabaceae)	Significantly reduced abundances of TGL, and increased abundance of generalist predators.	Chen,[96] Song et al.[20], Liu[35], Zhang et al.[94]
	T. repens or *Vigna sinensis* (L.) (Fabales: Fabaceae)	Increase abundance of *Empoasca vitis* (Göthe) (Hemiptera: Cicadellidae) and parasitoids.	Jiang et al.[97]
Vineyards	3: 7 mixture of *Fagopyrum esculentum* Moench (Caryophyllales: Polygonaceae) and *Helianthus annuus* L. (Asterales: Asteraceae)	Reduced adult abundance of *Erythroneura elegantula* Osborn (Hemiptera: Cicadellidae), and increased populations and species richness of general predators.	Nicholls et al.[98]
	3: 1 mixture of *Vicia benghalensis* L. (Fabales: Fabaceae) and *Hordeum* vulgare L. (Poales: Poaceae)	Significantly reduced nymphal abundance of *Erythroneura* spp. (Hemiptera: Cicadellidae) in mid- and late-season.	Costello and Daane[95]
	F. esculentum or *T. repens*	Neither the abundance nor the spatial and temporal distribution of *Erythroneura* spp. was significantly influenced in 1996 and 1997.	English-Loeb et al.[99]

provinces in China [27, 35, 109]. These peaks occur from March to May, and from September to October in longan orchards in Fujian province [42]. Along with other members of the family, *A. baccarum* has been suggested as a potential biocontrol agent for various economically significant arthropod pests, especially in apple orchards (Table 1.1) [26, 29, 110]. For a more comprehensive review on the life history and the usefulness of A. baccarum readers should consult Cuthbertson et al [26].

Despite their use in many agricultural systems, very little is known about the impact of different cover crops on *A. baccarum* and how they affect the TGL in intercropped tea plantations. This study aims to explore how intercropping with various cover crops in a tea plantation influences the abundances of *A. baccarum* and *E. onukii*, and the relationship between this pest and its predator. Hence, we conducted a two-year study to compare the influence of a) a grass cover crop (*P. notatum*), b) a legume cover crop (*C. rotundifolia*), c) bare ground, and d) natural ground cover on these two target organisms. We hypothesized that the intercropping cover crops in a tea plantation influence the abundance of both *A. baccarum* and *E. onukii*, and the relationship between the two species is affected by the treatments.

2.2 Monitoring, field studies and data

2.2.1 Study site and experimental design

The study was carried out from May 2006 to April 2008 in an Oolong tea plantation (clone Wuyi Shuixian) in the town of Xingcun ($27°38'51.4''N$ and $117°54'29.9''E$, $736m$ altitude) in the Wuyi Mountains, Fujian Province, China. The study site was a large seven-year-old tea plantation on red soil. Fertilizers were applied as conventional management practices. Germinating fertilizer was applied in March 2006, topdressing fertilizer in July, and basal fertilizer in November. Spring tea was harvested from mid-March to early-May, and autumn tea was picked from early-September to mid-October. Tea pruning, or skiffing, was done between mid-October and early-November. Further details of the study sites are available in Chen et al [111, 112]. The experimental design consisted of four treatments, each with three replicates: a) *P. notatum* cover crop (Pn), b) *C. rotundifolia* cover crop (Cr), c) bare ground (BG), and d) natural weedy ground cover (NGC). The experiment was set up on 12 experimental plots, each 17 m × 20 m in size, and at least 5 m apart (Figure .2.1). In order to decrease the edge effect and to increase the distance between samples, we avoided collecting in the near vicinity of margins of the plots.

As a baseline for the experiment, all plants were manually removed from the rows at the end of April 2006. Cover crop treatments of *P. notatum* and *C. rotundifolia* were

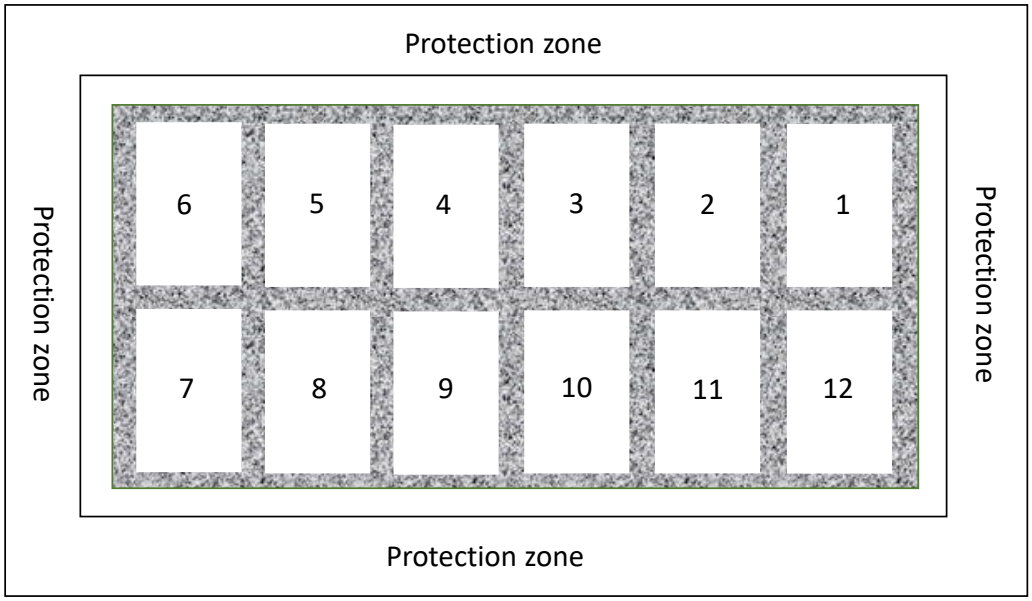

Figure 2.1: Layout of experimental plots in study site in Wuyi Mountains, Fujian province, China from May 2006 to April 2008. The blocks were intercropped with *P. notatum* (5, 9, 12), *C. rotundifolia*(2, 4, 7), natural ground cover (1, 6, 10) and bare ground (3, 8 , 11) respectively [112].

manually sown in May 2006 at a seed rate of 45 kg/ha and 7.5 kg/ha, respectively. In the bare ground treatment, all plants were manually removed each month. Existing vegetation was retained in the natural ground cover treatment. The *P. notatum*, *C. rotundifolia*, and natural ground cover plots were mown in September of each year to a height of 5 cm, and cover clippings were left on site. No herbicides or insecticides were applied on our experimental plots during the study period but plots were managed according to standard agronomic practices.

Although Chen [96] and Zhang et al. [94] used bare ground, which is traditional in monoculture tea plantations, as their control, in our field experiment the natural weedy ground cover served as the control treatment. Our main reason was that nowadays natural ground covers can be found more often in tea plantations. In recent years, manually clearing up of tea rows has been carried out less because of the increasing cost of labor and, in addition, the governmental ban on the use of herbicides in tea plantations made clearing up the rows difficult. No herbicides or insecticides were applied on our experimental plots during the study period but plots were managed according to standard agronomic practices.

2.2.2 Insect survey

Tea plant canopies were sampled every month from May 2006 to April 2008 in five, randomly-placed, 1 m × 1 m quadrats. Samples were collected manually by placing six white trays (36 cm × 45 cm) underneath the tea bushes and performing 30 sweeps with a net (38.1 cm in diameter) on the top of the bush (about 1 m height), and then beating the tea canopy 20 times. *A. baccarum* and *E. onukii* found in the nets and on the trays were transferred into plastic bags and frozen. Both nymphs and adults of the two species were collected.

Arthropods living in litter were surveyed using the dry sieve method. The litter and surface organic matter were collected in a square area of 0.33 m × 0.33 m, adjacent to

each quadrat used for tea canopy sampling. Sampling was done at the same time as for the tea canopies. Both nymphs and adults of *A. baccarum* and *E. onukii* were extracted from each sample using a set of three sieves of 12, 5, and 1 mm mesh sizes.

To sample *A. baccarum* and *E. onukii* in cover crop vegetations, five 1 m × 1 m quadrats were randomly positioned between tea rows in each treatment plot every month during the experiment. In each quadrat, 30 sweeps were performed using the same net as was used for sampling tea plants. *A. baccarum* and *E. onukii* were collected, transferred to a plastic bag and frozen. Specimens for all the surveys were preserved in 75% alcohol and stored in the laboratory. No cover samples were collected from the bare ground treatment. In all cases both nymphs and adults of both species were recorded.

2.3 Data analysis and statistical models

We used generalized linear mixed models (GLMMs) to test the impact of cover crop treatments on the abundance of *A. baccarum* and *E. onukii*, and to explore the relationship between these species over time. Since the abundance data of both species was strongly overdispersed in our dataset, and had significantly more zero counts than would be expected from a Poisson distribution, we applied zero inflated Poisson mixed models which combine binary logistic and Poisson distributions for the response variable [113]. When we analyzed the abundance of *A. baccarum* in tea canopies in the second year, we chose the negative binomial distribution since the standard error of the abundance

of *A. baccarum* was excessively large. We used the glmmTMB package [114] in the R software for our analysis [115]. Let Y_{ij} be the abundance of *A. baccarum* or *E. onukii* of observation $j(j = 1, \ldots, t_i)$ for plots $i(i = 1, \ldots, n)$, we denote

$$Y_{ij} \sim \begin{cases} 0, & with \quad probability \ \pi_{ij} \\ Poisson(\lambda_{ij}), & with \quad probability \ (1 - \pi_{ij}) \end{cases} \tag{2.1}$$

which means the zero counts values come from the strata of always-zero with probability of π_{ij} and not always-zero strata generated by Poisson distribution with probability of $(1 - \pi_{ij})$. For the positive abundance data, we consider a Poisson mixed model. Let ϵ_i be random effects. Conditional on ϵ_i, we assume that

$$E(Y_{ij} = y_{ij}|X_1, \epsilon) = g^{-1}(X_1\beta_1 + \epsilon\gamma) = \mu$$

with canonical log-linear link function $g = log(\mu)$, where X_1 is the design matrix of explanatory variables including the cover crop treatment, and sampling date (sampling date was treated as random effect in litter data due to the convergence problem of model estimate) and β_1 is the fixed effect. γ (plot) and ϵ are the random effects design matrix and random effects respectively. Hence, we have the zero inflated Poisson mixed model with two parts:

$$\text{Poisson mixed model: } log(\hat{\lambda}_{ij}) = X_1\beta_1 + \epsilon\gamma$$

$$\text{Zero inflation model: } logit(\hat{\pi}_{ij}) = X_2\beta_2$$

where β_2 and X_2 are the coefficients vector and design matrix of explanatory variables of the zero inflation model, respectively. Here, our model only involves the intercept terms. When we referred to the fixed effects β_1 of one variable, it indicated the effect among those that the abundance of species is not zero and held other variables constant.

We separately took the abundance of *A. baccarum* or *E. onukii* as dependent variables in the model to explore their interactions in four treatments. Since different methods were used to measure the abundance of *A. baccarum* and *E. onukii* among tea canopies, litter and cover crops, we separated the datasets by sampling strata. Moreover, we analyzed the two-year data by year to explore how the predictive variables affect the abundance of *A. baccarum* and *E. onukii* over time. The parameters of the model were estimated by maximum likelihood method, and a likelihood ratio test was conducted to examine if the independent variables are important predictors of the model. Tukey-tests were used to pairwise compare the four treatments, with an $\alpha = 0.05$ as the cutoff for significance.

Furthermore, we separately used the abundance of *E. onukii* or *A. baccarum* as a special independent predictive variables of each other to detect the relationship between their abundance in tea canopies. We also added the interaction term of abundance of *A. baccarum* or *E. onukii* with cover crop treatment into the model to help understand the impact of the four treatments on the relationship between *E. onukii* or *A. baccarum*.

2.4 Results

2.4.1 Population dynamics of the target species

A total of 2910 *A. baccarum* and 5414 *E. onukii* were recorded during the two-year period, from May 2006 to April 2008. Tea canopies had the highest abundance of *A. baccarum* (2700) and *E. onukii* (4490). The abundance of *A. baccarum* increased from 939 in the first year (from May 2006 to April 2007) to 1971 in the second year (from May 2007 to April 2008), and this increasing pattern was observed in all the four treatments (Table 2.2). However, the overall abundance of *E. onukii* was stable in both the first (2740) and second year (2674; Table 2.3).

In the first year, canopies of tea intercropped with *P. notatum* or *C. rotundifolia* had lower abundance of *E. onukii* than did tea canopies (mean,2.32,2.94 respectively) on bare ground (mean,4.49;Table 2.2). The numbers of *A. baccarum* present in the tea canopies of treatments intercropped with *P. notatum* (mean,1.48)and *C. rotundifolia* (mean,1.44) were higher in the first year than in the natural ground cover (mean, 0.46; Table 2.3).

Table 2.2: The abundance of *E. onukii* in tea canopies, litter, and cover crop vegetations in the Wuyi Mountains in the sampling years.

	NGC	BG	Pn	Cr	Total
May 2006 - April 2007					
Tea canopies	2.69 (4.425)*	4.49 (9.151)	2.32 (3.452)	2.94 (6.416)	2241
Litter	0.04 (0.207)	0.04 (0.276)	0.05 (0.219)	0.02 (0.182)	29
Cover crop vegetation	0.84 (1.551)	-	0.92 (2.081)	0.85 (1.608)	470
May 2007 - April 2008					
Tea canopies	3.5 (6.987)	2.85 (4.997)	3.7 (6.508)	3.58 (7.054)	2249
Litter	0.02 (0.134)	0.01 (0.11)	0.01 (0.11)	0.01 (0.11)	9
Cover crop vegetation	0.79 (1.282)	-	0.86 (1.53)	0.87 (1.582)	416

* Note: Mean (standard error) individuals of *E. onukii* per 1 m^2 in the tea canopies and cover crop vegetations and per 0.33 × 0.33 m^2 in the ground litters in four ground cover treatments applied to tea in the Wuyi Mountains in years one and two. Pn: intercropped with *P. notatum*; Cr: intercropped with *C. rotundifolia*; NGC: natural ground cover; BG: bare ground.

Table 2.3: The abundance of *A. baccarum* in tea canopies, litter, and cover crop vegetations in the Wuyi Mountains in the sampling years.

	NGC	BG	Pn	Cr	Total
May 2006 - April 2007					
Tea canopies	0.46 (1.326)*	1.52 (3.32)	1.48 (3.396)	1.44 (2.706)	882
Litter	0.01 (0.105)	0.02 (0.182)	0.11 (0.554)	0.07 (0.291)	37
Cover crop vegetation	0.04 (0.267)	-	0.04 (0.255)	0.03 (0.196)	20
May 2007 - April 2008					
Tea canopies	1.4 (2.714)	2.89 (11.567)	3.07 (4.484)	3.65 (7.826)	1818
Litter	0.08 (0.447)	0.15 (0.436)	0.2 (0.675)	0.18 (0.529)	101
Cover crop vegetation	0.08 (0.529)	-	0.1 (0.544)	0.14 (0.764)	52

* Note: Mean (standard error) individuals of *A. baccarum* per 1 m^2 in the tea canopies and cover crop vegetations and per 0.33 × 0.33 m^2 in the ground litters in four ground cover treatments applied to tea in the Wuyi Mountains in years one and two. Pn: intercropped with *P. notatum*; Cr: intercropped with *C. rotundifolia*; NGC: natural ground cover; BG: bare ground.

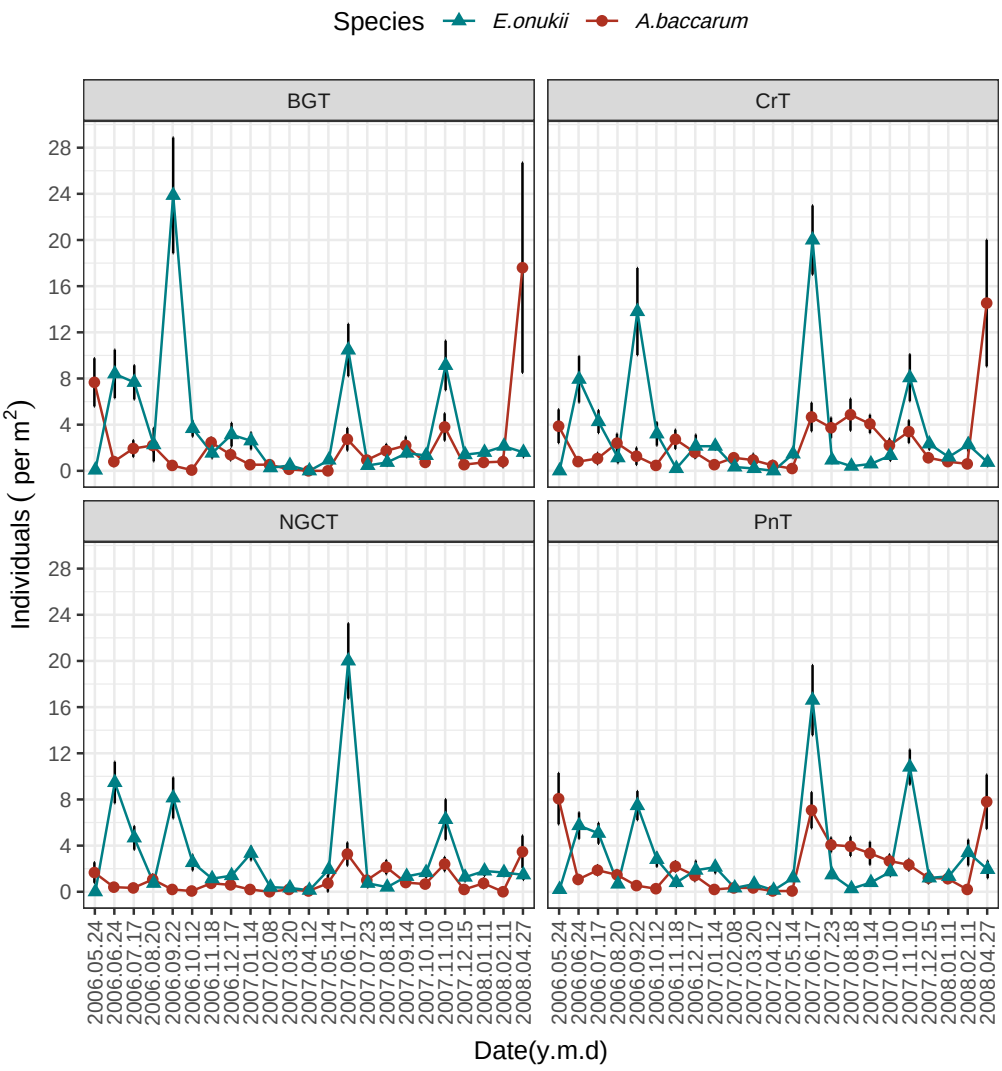

Figure 2.2: Mean (± SE) seasonal dynamics of *A. baccarum* and *E. onukii* per 1 m^2 in tea canopies in four treatments applied to tea in the Wuyi Mountains from May 2006 until April 2008. PnT: tea canopies intercropped with *P. notatum*; CrT: tea canopies intercropped with *C. rotundifolia*; BGT: tea canopies in bare ground; NGCT: tea canopies in natural ground cover.

2.4.2 Treatment effects on *Anystis baccarum*

The treatment effect on the abundance of *A. baccarum* was significant in tea canopies in both years (first year:$\chi^2 = 53.45, P < 0.001$; second year: $\chi^2 = 42.01, P < 0.001$; Figure 2.3A). The abundance of *A. baccarum* in tea canopies of both intercropping treatments was significantly higher in both years than that in natural ground cover and it was significantly higher in the first year in the bare ground treatment than in natural ground cover (Figure 2.3A). Additionally, the abundance of *A. baccarum* recorded in tea canopies of intercropping treatments was significantly higher than in bare ground in the second year (Figure 2.3A). In the litter, the treatment effect was statistically significant in the first year only (first year: $\chi^2 = 12.41, P = 0.006$; second year: $\chi^2 = 4.76, P = 0.190$; Figure 2.3B). In the first year, the abundance of *A. baccarum* was significantly greater in the litter of the *P. notatum* cover crop treatment than in the litter of the natural ground cover treatment (Figure 2.3B). In the cover crops, there was no significant difference in the abundance of *A. baccarum* among the three treatments in either of the years (first year: $\chi^2 = 0.44, P = 0.802$; second year: $\chi^2 = 2.37, P = 0.305$; Figure 2.3C).

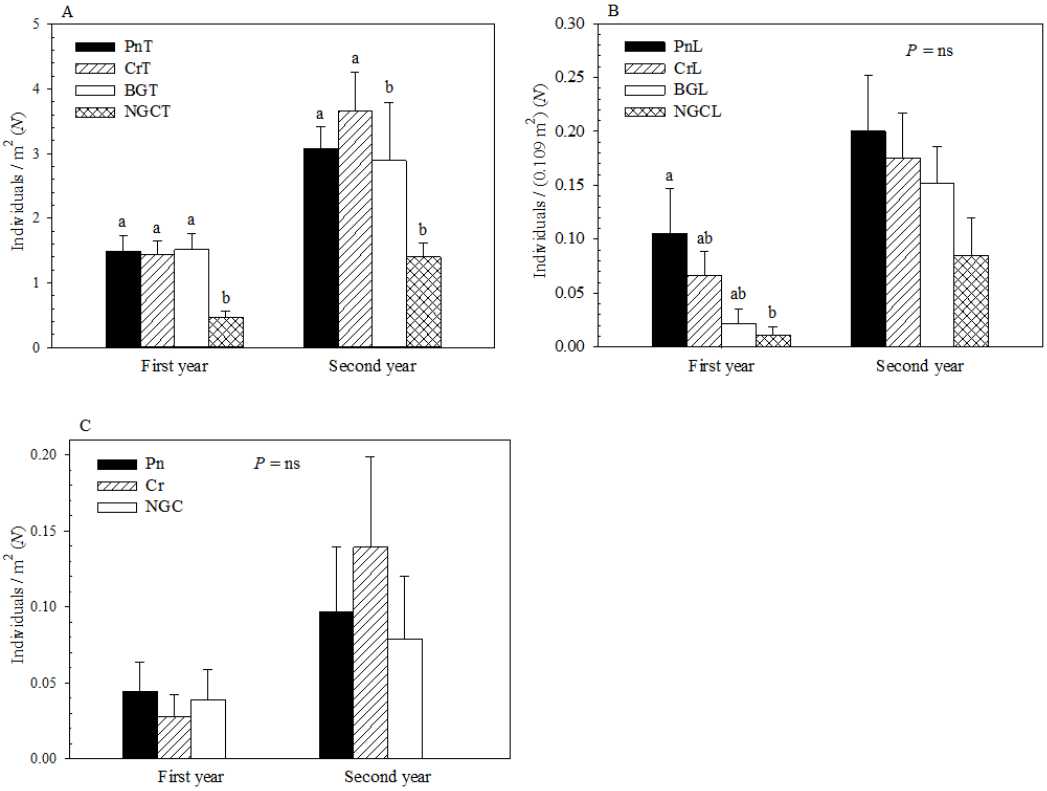

Figure 2.3: Mean (± SE) abundance of *A. baccarum* in tea canopies (A), litter (B), and cover crop vegetation (C) in four treatments applied to tea in the Wuyi Mountains in the first and second years. PnT: tea canopies intercropped with *P. notatum*; CrT: tea canopies intercropped with *C. rotundifolia*; BGT: tea canopies in bare ground; NGCT: tea canopies in natural ground cover; PnL: litter intercropped with *P. notatum*; CrL: litter intercropped with *C. rotundifolia*; BGL: litter in bare ground; NGCL: litter in natural ground cover; Pn: *P. notatum*; Cr: *C. rotundifolia*; NGC: natural ground cover. Within each cluster of bars, different letters indicate significant difference (Tukey-test, $P < 0.05$); and means denoted 'ns' are not significantly different (Tukey-test, $P > 0.05$).

2.4.3 Treatment effects on *Empoasca onukii*

The treatment effect was significant in tea canopies in both years (first year: $\chi^2 = 138.87, P < 0.001$; second year: $\chi^2 = 22.67, P < 0.001$; Figure 2.4A). When the abundances of *E. onukii* were modeled separately for years and strata, we observed a significantly greater abundance of *E. onukii* in the first year in tea canopies of the bare ground treatment than in any other treatments (Figure 2.4A). Moreover, *E. onukii* in the canopies of tea intercropped with *P. notatum* was significantly less abundant than in the treatment with *C. rotundifolia* (Figure 2.4A). In the second year, the abundance of *E. onukii* was significantly lower in tea canopies over the bare ground treatment than in any other treatments (Figure 2.4A). However, there was no significant difference between treatments in the abundance of *E. onukii* in litter samples and in samples from the cover crop vegetation in either of the years (first year: litter: $\chi^2 = 2.02, P = 0.568$, cover crop vegetation: $\chi^2 = 1.41, P = 0.495$; second year: litter: $\chi^2 = 0.31, P = 0.958$, cover crop vegetation: $\chi^2 = 0.96, P = 0.619$; Figure 2.4B and 2.4C).

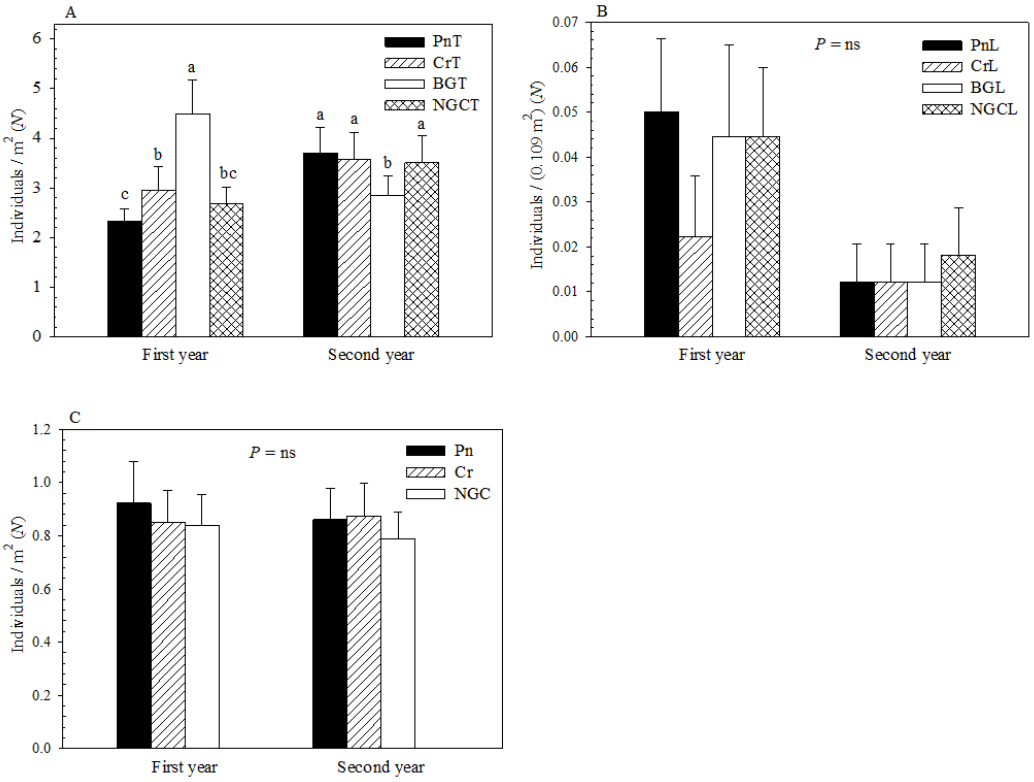

Figure 2.4: Mean (± SE) abundance of *E. onukii* in tea canopies (A), litter (B), and cover crop vegetation (C) in four treatments applied to tea in the Wuyi Mountains in the first and second years. PnT: tea canopies intercropped with *P. notatum*; CrT: tea canopies intercropped with *C. rotundifolia*; BGT: tea canopies in bare ground; NGCT: tea canopies in natural ground cover; PnL: litter intercropped with *P. notatum*; CrL: litter intercropped with *C. rotundifolia*; BGL: litter in bare ground; NGCL: litter in natural ground cover; Pn: *P. notatum*; Cr: *C. rotundifolia*; NGC: natural ground cover. Within each cluster of bars, different letters indicate significant difference (Tukey-test, $P < 0.05$); and means denoted 'ns' are not significantly different (Tukey-test, $P > 0.05$).

2.4.4 Relationship between *A. baccarum* and *E. onukii*

A. baccarum was found throughout the year in the tea plantation, but with lower abundance in winter. In tea canopies, *A. baccarum* showed three population peaks in the first year, on May 24th, 2006, August 20th, 2006, and November 18th, 2006. It also showed two population peaks in the second year on June 17th, 2007 and April 27th, 2008 (Figure 2.2). *E. onukii* showed two population peaks in the first year on June 24th, 2006 and September 22nd, 2006. Similarly, two population peaks were recorded in the second year on June 17th, 2007 and November 10th, 2007 (Figure 2.2). In other words, the first population peak of *E. onukii* attacked primarily the summer tea crop, the second population peak of *E. onukii* attacked primarily the autumn tea crop. The population dynamics of the two species showed that there is a negative correlation between the abundance of *E. onukii* and *A. baccarum* in tea canopies (Figure 2.2). In the first year, when the abundance of *A. baccarum* decreased, *E. onukii* abundances increased but this pattern reversed in intercropping treatments in the second year (Figure 2.2). On the other hand, in the second year, *A. baccarum* and *E. onukii* populations showed parallel growth trends in both bare ground and natural ground cover treatments (Figure 2.2). Since the correlations may be resulted from the seasonal dynamics, to further understanding their correlations, we constructed the zero inflation Poisson model.

Since no *A. baccarum* were recorded in over 90% of the cover crop vegetation and

litter samples, only samples taken from the tea canopies were considered for our model investigating the relationship between *A. baccarum* and *E. onukii*. In both years, the intercept term in zero inflation models were significant (Tables 2.4 and 2.5), which indicated the necessity of using these models. In the first year, there was no significant correlation between the abundance of *A. baccarum* and *E. onukii* in tea canopies (Table 2.4). However, in the second year, there was some indication of a positive correlation between the abundance of *A. baccarum* and *E. onukii*. The abundance of *A. baccarum* significantly increased with the growing abundance of *E. onukii* (Table 2.4). In all four treatments, the estimated abundance of A. baccarum in tea canopies increased by 3.6% ($e^{0.032}$; Table 2.4) per unit of *E. onukii* increase.

There was no significant correlation between the abundance of *E. onukii* and *A. baccarum* in tea canopies in the first year (Table 2.5). However, in the second year, there is an indication that the abundance of *E. onukii* increased with the increasing number of *A. baccarum* (Table 2.5). Also, the strength of correlation between abundances of the two species was different for different treatments. Compared to the natural ground cover, other treatments showed that there is a pattern that this positive relationship between the two species turns into zero, which may be the result of the control effect of *A. baccarum* on the *E. onukii*. The estimated abundance of *E. onukii* in tea canopies of the treatment intercropped with *P. notatum* decreased by 5.4% ($e^{-0.056}$) per unit of *A. baccarum* increased than that in natural ground cover (Table 2.5). In all four treatments, the

strongest reciprocal correlation of *A. baccarum* on *E. onukii* was shown in tea canopies intercropped with *P. notatum*, followed by the bare ground treatment (4.8%; $e^{-0.049}$) and the treatment of intercropping with *C. rotundifolia* (4.4%; $e^{-0.045}$), compared to the reference of tea canopies growing over natural ground cover (Table 2.5).

2.5 Discussion

In this chapter, our main interest is to investigate how the abundances of the TGL and a predatory mite were affected by experimental cover crop alterations. Conducting the statistical analysis based on the experimental data, we show that intercropping cover crops harbor a large number of the predatory mite, *A. baccarum*, and that the intercropping treatments caused a significant increase in the mite's abundance in tea canopies when compared with the natural ground cover treatment. These results are consistent with the observations reported by Liu [116] who found that cover crops increased the abundance of *A. baccarum* in a tea plantation.

A. baccarum is a habitat generalist, it lays eggs in a wide variety of habitats, including tea canopies, litter, as well as in cover crop vegetation [26, 29, 108] and therefore, it is unlikely to be directly influenced by available extra habitat. On the other hand, intercropping cover crops may provide increased amount of food sources and, likely, also a greater protection from predators [8, 92, 116]. This theory is supported by the fact that the treatment effect was more pronounced in tea canopies than it was in cover crop

Table 2.4: Model estimation of the relationship between abundance of *A. baccarum* and *E. onukii* in tea canopies

In the first year	Estimate[a]	SE	In the second year	Estimate	SE
(Intercept)	1.182***[b]	0.228	(Intercept)	-2.337***	0.533
E. onukii	0.004	0.029	*E. onukii*	0.032***	0.012
PnT	0.841***	0.166	PnT	0.968***	0.185
CrT	0.934***	0.162	CrT	0.982***	0.178
BGT	0.808***	0.163	BGT	0.528***	0.234
E. onukii: PnT	-0.014	0.04	*E. onukii*: PnT	0.021	0.02
E. onukii: CrT	0.023	0.029	*E. onukii*: CrT	-0.025	0.016
E. onukii: BGT	-0.007	0.03	*E. onukii*: BGT	-0.035*	0.022
Sampling date[c]			Sampling date		
Zero inflation model					
(Intercept)	-0.517***	0.141	(Intercept)	2.069***	0.428

[a] Estimate: the coefficients of the model. Dependent variable: the abundance of *A. baccarum*. Set 24 May 2006 and 14 May 2007 as the baseline of the month in the first and second years, respectively. NGCT as the baseline of treatment, tea canopies in natural ground cover abbreviated NGCT.

[b] Significance: ***p <0.001; *p <0.05.

[c] The sampling date was included in the model due to the strong seasonal effect, which can be seen clearly in Figure 3.

PnT, tea canopies intercropped with *P. notatum*; CrT, tea canopies intercropped with *C. rotundifolia*; BGT, tea canopies in bare ground; *E. onukii*: PnT, the interaction of *E. onukii* with PnT; *E. onukii*: CrT, the interaction of *E. onukii* with CrT; *E. onukii*: BGT, the interaction of *E. onukii* with BGT.

Table 2.5: Model estimation of the relationship between abundance of *E. onukii* and *A. baccarum* in tea canopies

In the first year	Estimate[a]	SE	In the second year	Estimate	SE
(Intercept)	-2.738***[b]	0.527	(Intercept)	0.345*	0.162
A. baccarum	0.035	0.055	*A. baccarum*	0.059***	0.012
PnT	-0.118*	0.079	PnT	0.196*	0.079
CrT	0.069	0.072	CrT	0.153	0.087
BGT	0.56***	0.065	BGT	-0.078	0.075
A. baccarum: PnT	-0.014	0.04	*A. baccarum*: PnT	-0.056***	0.014
A. baccarum: CrT	0.023	0.029	*A. baccarum*: CrT	-0.045**	0.016
A. baccarum: BGT	-0.007	0.03	*A. baccarum*: BGT	-0.049***	0.013
Sampling date[c]			Sampling date		
Zero inflation model					
(Intercept)	-1.922***	0.202	(Intercept)	-1.812***	0.203

[a] Estimate: the coefficients of the model. Dependent variable: the abundance of *E. onukii*. Set 24 May 2006 and 14 May 2007 as the baseline of the month in the first and second years, respectively. NGCT as the baseline of treatment, tea canopies in natural ground cover abbreviated NGCT.

[b] Significance: ***p <0.001;**p <0.01; *p <0.05.

[c] The sampling date was included in the model due to the strong seasonal effect, which can be seen clearly in Figure 3.

PnT, tea canopies intercropped with *P. notatum*; CrT, tea canopies intercropped with *C. rotundifolia*; BGT, tea canopies in bare ground; *A. baccarum*: PnT, the interaction of *A. baccarum* with PnT; *A. baccarum*: CrT, the interaction of *A. baccarum* with CrT; *A. baccarum*: BGT, the interaction of *A. baccarum* with BGT.

vegetation. The observed correlation between the two species in tea canopies suggests that *A. baccarum* has an impact on the seasonal dynamics of *E. onukii* (Figure 2.2). Furthermore, it also seems to be plausible that cover crops play an important role in driving predatory mite abundances only at certain periods. When the TGL, as the primary prey of the predatory mite, is scarce or cannot be found, cover crop vegetation may be an important source for providing alternative prey species. During these periods of prey shortage *A. baccarum* can move from tea canopies closer to the ground. In these times the mite is more likely to lay its eggs in the litter. Indeed, Sorensen et al. [107] showed that *Anystis agilis* (Banks) (Acari: Anystidae) populations decreased from June to July in Californian vineyards, possibly because adult mites migrated down the tree trunk to the soil to oviposit. Lange et al. [117] reported similar findings in *A. baccarum* in blackcurrant plants in Russia.

Earlier studies reported lower abundances of TGLs in the intercropped tea plantations than in bare ground [94], or in rows with traditional clearing tillage [20, 22]. Compared to the bare ground treatment, we also find an indication that cover crops influence TGL abundance in tea canopies. Since the results between the two sampled years were different, neither the nature of this effect nor the main drivers are clear. Moreover, compared to our natural ground cover control, the effect of cover crops on TGL abundances was not observed. This is in line with Ye et al. [21], who found that there was no significant difference of TGL abundances between intercropping Wuniuzao-waxberry treatment and

traditional clearing tillage control. Further still, Jiang et al. [97] found that intercropping tea treatments resulted in a significantly greater abundance of TGL than was found in conventional clearing tillage. This latter phenomenon is likely to be due to the increased structural complexity of the vegetation that may also positively affect herbivore populations. How this complexity influences predator–pest dynamics, and how this can be translated to effective pest control remains a question to be investigated. Whereas the treatment effect on *E. onukii* was unclear, the negative correlation between this leafhopper and *A. baccarum* suggests a suppression effect in three of our treatments (Table 2.5). Compared to natural ground cover, the estimated abundance decrease of *E. onukii* in tea canopies intercropped with *P. notatum* and *C. rotundifolia* was 5.4% and 4.4%, respectively, with the increase of *A. baccarum* per unit abundance. Indeed, in a previous study, Liu [116] suggested that reductions in TGL abundance were attributed to the enhanced density of *A. baccarum*, which was consistently found at higher densities in tea intercropped with *A. conyzoides* and *C. tora* than in monoculture tea. *Festuca arundinacea* Schreb. (Poales: Poaceae) intercropping treatment has the potential to improve the controlling effect of *Tetranychus urticae* Koch (Acari: Tetranychidae) in clementine mandarins when compared to natural ground cover or bare ground [118, 119]. Nevertheless, without targeted exclusion experiments, it is not possible to establish that the increasing mite abundances are directly responsible for declining TGL populations. The fact that, despite the greater abundance of the predatory mite, a significant decrease in

E. onukii was not detectable in the first year (Table 2.5) which further highlights the potential importance of the periodical impact of cover crops. One of the reasons why increased predator numbers did not directly translate to declining pest numbers can be that the predatory mite may need some time to increase its population to a level that can efficiently suppress pest populations. Moreover, the generalist nature of the predatory behavior of *A. baccarum* may be a further explanation. Although this mite is a valuable natural enemy of insect pests in tea plantations, it disperses throughout the habitat and also consumes a variety of invertebrates, including phytophagous tea mites, other leafhoppers, aphids, whiteflies, and thrips. Therefore, its control effect on *E. onukii* may be masked. Furthermore, the phenology of parasitoids or specialist predators typically mirrors that of their prey, with some lag behind [120]. However, the polyphagous nature of *A. baccarum*, as many other species are likely to have been simultaneously available to prey upon, may mean that this predator is not especially reliant on availability of *E. onukii* [27, 33, 36]. Thus, this asynchronous phenology may be another factor why the controlling effect of the predatory mite was not clear. Similarly to previous studies conducted in tea plantations [27, 109] or longan orchards [42], in our study, *A. baccarum* occurred from January to February, from April to June, from August to September, and in November, without obvious overwintering periods. However, *E. onukii* peaked from May to July and from September to November, aligning with the activity period of *A. baccarum* only to some extent.

Our findings support the hypothesis that intercropping system can enhance the abundance of predatory mite. The effects of this increased abundance of the predatory mite on leafhopper pest populations are, however, yet unclear and need to be investigated further. Whilst both clearing tea rows up completely and leaving natural weedy cover are conventional ways of tea production, in this study we did not find any strong evidence to support their functions against *E. onukii*, and both of them have considerable drawbacks. As well as increasing costs of manual labor in China making this practice uneconomic, clearing-up tea rows also minimizes the chance for any kind of biological control. Similarly, natural weedy vegetation may compete with the tea crop, and, although it enables beneficial insect populations to grow, its regular removal it can only provide a temporarily suitable environment. On the other hand, since we did not find any effect of cover crop treatments decreasing tea production, the additional benefits, such as enhancing biological pest management [20] and weed control [102], are likely to supersede the others. Additional potential benefits of cover crops that we did not investigate in this study include providing nectar, pollen, or honeydew for natural enemies, alternative hosts for herbivores, or mitigating water runoff and soil erosion [8, 100, 102, 104]. Hence, we believe that tea production is still likely to benefit from well-chosen cover crop vegetation. Species choice (including combinations), sowing times, and other management practices, along with the other potential benefits need further investigation, though, before final cost-benefit assessments, or practical applications. In forthcoming

research an emphasis should be put on the temporal aspect these practices.

2.6 Conclusion

Tea plantations are long-lasting agro ecosystems but still have high levels of human disturbance, mainly through insecticide uses. As tea is a perennial, evergreen crop, the habitats it provides for a variety of phytophagous and beneficial arthropods are relatively stable. This stability favors the build-up and maintenance of effective natural enemy communities, which, in turn, can effectively control tea pests and, therefore, they can lead to a reduced need for pesticide use.

In this chapter, we have shown that intercropping treatments help to enhance the densities of the predatory mite, *A. baccarum*, and may reduce the populations of the leafhopper pest, *E. onukii*. The direct interaction between predator and *E. onukii* is not clear though, neither is it clear how alternative intercropping treatments with other cover plants can influence the abundance of *A. baccarum* and *E. onukii* . Therefore, further research on the effects of intercropping system in tea production is necessary. Further studies are also required to enhance understanding of the trophic relationship among *A. baccarum* and *E. onukii*, and other natural enemies or preys, and the mechanisms by which cover crop vegetation facilitates the suppression of pest in tea plantations. Future research should also consider all development stages and instars of both *A. baccarum* and *E. onukii*. Additional alternative cover crop species, or species combinations, have

the potential to be more effective in supporting management of the critical tea pest, *E. onukii*, and other pest species and even providing additional ecosystem services. Furthermore, with no negative effect from the tea management point of view, other, previously described, benefits are likely to make cover crops a useful management practice that in many cases outperform conventional systems.

3 Dynamics complexity of generalist predatory mite and the leafhopper pest in tea plantations

This work has been conducted in collaboration with Dr. Zhu, H., Dr. Chen, L. L., and Dr. You, M. S. I have collaborated in constructing the models, theoretical analyses and numerical simulations.

3.1 Introduction

In chapter 2, we have applied the statistical model to discuss the correlation between *E. onukii* and *A. baccarum* abundance in the tea plantation with different crop cover treatment. The abundance of *A. baccarum* in a tea plantation is influenced by intercropping treatment significantly. But compared to natural ground cover crops, the effect of cover crops on *E. onukii* was not observed. The effects of this increased abundance of the *A. baccarum* on *E. onukii* populations are not unclear and need to be investigated further. In this chapter, we aim to use the dynamical system to analyze the relationship between

these two species.

Mathematical models have been made to understand the population dynamics in ecology for many years since the pioneering work of Lotka and Volterra [48]. However, there are less modeling studies on the dynamics of tea garden ecosystems which can be more complicated with thousands of different species, providing a relatively steady microclimate and food supply of insect and mite communities [3]. The role of generalist predators in controlling pests has also been explored in some cropping systems through field experiments [72, 121]. Therefore, we will explore the interaction between generalist predator and its preys to find ways to optimize the beneficial synergies of pest control [72]. In particularly, we will study the dynamics of *E. onukii* and *A. baccarum* for seeking a sustainable way for pest suppression in tea plantations.

To understand the interaction of *E. onukii* and *A. baccarum*, Chen et al. [112, 122] carried out field studies in the Wuyi mountain area, the north of Fujian province of China. The abundance data for the two species were collected over a two-year period and presented in Figure 3.1. One can see from the figure that in the first year, there is a negative correlation between the two species. However, it did not show the same trend in the second year. A significant decrease in the population of *E. onukii* was not detectable despite the greater abundance of *A. baccarum* in the second year [122]. One can also observe that when *E. onukii* is abundant, ideally the *A. baccarum* mainly feed on *E. onukii* or may feed on other preys as well, so that the number of *E. onukii* is reduced to only a

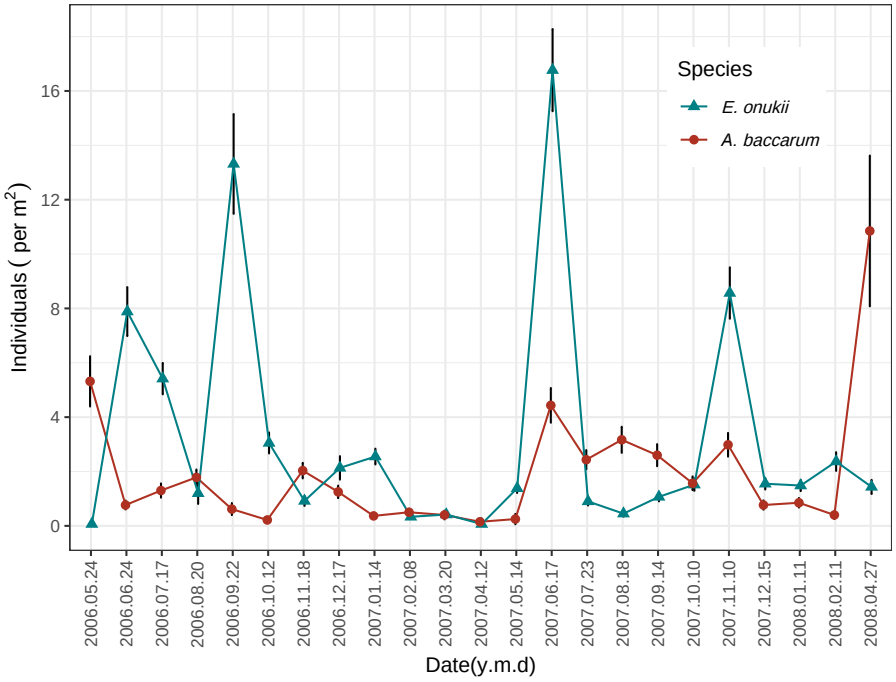

Figure 3.1: Average abundance (± standard error) of *E. onukii* and *A. baccarum* per 1 m^2 in tea canopies in the tea plantations in the Wuyi Mountains from May 2006 until April 2008.

certain extent. Therefore, the control of the target pest *E. onukii* using *A. baccarum* is much more complicated as *A. baccarum* is a generalist predator.

It is not difficult to directly make up a predator-prey type of model for the pest and predator mite. However, to understand the population dynamics between these two species and to promote the use of *A. baccarum* to control *E. onukii*, we will use the results of field studies [112, 122] and build a simpler dynamical model to study the interaction of the adults population, which will allow us to explore the factors and reason

leading to complex dynamics using bifurcation theory, and to find threshold conditions for controlling *E. onukii* using its generalist natural enemy.

Let us consider a tea plantation with fixed area where tea trees grow. We are interested in the fresh tender leaves which can be measured by the weight or equivalently transformed single-side surface area of leaves. Let K be the total tea leaves surface area (m^2) and $E(t)$ denote the adult population of *E. onukii*, the number of *E. onukii* per unit tea leaves surface area (m^2) at time t. We assume that the average number of *E. onukii* that per unit tea leaves surface area can carry is n_e. Hence, it is plausible to assume that *E. onukii* satisfy a logistic growth with an intrinsic reproduction rate $r_1 > 0$ and the carrying capacity $K_1 = Kn_e > 0$ in the absence of *A. baccarum*.

Let $M(t)$ denote the adult population of *A. baccarum*, the number of *A. baccarum* per unit tea leaves surface area (m^2) at time t and the average number of *A. baccarum* per unit tea leaves surface area is n_m. As a generalist predator, *A. baccarum* can prey on other pests and maintain its population without *E. onukii*. Hence, we assume that the *A. baccarum* reproduces also following a logistic growth with a constant intrinsic growth rate $r_2 > 0$ and a carrying capacity $K_2 = Kn_m > 0$ in the absence of *E. onukii*. In fact, the generalist predators are more common in ecosystems than the specialist predator. We observe that the euryphagous nature of *A. baccarum* is conducive to maintaining its population to suppress the *E. onukii* when the outbreak occurs even when the density of *E. onukii* is relatively low. If the *A. baccarum* are monophagous, there may not be

enough to control the *E. onukii* due to the decreasing of *E. onukii* population. Hence, we will develop a predator prey model considering *A. baccarum* as a generalist predator.

In order to describe the predator-prey relationship between the *E. onukii* and the *A. baccarum*, we look at it from a micro perspective. Since each species of insect will be active for certain amount of time per day, we assume that *E. onukii* and *A. baccarum* spend T_e and T_m hours foraging per day ($0 < T_m, T_e < 24h$) [30, 123]. During the period of T_m, each *A. baccarum* can attack N_E number of *E. onukii*. The factors affecting N_E are: the area and time needed to search *E. onukii*, the successful search rate of *A. baccarum*, attack rate of *A. baccarum* and the number of *E. onukii*. If searching is successful, *A. baccarum* needs T_h time on average to handle the prey (pursue, capture, kill and eat) [30]. Hence, the number of *E. onukii* attacked by one *A. baccarum* equals $N_E = spT_sKE$, where s is the successfully searching rate of *A. baccarum* per unit area per unit of time. p is the capture probability of *A. baccarum* after search. T_s is the time per day that *A. baccarum* spend for searching, K is the total tea leaves surface area, and E is the number of *E. onukii* per unit tea leaves surface area (m^2). Note that we have $T_s = T_m - T_hN_E$. Then, we have

$$N_E = P(E) = \frac{spT_mKE}{1 + spT_hKE} = \frac{\frac{T_m}{T_h}E}{\frac{1}{spT_hK} + E} = \frac{mE}{a + E}$$

where $m = \frac{T_m}{T_h}$, which is the maximum number of *E. onukii* that *A. baccarum* can handle in the time period T_m for foraging. Another important parameter $a = \frac{1}{spT_hK}$, describes the number of *E. onukii* handled by *A. baccarum* in the average time period that *A.*

baccarum successfully search and capture one *E. onukii*. Each *A. baccarum* on average preys N_E number of *E. onukii*. And $P(E)$ is the widely used functional response, Holling type II, in the predator prey model. We derive the process to determine the meaning of the parameters in our model, which will help the model analysis incorporating our field experimental data in future work. Hence we have the following model

$$\begin{cases} \dfrac{dE}{dt} &= r_1 E(1-\dfrac{E}{K_1}) - \dfrac{mEM}{a+E}, \\ \dfrac{dM}{dt} &= r_2 M(1-\dfrac{M}{K_2}) + \dfrac{cmEM}{a+E}, \end{cases} \tag{3.1}$$

where all the parameters r_1, r_2, K_1, K_2, a, m are positive constants as defined above, and c is the conversion rate.

For the model (3.1), we can rewrite as

$$\begin{cases} \dfrac{dE}{dt} &= E(r_1 - \dfrac{r_1}{K_1}E - \dfrac{m}{a+E}M), \\ \dfrac{dM}{dt} &= M(r_2 - \dfrac{r_2}{K_2}M + \dfrac{cm}{a+E}E). \end{cases} \tag{3.2}$$

It turns out that system (3.2) is a model on the bookshelf. One can see that system (3.2) can be regarded as a generalized Lotka–Volterra model with a fractional response function. Recall that for a quadratic Lotka–Volterra system, it is well-known that it has relative simple dynamics, and in particular the system does not even have a limit cycle [124]. As far as we can tell that Alexeev (1973) [125] and Bazykin (1974) [126] are among the first researchers considered the predator competition for resources other than

prey and studied the following model,

$$\begin{cases} \dfrac{dx}{dt} &= ax - \dfrac{bxy}{1+Ax} - ex^2, \\ \dfrac{dy}{dt} &= -cy + \dfrac{dxy}{1+Ax} - hy^2, \end{cases} \tag{3.3}$$

where a is the reproduction rate of prey population in the absence of the predator. b is the per capita rate of the consumption of prey by the predators. The parameter $c >$ is the natural mortality rate of the predator, $\frac{d}{b}$ reflects the fraction of prey biomass that is converted into predator biomass. $\frac{1}{A}$ is the prey population density at which the predator's consumption is half the maximum value or half saturation level. e is the coefficient of competition among prey. h is the coefficient of competition for resources other than prey [49]. The system (3.3) depends on four parameters after rescaling and the related dynamics are well discussed in Bazykin (1998) [49]. But the predator in this model is a specialist predator that only relies on the prey population. When $c < 0$, that the predator also has the reproduction rate, the system (3.3) is consistent with the model (3.1). It is worth mentioning that Magal et al. [77] also used the model to explore the spatial dynamics of host and generalist parasitoids with logistic growth, and investigated the biological control of the leaf miner population. Their non-spatial model is the same as (3.1). Recently, Seo and Wolkowicz [78] identified some cases missed in the non-spatial model analysis of Magal et al. [77], and they gave a more detailed bifurcation analysis and presented a bifurcation diagram using K_1 and K_2 as bifurcation parameters, they analyzed the impact of different K_1 and K_2 on pest control and proposed possible pest

reduction strategies. More recently, Xiang et al. [79] also studied the nilpotent singularity of the model and presented the bifurcations associated with the nilpotent singularity of elliptic and focus type. Here we suggest and use the terms and classification given by Dumortier et al. [127] and in Zhu and Rousseau [128] in classifying the non-cusp type of nilpotent singularities.

The dynamics of generalist predator-prey model (3.2) are much more complicated then most of the specialist predator-prey models. The model can undergo Hopf bifurcation, degenerate Hopf bifurcation, and Bogdanov-Takens (BT) bifurcations of codimension 2 and 3, bifurcations of nilpotent focus and elliptic point. The three types of codimension 3 bifurcations of nilpotent singularities were presented in the study of Xiang et al. [79], but how these codimension 3 bifurcations are organized in the system are not discussed. From the available studies, the system can have two limit cycles [78, 79, 76], just like the specialist predator-prey model with other Holling types of response function studied in [60]. Currently, the available bifurcation studies are only partial unfolding of the complex dynamics from the degenerate nilpotent singularity, the understanding of the local dynamics still remains incomplete, not to say the global dynamics of the system.

The model exhibits three boundary equilibria and up to three coexistence equilibria, and the complicated dynamics involves Bogdanov-Takens bifurcation of codimension 2 and 3, and bifurcations of nilpotent singularity of focus and elliptic type of codimension 3 or 4. As described by Xiao and Zhu [70], the predator-prey system of the form (3.2)

can be locally transformed into a generalized Liénard-type system. There have been extensive global analysis of Liénard system involving the nilpotent singularities. For the related bifurcation studies, we only refer to Dangelmayr and Guckenheimer [129], Khibnik et al. [130] and a recent work of Chen and Zhu [131] and references therein. In this chapter, we will present a full bifurcation analysis of the system (3.2). Using normal form theory we will show that it is the nilpotent focus of codimension 4 that serves as an organizing center of the codimension 3 nilpotent bifurcations. We will also present the bifurcation diagrams near the nilpotent singularities of focus and elliptic type of codimension 3 using r_1, r_2, K_1 and K_2 as bifurcation parameters. For system (3.2), one interesting observation is that we numerically show the existence of three limit cycles in the generalist predator-prey systems.

The chapter is organized as the following. We present the existence and number of equilibria and local stability in Section 2. In Section 3, we study the bifurcation and complex dynamics of the system. We prove the existence of saddle-node bifurcation of codimension 1 and 2, Hopf bifurcation, BT bifurcation and nilpotent singularity of codimension 3 and 4. We also provide the one and two-parameter bifurcation diagrams and the bifurcation diagram near the nilpotent singularity of codimension 3. Section 4 contains the phase portraits of system (3.1) with different parameters. We present an example numerically to show the existence of three limit cycles. Our numerical simulation illustrates the different types of coexistence of *A. baccarum* and *E. onukii* and the

large amplitude oscillation of this two species population is possible. Finally, in Section 5, we summarize our results and discuss the implications for pest control based on our dynamical findings. Some of the calculations were assisted by the use of Maple [132]. The phase portraits and one and two-parameter bifurcation diagrams were produced by the Matlab [133].

3.2 Equilibrium states and local stability

3.2.1 Existence and number of equilibria

Our model (3.1) always has three boundary equilibria, $S_{00}(0,0)$, $S_{10}(K_1,0)$ and S_{01} $(0,K_2)$, which represent three trivial equilibrium states respectively. For co-existence equilibrium state, one can verify that any positive equilibrium $\bar{S}(\bar{E},\bar{M})$, if it exists, is the intersection of the two curves

$$\begin{aligned} U_1(E) &= \frac{r_1(K_1-E)(a+E)}{K_1 m} = \frac{r_1 E}{P(E)}(1-\frac{E}{K_1}), \\ U_2(E) &= K_2\left[\frac{mcE}{r_2(a+E)}+1\right] = K_2[\frac{c}{r_2}P(E)+1], \end{aligned} \tag{3.4}$$

and its E coordinate satisfies

$$\begin{aligned} U(E) =& E^3-(K_1-2a)E^2+\left[a^2-2aK_1+\frac{K_1K_2cm^2}{r_1r_2}+\frac{mK_1K_2}{r_1}\right]E-a^2K_1 \\ &+\frac{maK_1K_2}{r_1}=0. \end{aligned} \tag{3.5}$$

The cubic equation (3.5) has at most 3 positive solutions. We are only interested in the non-negative solutions of equation (3.5).

We first use K_1 and K_2 as parameters to discuss the number of positive equilibria. The equation (3.5) has at least one positive solution when $K_2 < \frac{r_1 a}{m}$. For the case of $K_2 > \frac{r_1 a}{m}$, some calculations and results can be found in [78, 79]. Using the formula of Fan in [134], we can compute the discriminant of (3.5) to get

$$\Delta = B^2 - 4AC, \tag{3.6}$$

where

$$\begin{aligned}
A &= (K_1 + a)^2 - \frac{3mK_1K_2\delta}{r_1 r_2}, \\
B &= 2a(K_1 + a)^2 - \frac{3mK_1K_2[K_1\delta + a(7r_2 - cm)]}{r_1 r_2}, \\
C &= \left[a^2 - 2aK_1 + \frac{K_1K_2cm^2}{r_1 r_2} + \frac{mK_1K_2}{r_1}\right]^2 + 3(K_1 - 2a)(-a^2K_1 + \frac{maK_1K_2}{r_1}),
\end{aligned}$$

and $\delta = r_2 + cm$. Collecting in terms of r_1, Δ becomes

$$\Delta = \tilde{A}r_1^2 + \tilde{B}r_1 + \tilde{C}, \tag{3.7}$$

where $\tilde{C} = 4m\delta^3$ and

$$\begin{aligned}
\tilde{A} &= \frac{4ac(K_1 + a)^3 r_2^2}{K_1^2 K_2^2}, \\
\tilde{B} &= -\frac{(K_1 + a)^2 r_2^3 + 2K_2cm(K_1 + a)(K_1 + 10a)r_2^2 + c^2m^2(K_1^2 + 20K_1a - 8a^2)r_2}{K_1K_2}.
\end{aligned}$$

The sign of Δ decides the number of real roots of (3.5). The equation $\Delta = 0$ may have two real roots if $\Delta_r > 0$ which are denoted as $r_{1i} = r_{1i}(K_1, K_2)(i = 1, 2)$:

$$r_{11}(K_1, K_2) = \frac{-B + \sqrt{\Delta_r}}{2A}, \;\; r_{12}(K_1, K_2) = \frac{-B - \sqrt{\Delta_r}}{2A},$$

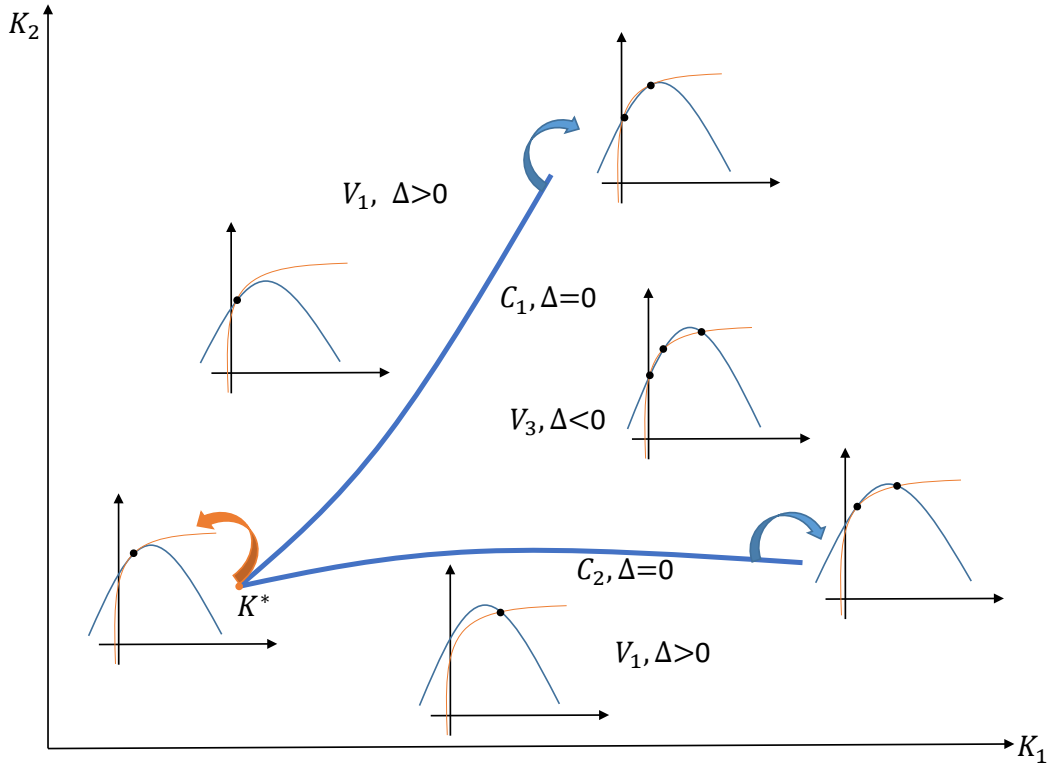

Figure 3.2: Existence of positive equilibria (number and position) of system (3.1) with K_1 and K_2 as parameters. The light blue curve is $U_1(E)$; the orange curve is $U_2(E)$.

where $\Delta_r = \frac{r_2^2[K_1\delta+ar_2][K_1\delta+a(r_2-8cm)]^3}{K_1^2K_2^2}$.

For $r_2 < 8cm, K_2 < \frac{r_1a}{m}$ and $K_1 > \frac{a}{8}(8cm - r_2)$, $r_{1i} = r_{1i}(K_1, K_2)(i = 1, 2)$ defines two curves C_1 and C_2 in (K_1, K_2) plane

$$C_1 = \left\{(K_1, K_2)\middle| r_1 = r_{11}(K_1, K_2),\ K_1 > \frac{a}{\delta}(8cm - r_2), K_2 < \frac{r_1a}{m}\right\},$$

$$C_2 = \left\{(K_1, K_2)\middle| r_1 = r_{12}(K_1, K_2), K_1 > \frac{a}{\delta}(8cm - r_2), K_2 < \frac{r_1a}{m}\right\},$$

and they subdivide the nonnegative cone of $(K_1, K_2$ plane into three open regions (see

Figure (3.2)):

$$V_1 = \{(K_1, K_2), \Delta > 0\},$$

$$V_2 = \{(K_1, K_2), C_1 \cup C_2\},$$

$$V_3 = \{(K_1, K_2), \Delta < 0\}.$$

In V_1, V_2 and V_3, system (3.1) has one, two and three positive equilibria respectively.

3.2.2 Local stability of equilibria

The equilibrium S_{00} has two positive eigenvalues r_1 and $r_2 > 0$, it is a unstable node. $S_{10}(K_1, 0)$ is always a saddle which means that as a generalist predator, the *A. baccarum* will never go extinction.

For the pest free equilibrium point $S_{01}(0, K_2)$, it has two eigenvalues, one is $-r_2 < 0$, the other is $r_1 - \frac{mK_2}{a}$. Hence it is locally asymptotically stable if $K_2 > \frac{r_1 a}{m}$, is a saddle if $\frac{r_1 a}{m} > K_2$, and it will be a saddle-node when $K_2 = \frac{r_1 a}{m}$. In later section, we will see that S_{01} can be a saddle-node of codimension 2.

Now, we discuss the local stability of the coexistence or positive equilibria. Using the expressions of $U_1(E)$ and $U_2(E)$, we can rewrite the system (3.1) as

$$\begin{cases} \dfrac{dE}{dt} &= P(E)[U_1(E) - M], \\ \dfrac{dM}{dt} &= \dfrac{r_2}{K_2} M[U_2(E) - M]. \end{cases} \tag{3.8}$$

The Jacobian matrix of system (3.8) is

$$J(E) = \begin{pmatrix} P(E)U_1'(E) + P'(E)[U_1(E) - M] & -P(E) \\ \\ \frac{r_2}{K_2}MU_2'(E) & -\frac{r_2}{K_2}M + \frac{r_2}{K_2}[U_2(E) - M] \end{pmatrix}. \tag{3.9}$$

For any positive equilibrium, if exists, the characteristic equation at the equilibrium $\overline{S}(\overline{E}, \overline{M})$ is of the form

$$\lambda^2 - \left[P(E)U_1'(E) - \frac{r_2}{K_2}\overline{M}\right]\lambda + P(E)\frac{r_2}{K_2}\overline{M}\big[U_2'(E) - U_1'(E)\big] = 0. \tag{3.10}$$

If λ_1 and λ_2 are the two eigenvalues, then we have the trace and determinant of $J(E)$ are

$$\begin{aligned} T(J(\overline{S})) &= \lambda_1 + \lambda_2 = P(\overline{E})U_1'(E) - \tfrac{r_2}{K_2}\overline{M}, \\ D(J(\overline{S})) &= \lambda_1\lambda_2 = P(\overline{E})\tfrac{r_2}{K_2}\overline{M}\big[U_2'(\overline{E}) - U_1'(\overline{E})\big], \end{aligned} \tag{3.11}$$

where

$$U_1'(\overline{E}) = \frac{r_1(-a - 2\overline{E} + K_1)}{K_1 m}, \quad U_2'(\overline{E}) = \frac{K_2 acm}{r_2(a + \overline{E})^2}.$$

For any $\overline{S}$, sign of the $D(\overline{E})$ is determined by the slope difference of the two curves $M = U_1(E)$ and $M = U_2(E)$ at the intersection. As shown in Figure 3.3, if we denote $k_i = U_i'(\overline{E})$ $(i = 1, 2)$ then when $k_1 > k_2$, $D(J(\overline{S})) < 0$, the equilibrium point is a saddle. If $k_1 < k_2$, then $D(J(\overline{S})) > 0$, and the real part of the eigenvalues will be both positive or negative depending on the sign of $T(J(\overline{S}))$.

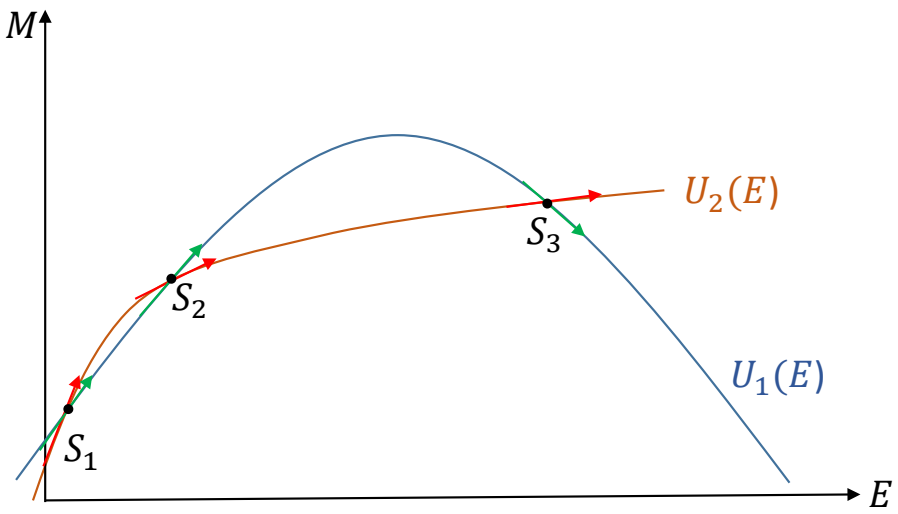

Figure 3.3: The existence and stability of the three positive equilibria S_1, S_2 and S_3 for $(K_1, K_2) \in V_3$.

It follows from (3.11) that a Hopf bifurcation may occur at $\overline{S}$ if $T(J(\overline{S})) = 0$. Also, if $k_1 = k_2$, $D(J(\overline{S})) = 0$, a saddle-node bifurcation may occur. Furthermore, the equilibrium will be nilpotent if $T(J(\overline{S})) = D(J(\overline{S})) = 0$.

To summarize, as shown in Figure 3.2 and 3.3, we have the following proposition on the number and local stability of positive equilibria.

Proposition 3.2.1. *Consider the system* (3.1) *with parameters* K_1 *and* $K_2 < \dfrac{r_1 a}{m}$. *For any* r_1, r_2, a, c, $m > 0$, *we have*

(1) If $(K_1, K_2) \in V_1$ *(*$\Delta > 0$*), system has a unique positive equilibrium* S_1, *it is a non-saddle.*

(2) If $(K_1, K_2) \in V_2$, *(*$\Delta = 0$*),*

(2.1) If $r_2 < 8cm$, $K_1 > 2a$, $\Delta_r = 0$ *and* $(K_1, K_2) = (K_1^*, K_2^*) = C_1 \cap C_2$ *with*

$$K_1^* = \frac{a(8cm - r_2)}{\delta}, \;\; K_2^* = \frac{27 r_1 r_2 c^2 m a}{\delta^2 (8cm - r_2)}, \tag{3.12}$$

then, system has a unique degenerate positive equilibrium which we denote it as $S_{123} = (E_{123}, M_{123})$ *with*

$$E_{123} = \frac{K_1^* - 2a}{3}, \;\; M_{123} = \frac{2r_1 (K_1^* + a)^2}{9 K_1^* m}. \tag{3.13}$$

(2.2) If $\Delta_r > 0$ *or when* $(K_1, K_2) \in C_1 \cup C_2 / (K_1^*, K_2^*)$*, system has two positive equilibria.*

(i) When $(K_1, K_2) \in C_1 / (K_1^*, K_2^*)$*, system has the two positive equilibria are* $S_1(E_1, M_1)$ *and* $S_{23}(E_{23}, M_{23})$*, and* S_{23} *is of multiplicity 2 and a saddle-node if* $T(S_{23}) \neq 0$.

(ii) When $(K_1, K_2) \in C_2 / (K_1^; K_2^*)$*, the system has two positive equilibria* $S_{12}(E_{12}, M_{12})$ *and* $S_3(E_3, M_3)$*, and* S_{12} *is of multiplicity 2 and a saddle-node if* $T(S_{12}) \neq 0$.

(3) If $(K_1, K_2) \in V_3$ *(*$\Delta < 0$*), system has three distinct positive equilibria. We denote these three equilibria as* $S_i(E_i, M_i)$ *with* $i = 1, 2, 3$ *and* $E_1 < E_2 < E_3$. *The middle one* S_2 (E_2, M_2) *is always a saddle.*

3.3 Bifurcation and complex dynamics

For system (3.1), when K_1 and K_2 change, it can have up to three positive equilibria which will undergo various type of bifurcations. Among the rest of 5 model parameters r_1, r_2, a, c, m, we will select to add the parameters r_1 and r_2 to study the bifurcations, hence we will use K_1, K_2 and r_1, r_2 to present the bifurcations in the parameter space (K_1, K_2, r_1, r_2).

3.3.1 Saddle-node bifurcations

System may undergo saddle-node bifurcations at a positive equilibrium and boundary equilibrium $S_{01}(0, K_2)$.

It follows from the Prop. (3.2.1) that S_1 and S_2 coalesce at S_{12} if $(K_1, K_2) \in C_2$. Note that $U_2'(E) = \frac{acmK_2}{r_2(a+E)^2} > 0$, hence when exists, S_{12} is always located to the left of the hump of the parabola. From (3.11), we have $D(J(S_{12})) = 0$, and the associated eigenvalues, one is zero, and the other

$$\begin{aligned}\lambda_2 = T_\Delta &= P(E_{12})U_1'(E_{12}) - \frac{r_2}{K_2}M_{12} \\ &= -\frac{2r_1E_{12}^2 + [(\delta - r_1)K_1 + r_1a]E_{12} + K_1ar_2}{K_1(a + E_{12})} = -\frac{h(E_{12})}{K_1(a + E_{12})},\end{aligned}$$

here we define that

$$h(\overline{E}) = 2r_1\overline{E}^2 + [\delta K_1 + r_1(a - K_1)]\overline{E} + K_1r_2a, \tag{3.14}$$

with $\overline{E} = E_{12}$, $0 < E_{12} < \frac{K_1-a}{2}$.

Note that $\frac{dh(E_{12})}{dr_1} = E_{12}(2E_{12} - K_1 + a) < 0$, therefore λ_2 will change sign at most once, and $h(r_{11}) < h(r_{12})$. Hence, we only need to find the nilpotent equilibria that $T_\Delta = 0$, which separate the stable and unstable saddle-node bifurcation.

For the equilibrium S_{12}, if $T_\Delta = T(J(S_{12})) \neq 0$, we can linearize the system at S_{12} and diagonalize the linear part to obtain

$$\begin{cases} \dot{x} &= A_{20}x^2 + xO(y) + O(|y|^2, |x,y|^3), \\ \dot{y} &= T_\Delta y + O(|x,y|^2), \end{cases} \tag{3.15}$$

where

$$\begin{aligned} A_{20} &= \frac{E_{12}(\delta E_{12} + r_2 a)}{r_2(a + E_{12})^3 h(E_{12})}\{r_1 r_2 (K_1 + a)(a + E_{12})^2 + K_1 K_2 m[a(cm - 2r_2) \\ &\quad - 2\delta E_{12}]\}, \\ E_{12} &= \frac{m\delta K_1^2 K_2 + am(7r_2 - 2cm)K_1 K_2 - 2ar_1 r_2 (K_1 + a)^2}{2r_1 r_2 (K_1 + a)^2 - 6m\delta K_1 K_2}. \end{aligned}$$

Obviously, A_{20} determines the codimension of the saddle-node bifurcation if $T_\Delta \neq 0$. If $A_{20} \neq 0$, then it follows from (3.15) that S_{12} is a saddle-node (for S_{23}, the calculation is similar).

If $A_{20} = 0$, we have

$$\begin{aligned} &r_1 r_2 \delta^2 K_1^3 K_2 - 4m\delta^3 K_1^2 K_2^2 + 2ar_1 r_2 \delta(10cm + r_2)K_1^2 K_2 \\ &\quad + a^2 r_1 r_2 (r_2^2 + 20cmr_2 - 8c^2 m^2)K_1 K_2 - 4acr_1^2 r_2^2 (K_1 + a)^3 = 0. \end{aligned} \tag{3.16}$$

One can verify that for any positive model parameters, if $K_1 = K_1^*, K_2 = K_2^*$, then $A_{20} = 0$, which corresponds to the case $S_{12} = S_{23} = S_{123}$.

Substituting the expressions (3.12) for $K_1 = K_1^*, K_2 = K_2^*$ into $T_\Delta = 0$, we can solve to get a unique solution

$$r_1 = r_1^* = \frac{2\delta(8cm - r_2)}{3(2cm - r_2)}.$$

Therefore, T_Δ changes sign at (K_1^*, K_2^*, r_1^*). When $(K_1, K_2, r_1) = (K_1^*, K_2^*, r_1^*)$, S_{123} becomes a nilpotent equilibrium which will be discussed further in Section 3.3.4.

Proposition 3.3.1. *For the system* (3.1) *with* $(K_1, K_2) \in C_1 \cup C_2 / (K_1^*, K_2^*)$ *(* $\Delta = 0$ *and* $T_\Delta \neq 0$*), we have*

(1) When exist, S_{12} *and* S_{23} *are saddle-nodes of codimension 1 for* (K_1, K_2) *on* C_2 *and* C_1 *respectively.*

(2) If $K_1 = K_1^*, K_2 = K_2^*$ *but* $r_1 \neq r_1^*$*, the unique positive equilibrium* $S_{12} = S_{23} = S_{123}$ *will be a saddle-node of codimension 2.*

Now we study the bifurcation of the boundary equilibrium $S_{01}(0, K_2)$. When $K_2 = \frac{r_1 a}{m}$, one can calculate to verify that S_{01} has two eigenvalues 0 and $-r_2$, hence it is a saddle-node. Translate the $S_{12}(0, K_2)$ into the origin by letting $x = E, y = M - \frac{r_1 a}{m}$, we obtain

$$\begin{cases} \dot{x} &= \dfrac{r_1(K_1 - a)}{K_1 a}x^2 - \dfrac{m}{a}xy + \dfrac{m}{a^2}x^2 y - \dfrac{r_1}{a^2}x^3 + O(|x, y|^4), \\ \dot{y} &= cr_1 x - r_2 y - \dfrac{cr_1}{a}x^2 + \frac{cm}{a}xy - \frac{r_2 m}{r_1 a}y^2 - \frac{cm}{a^2}x^2 y + \dfrac{cr_1}{a^2}x^3 + O(|x, y|^4). \end{cases} \tag{3.17}$$

If we make a change of variables as $u = x$, $v = \frac{cr_1}{r_2}x + y$, then system (3.17) becomes

$$\begin{cases} \dot{u} &= \tilde{a}_{20}u^2 + \tilde{a}_{11}uv + \tilde{a}_{30}u^3 + \tilde{a}_{21}u^2v + O(|u,v|^4), \\ \dot{v} &= -r_2v + \tilde{b}_{20}u^2 + \tilde{b}_{11}uv + \tilde{b}_{02}v^2 + O(|u,v|^3), \end{cases} \tag{3.18}$$

where

$$\tilde{a}_{20} = \frac{r_1((r_2 - cm)K_1 - r_2a)}{ar_2K_1},\ \tilde{a}_{11} = -\frac{m}{a},\quad \tilde{a}_{30} = \frac{r_1(cm - r_2)}{a^2r_2},\quad \tilde{a}_{21} = \frac{m}{a^2},$$
$$\tilde{b}_{20} = -\frac{((r_1(cm - r_2) - r_2^2)K_1 + r_1r_2a)r_1c}{aK_1r_2^2},\quad \tilde{b}_{11} = \frac{cm(r_1 - r_2)}{ar_2},\quad \tilde{b}_{02} = -\frac{r_2m}{r_1a}.$$

Therefore, S_{01} is a saddle-node of codimension 1 when $\tilde{a}_{20} \neq 0$.

When $S_{12} = S_{01}$, we have $K_1 = \frac{r_2a}{r_2 - cm}$ ($r_2 > cm$), and we can verify that $\tilde{a}_{20} = 0, \tilde{a}_{30} \neq 0$. Also, when $S_{123} = S_{01}$, we have $K_1 = 2a, r_2 = 2cm$, and $\tilde{a}_{20} = 0, \tilde{a}_{30} \neq 0$. Unlike in [79], this is a more degenerate case which may involve canard cycles and deserves further investigation [135].

Summarizing the above discussion, we have the following proposition.

Proposition 3.3.2. *For the pest free equilibrium $S_{01}(0, K_2)$, if $K_2 = \frac{r_1a}{m}$,*

(1) it is a saddle-node of codimension 1.

(2) when $K_1 = \frac{r_2a}{r_2 - cm}$, and $(r_2 > cm)$, S_{01} is a saddle-node of codimension 2.

3.3.2 Hopf bifurcations

Though the Hopf bifurcations were analyzed in Seo and Wolkowicz in details [78], but their analysis did not capture all the possible cases, we will present the Hopf bifurcation

analysis and add the other two types of (K_1, K_2) plane bifurcation diagrams which were missing in their analysis. From the Prop. 3.2.1, when exists, the equilibria S_1 and S_3 may undergo Hopf bifurcation(s) if

$$T(J(\overline{S})) = k_1 P(\overline{E}) - \frac{r_2}{K_2}\overline{M} = -\frac{h(\overline{E})}{K_1(a+\overline{E})} = 0, \tag{3.19}$$

where $h(\overline{E})$ is defined in (3.14).

Denote the discriminant of equation $h(\overline{E}) = 0$ as Δ_1, and collect in terms of parameter K_1,

$$\Delta_1 = (\delta - r_1)^2 K_1^2 + 2r_1 a(cm - r_1 - 3r_2)K_1 + a^2 r_1^2,$$

with its discriminant denoted as $\Delta_2 = -32a^2 r_1^2 r_2(cm - r_1 - r_2)$. The equation $h(\overline{E}) = 0$ may have two roots if $\Delta_1 > 0$ which we denote them respectively as

$$H_1 = \frac{r_1(K_1 - a) - K_1\delta + \sqrt{\Delta_1}}{4r_1}, \quad H_2 = \frac{r_1(K_1 - a) - K_1\delta - \sqrt{\Delta_1}}{4r_1}.$$

For $H_{1,2}$ to be real numbers, it also requires

$$K_1 > \frac{r_1 a}{r_1 - \delta} \quad (0 < r_1 < \delta).$$

When $\Delta_2 < 0$, then $r_1 < cm - r_2$, Δ_1 is always greater than 0. When $\Delta_2 \geq 0$, then $r_1 \geq cm - r_2$, $\Delta_1 > 0$ when $K_1 \geq K_1^+$ or $K_1 \leq K_1^-$, with

$$K_1^+ = \frac{2r_1 a(r_1 + 3r_2 - cm) + \sqrt{\Delta_2}}{2(r_1 - \delta)^2}, \quad K_1^- = \frac{2r_1 a(r_1 + 3r_2 - cm) - \sqrt{\Delta_2}}{2(r_1 - \delta)^2}.$$

To ensure $K_1^{\pm}$ are positive, it requires

$$r_1 \geq cm - r_2 = \max\{cm - r_2, cm - 3r_2\}.$$

Also, one can easily find that $K_1^+ > \frac{r_1 a}{r_1 - \delta}$. Hence, we have the following condition to ensure $\Delta_1 > 0$,

$$\begin{aligned} K_1 &> \frac{r_1 a}{r_1 - \delta}, \quad 0 < r_1 < cm - r_2, \\ K_1 &\geq K_1^+, \quad cm - r_2 \leq r_1 < \delta. \end{aligned} \tag{3.20}$$

Substituting H_1 and H_2 into $U(\overline{E})$ yields the set of Hopf bifurcation which is defined by a curve $H(K_1, K_2, r_1) = 0$ given by

$$K_2 = \frac{p_3 \pm p_2\sqrt{\Delta_1}}{4(p_1 \mp \delta\sqrt{\Delta_1})mr_1K_1} \tag{3.21}$$

where

$$\begin{aligned} p_1 &= \delta(\delta - r_1)K_1 + r_1 a(\delta - 4r_2), \\ p_2 &= -r_2[(r_1^2 - \delta^2)K_1^2 + 2ar_1(\delta + 2r_1 + r_2)K_1 - a^2 r_1^2], \\ p_3 &= -r_2[(\delta + r_1)(\delta - r_1)^2 K_1^3 - ar_1[-3r_1^2 + 2(\delta + r2)r_1 + \delta(\delta + 6r_2)]K_1^2 \\ &\quad - a^2 r_1^2(\delta - 11r_1 - 10r_2)K_1 + a^3 r_1^3]. \end{aligned}$$

On the other hand, for Hopf bifurcation to occur, we need $D(J(\overline{S})) > 0$ ($k_1 < k_2$), which is equivalent to

$$\begin{aligned} &2r_1r_2\overline{E}^3 - r_1r_2(K_1 - 5a)\overline{E}^2 - 2ar_1r_2(K_1 - 2a)\overline{E} + a(K_1K_2cm^2 - K_1ar_1r_2 \\ &+ a^2r_1r_2) > 0 \end{aligned} \tag{3.22}$$

Substituting $H_{1,2}$ into the (3.22) and we obtain

$$K_2 > \frac{r_2(\hat{p}_1 - \hat{p}_2\sqrt{\Delta_1})}{8K_1acm^2r_1^2} \text{ (for } H_1), K_2 > \frac{r_2(\hat{p}_1 + \hat{p}_2\sqrt{\Delta_1})}{8K_1acm^2r_1^2} \text{ (for } H_2), \tag{3.23}$$

where

$$\begin{aligned}\hat{p}_1 =&\delta(\delta - r_1)^2K_1^3 - 2r_1a[(-cm - 2r_2)r_1 - \delta(cm + 4r_2)]K_1^2 + r_1^2a^2(cm + 4r_1 \\ &+ 15r_2)K_1 - 4a^3r_1^3, \\ \hat{p}_2 =&\delta(\delta - r_1)K_1^2 - r_1a(3cm + 5r_2)K_1 + 4a^2r_1^2.\end{aligned}$$

Therefore, under condition of (3.20) and (3.23), a Hopf bifurcation may occur at $\overline{E} = H_1$, $\overline{E} = H_2$ or at $\overline{E} = H_1 = H_2$ when $\Delta_1 = 0$, except when $\overline{E} = E_{12}$ or $\overline{E} = E_{23}$ or $\overline{E} = E_{12} = E_{23} = E_{123}$ where the degenerate equilibrium point occurs and the Hopf bifurcation curve is given by (3.21).

Next, we verify the transversality condition. Let γ be the real part of the eigenvalue of S_1 or S_3, then

$$\gamma = \frac{1}{2}T(\overline{E}) = -\frac{2r_1\overline{E}^2 + [\delta K_1 + r_1(a - K_1)]\overline{E} + K_1r_2a}{2K_1(a + \overline{E})}.$$

A straightforward calculation gives

$$\frac{\partial\gamma}{\partial K_2} = \frac{\partial\gamma}{\partial\overline{E}}\frac{\partial\overline{E}}{\partial K_2} = \frac{-2r_1\overline{E}^2 - 4r_1a\overline{E} - r_1a^2 + K_1(r_1 - cm)a}{2K_1(a + \overline{E})^2}\frac{\partial\overline{E}}{\partial K_2},$$

where

$$\frac{\partial\overline{E}}{\partial K_2} = \frac{-K_1m[(cm + r_2)\overline{E} + r_2a]}{r_1r_2[3\overline{E}^2 - 2(K_1 - 2a)\overline{E} + a^2 - 2K_1a] + K_1K_2cm^2 + K_1K_2mr_2}.$$

Since $\overline{E}$, K_1, r_2, c, m, a are all positive, $\frac{\partial \overline{E}}{\partial K_2} \neq 0$. Also, we find $\frac{\partial \gamma}{\partial \overline{E}} = 0$ only when $\overline{E} = \hat{E} = \frac{-2r_1a+\sqrt{2r_1a[K_1(r_1-cm)+r_1a]}}{2r_1}$ and the coordinate $\hat{E}$ does not satisfy $U(\hat{E}) = 0$. For the positive equilibrium $\overline{S}(\overline{E}, \overline{M})$, $\frac{\partial \gamma}{\partial \overline{E}} \neq 0$. Hence, $\frac{\partial \gamma}{\partial K_2} \neq 0$, the transversality condition is satisfied.

Moreover, we can find the point that $D(J(\overline{S})) = 0$, which is the intersection of Hopf and saddle-node bifurcation curves. It separates the Hopf bifurcation and neutral saddle curves. We now plot the curves $\Delta = 0$ and $H(K_1, K_2, r_1) = 0$ in (K_1, K_2) plane when $r_1 = r_1^*$ for different r_2. A numerical generated partial bifurcation diagram contains both Hopf and saddle-node bifurcations is presented in (K_1, K_2) plane in Figure 3.4. This is the slices of the bifurcation diagram near the degenerate equilibrium point when r_1 is fixed. Also, the bifurcation diagram with r_1 varying are presented in Figure 3.8 and Figure 3.9. In this paper, we discussed the bifurcation diagram involving four parameters through the slices.

Different cases can happen with the two curves are tangent at different positions (Figure 3.4(a), 3.4(b), 3.4(c)) which corresponds to different type of nilpotent singularities. The curve in blue is for saddle-node bifurcation, $\Delta = 0$, which has two parts of stable and unstable saddle-node bifurcation separated by a point associated with nilpotent equilibrium point (Figure 3.4(a), 3.4(b)) or Bogdanov-Takens point (Figure 3.4(c)); while the curve in red, $H = 0$ is composed of curves segment of Hopf bifurcation curve and neutral saddle curve which are separated by the point corresponding to the nilpotent equilibrium

(Figure 3.4(a), 3.4(b)) or Bogdanov-Takens point (Figure 3.4(c)).

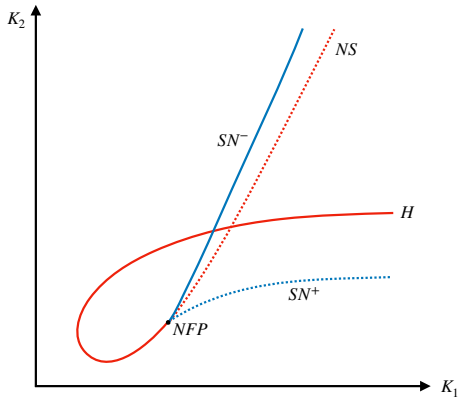

(a) $r_2 = 0.5, a = 1, c = 1, m = 1$

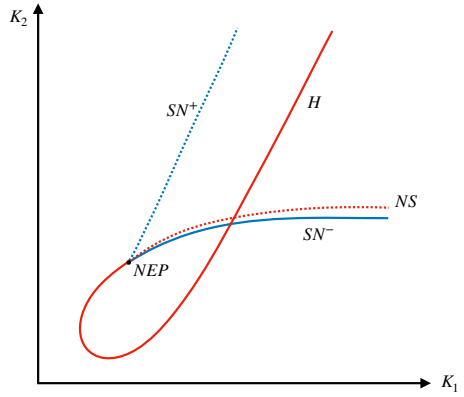

(b) $r_2 = 1.6, a = 1, c = 1, m = 1$

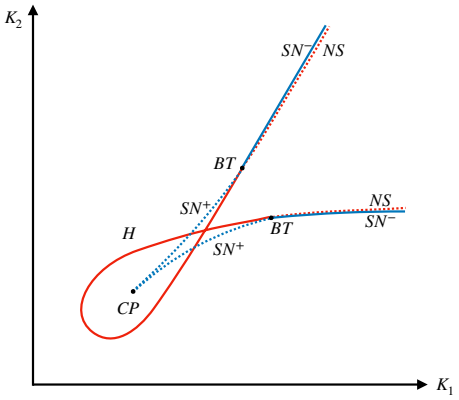

(c) $r_2 = \frac{8}{7}, a = 1, c = 1, m = 1$

Figure 3.4: The diagram of Hopf and saddle-node bifurcations in (K_1, K_2) plane when $r_1 = r_1^*$ with different r_2. $SN^{\pm}$ is the unstable (blue dot line) and stable (blue solid line) saddle node bifurcation curve respectively; NS is the neutral saddle curve (red dot line); H is the Hopf bifurcation curve (red solid line); NFP is the nilpotent focus point of codimension 3; NEP is the nilpotent elliptic point of codimension 3; CP is the cusp point; BT is the Bogdanov-Takens point.

3.3.3 Bogdanov-Takens bifurcation

The analysis of Bogdanov-Takens bifurcation of codimension 2 was not included in the studies of Seo and Wolkowicz [78] and Xiang et al. [79], we will briefly present the bifurcation for the purpose of completeness.

Theorem 3.3.3. *Suppose*

$$K_2 = \widetilde{K}_2 = \frac{r_2(a+\overline{E})^2(r_2 a + \overline{E}\delta)}{m^2 ac\overline{E}}, \quad r_1 = \widetilde{r}_1 = \frac{K_1(r_2 a + \delta\overline{E})}{\overline{E}(-a - 2\overline{E} + K_1)},$$

$K_1 > a + 2\overline{E}$ *and* $\hat{m}_{20} \neq 0$, $\hat{m}_{11} \neq 0$, *system* (3.1) *localized at* $\overline{S}$ *is topologically equivalent to*

$$\begin{cases} \dot{x} &= y, \\ \dot{y} &= sgn(\hat{m}_{20})x^2 + sgn(\hat{m}_{11})xy + O(|x,y|^3). \end{cases} \tag{3.24}$$

Proof. Firstly, we bring the co-existence equilibrium point $\overline{S}$ to the origin by the translation [136, 137] $X = E - \overline{E}, Y = M - \overline{M}$ and we obtain

$$\begin{pmatrix} \dot{X} \\ \\ \dot{Y} \end{pmatrix} = J(\overline{S}) \begin{pmatrix} X \\ \\ Y \end{pmatrix} + \begin{pmatrix} l_{20}X^2 + l_{11}XY + l_{21}X^2Y + l_{30}X^3 \\ \\ m_{20}X^2 + m_{11}XY + m_{02}Y^2 + m_{21}X^2Y + m_{30}X^3 \end{pmatrix} + O(|X,Y|^4), \tag{3.25}$$

where

$$J(\overline{S}) = \begin{pmatrix} l_{10} & l_{01} \\ \\ l_{10} & l_{01} \end{pmatrix}, \quad l_{10} = \frac{\widetilde{r}_1\overline{E}(K_1 - a - 2\overline{E})}{K_1(a+\overline{E})}, \quad l_{01} = -\frac{m\overline{E}}{a+\overline{E}},$$
$$m_{10} = \frac{\widetilde{K}_2 acm(r_2 a + \delta\overline{E})}{r_2(a+\overline{E})^3}, \quad m_{01} = -\frac{r_2 a + \delta\overline{E}}{a+\overline{E}}, \quad l_{11} = -\frac{m\overline{E}}{(a+\overline{E})^2},$$
$$l_{20} = -\frac{\widetilde{r}_1(\overline{E}^2 + 3a\overline{E} + a^2 - K_1 a)}{K_1(a+\overline{E})^2}, \quad l_{21} = \frac{am}{(a+\overline{E})^3}, \quad l_{30} = \frac{\widetilde{r}_1 a(\overline{E} - K_1)}{K_1(a+\overline{E})^3},$$
$$m_{11} = \frac{acm}{(a+\overline{E})^2}, \quad m_{20} = -\frac{\widetilde{K}_2 acm(r_2 a + \delta\overline{E})}{r_2(a+\overline{E})^4}, \quad m_{02} = -\frac{r_2}{\widetilde{K}_2},$$
$$m_{21} = -\frac{acm}{(a+\overline{E})^3}, \quad m_{30} = \frac{\widetilde{K}_2 acm(r_2 a + \delta\overline{E})}{r_2(a+\overline{E})^5}.$$

Then under following transformation

$$\begin{pmatrix} X \\ \\ Y \end{pmatrix} = \widetilde{P} \begin{pmatrix} x \\ \\ y \end{pmatrix}, \quad \widetilde{P} = (\widetilde{V}_1, \widetilde{V}_2),$$

where

$$\widetilde{V}_1 = \begin{pmatrix} 1 \\ \\ k_1 \end{pmatrix}, \quad \widetilde{V}_2 = \begin{pmatrix} \frac{1}{P(\overline{E})k_1} \\ \\ 0 \end{pmatrix},$$

and $|\widetilde{P}| \neq 0$, then we have

$$\begin{cases} \dot{x} &= y + \bar{l}_{20}x^2 + \bar{l}_{11}xy + \bar{l}_{02}y^2 + O(|x,y|^3), \\ \\ \dot{y} &= \overline{m}_{20}x^2 + \overline{m}_{11}xy + \overline{m}_{02}y^2 + O(|x,y|^3), \end{cases} \tag{3.26}$$

where

$$\bar{l}_{20} = -\frac{r_2 a + \delta\overline{E}}{(a+\overline{E})^2}, \quad \bar{l}_{11} = \frac{acm - 2r_2 a - 2\delta\overline{E}}{(r_2 a + \delta\overline{E})(a+\overline{E})}, \quad \bar{l}_{02} = -\frac{1}{r_2 a + \delta\overline{E}},$$
$$\overline{m}_{20} = \frac{(K_1 - 2a - 3\overline{E})(r_2 a + \delta\overline{E})^2}{(a+\overline{E})^3(K_1 - a - 2\overline{E})}, \quad \overline{m}_{02} = \frac{(K_1 - a - 3\overline{E})}{\overline{E}(K_1 - a - 2\overline{E})},$$
$$\overline{m}_{11} = \frac{-6\delta\overline{E}^3 + [2K_1\delta - 4a(3r_2 + cm)]\overline{E}^2 + r_2 a(3K_1 - 7a)\overline{E} + r_2 a^2(K_1 - a)}{\overline{E}(-a - 2\overline{E} + K_1)(a+\overline{E})^2}.$$

Then we use the following near-identity transformation

$$u = x, \quad v = y + \bar{l}_{20}x^2 + \bar{l}_{11}xy + \bar{l}_{02}y^2 + O(|x,y|^3),$$

and if we change u, v into x, y, we obtain

$$\begin{cases} \dot{x} &= y, \\ \dot{y} &= \hat{m}_{20}x^2 + \hat{m}_{11}xy + O(|x,y|^3), \end{cases} \tag{3.27}$$

where

$$\hat{m}_{20} = \overline{m}_{20} = \frac{(K_1 - 2a - 3\overline{E})(r_2 a + \delta\overline{E})^2}{(a+\overline{E})^3(K_1 - a - 2\overline{E})},$$
$$\hat{m}_{11} = \overline{m}_{11} + 2\bar{l}_{20} = \frac{-2\delta\overline{E}^2 - 4r_2 a\overline{E} - r_2 a(K_1 - a)}{\overline{E}(a+\overline{E})(K_1 - a - 2\overline{E})}.$$

If $\hat{m}_{20} \neq 0$ ($K_1 \neq \frac{K_1 - 2a}{3}$) and $\hat{m}_{11} \neq 0$, and we make a rescaling of coordinates and time by

$$X = \frac{\hat{m}_{20}}{\hat{m}_{11}^2}x, \quad Y = \frac{\hat{m}_{20}^2}{\hat{m}_{11}^3}y, \quad \tau = \frac{\hat{m}_{11}}{\hat{m}_{20}}t,$$

and rewrite X, Y, τ into x, y, t, the system (3.27) is topologically equivalent to system (3.24). Also, we can verify that $\hat{m}_{20} = 0$ when $\overline{S} = S_{123}$. We will discuss it in details in the section 3.3.4. □

And if $T^{'}(J(\overline{S})) = 0$, we have

$$K_1 = \frac{2\delta\overline{E}^2 + r_2 a(4\overline{E} + a)}{r_2 a}. \tag{3.28}$$

When K_1, K_2, r_1 satisfy the condition in theorem 3.3.3 and 3.28, we can verify that

$$\hat{m}_{11} = 0, \;\; \hat{m}_{20} = \frac{(r_2 a + \delta\overline{E})(2\delta\overline{E}^2 + r_2 a\overline{E} - r_2 a^2)}{2\overline{E}(a + \overline{E})^3} \neq 0.$$

Hence, $\overline{S}$ is a cusp point at least codimension 3. To determine its codimension, we need to calculate the coefficient of $x^3 y$ term in the normal form 3.24. We will not do the computation here as Xiang et al. [79] showed that the existence of cusp type Bogdanov-Takens bifurcation of codimension 3.

3.3.4 Bifurcations for the nilpotent singularity

Though the relative bifurcations called focus and elliptic type of BT bifurcation of codimension 3 were carried out in Xiang et al. [79], we present the analysis of bifurcations for the nilpotent singularity followed the terms and classification given by Dumortier et al. [127] and in Zhu and Rousseau [128], to find the organizing center for the system (3.1). Also, we present the bifurcation diagram near the focus and elliptic type of nilpotent singularity of codimension 3 based on the analysis of Dumortier et al. [127], which is not included in Seo and Wolkowicz [78] and Xiang et al. [79].

It follows from the Prop. 3.2.1 and 3.3.1 and the discussion about Hopf bifurcations, a straightforward calculation can conclude that the system (3.1) has a unique positive

equilibrium S_{123} which can now be written and denoted as $S^* = (E^*, M^*)$ with

$$E^* = \frac{a(2cm - r_2)}{\delta}, \quad M^* = \frac{12mc^2a}{2cm - r_2},$$

if

$$K_1 = K_1^* = \frac{a(8cm - r_2)}{\delta}, \quad K_2 = K_2^* = \frac{18r_2ac^2m}{(2cm - r_2)\delta}, \quad r_1 = r_1^* = \frac{2\delta(8cm - r_2)}{3(2cm - r_2)}. \tag{3.29}$$

Theorem 3.3.4. *For system* (3.1) *with all positive parameters and* (K_1, K_2, r_1) *satisfying* (3.29)*, the equilibrium* $S^*(E^*, M^*)$ *is a nilpotent singularity of codimension at least 3, and the system* (3.1) *localized at* S^* *is topologically equivalent to*

$$\begin{cases} \dot{x} &= y, \\ \dot{y} &= -x^3 + bxy - x^2y + y^2Q_{12}(x, y), \end{cases} \tag{3.30}$$

where $b = \frac{7r_2 - 8cm}{2(2cm - r_2)}$.

Furthermore, if we fix the parameters a, c, m*, and depending on the value of* r_2*, we have*

(1) When $\frac{24\sqrt{2}-8}{17}cm < r_2 < 2cm$*,* S^* *is a codimension 3 nilpotent sigularity of elliptic type.*

(2) When $0 < r_2 < \frac{8}{7}cm$*,* $\frac{8}{7}cm < r_2 < \frac{24\sqrt{2}-8}{17}cm$*,* S^* *is a nilpotent singularity of the focus type of codimension 3.*

(3) when $r_2 = \frac{8}{7}cm$ *or* $\frac{24\sqrt{2}-8}{17}cm$*, the equilibrium* S^* *is nilpotent point of codimension* ≥ 4*.*

Proof. Firstly, we translate the degenerate equilibrium S^* to the origin by $X = E - E^*$, $Y = M - M^*$ and expand system (3.1) in the neighborhood of the new origin, we will have

$$\begin{pmatrix} \dot{X} \\ \dot{Y} \end{pmatrix} = J(S^*) \begin{pmatrix} X \\ Y \end{pmatrix} + \begin{pmatrix} a_{20}X^2 + a_{11}XY + a_{21}X^2Y + a_{30}X^3 \\ b_{20}X^2 + b_{11}XY + b_{02}Y^2 + b_{21}X^2Y + b_{30}X^3 \end{pmatrix} + Q_1(X, Y), \tag{3.31}$$

where $Q_1(X, Y) = O(|X, Y|^4)$ and

$$J(S^*) = \begin{pmatrix} a_{10} & a_{01} \\ b_{10} & b_{01} \end{pmatrix}, \quad a_{10} = \frac{2\delta}{3}, \quad a_{01} = \frac{(-2cm + r_2)}{3c}, \quad b_{10} = \frac{4c\delta^2}{3(2cm - r_2)},$$
$$b_{01} = -\frac{2\delta}{3}, \quad a_{11} = -\frac{\delta^2}{9amc^2}, \quad a_{20} = \frac{-2(cm - 2r_2)\delta^2}{9mca(2cm - r_2)}, \quad a_{21} = \frac{\delta^3}{27a^2m^2c^3},$$
$$a_{30} = -\frac{4\delta^4}{27a^2c^2m^2(2cm - r_2)}, \quad b_{11} = \frac{(\delta^2}{9acm}, \quad b_{20} = -\frac{4\delta^3}{9am(2cm - r_2)},$$
$$b_{02} = -\frac{(2cm - r_2)\delta}{18amc^2}, \quad b_{21} = -\frac{\delta^3}{27a^2c^2m^2}, \quad b_{30} = \frac{4\delta^4}{27a^2cm^2(2cm - r_2)}.$$

Next we transform the linear part of the system (3.31) to the Jordan canonical form and find that $J(S^*)$ is nilpotent. Note that the generalized eigenvectors associated with the zero eigenvalues are $V_1 = (\frac{2cm - r_2}{2c}, \delta)'$, $V_2 = (0, -\frac{3}{2})'$ which satisfy $J(S^*)V_1 = 0, J(S^*)V_2 = V_1$. Let $P = (V_1, V_2)$, then under the non-singular linear transformation

$$\begin{pmatrix} X \\ Y \end{pmatrix} = P \begin{pmatrix} x \\ y \end{pmatrix},$$

with $|P| = -\frac{3(2cm-r_2)}{4c} < 0$, system (3.31) becomes

$$\begin{cases} \dot{x} &= y + \widetilde{a}_{20}x^2 + \widetilde{a}_{30}x^3 + y(\widetilde{a}_{11}x + \widetilde{a}_{21}x^2) + \widetilde{Q}_{11}(x,y), \\ \dot{y} &= \widetilde{b}_{30}x^3 + y(\widetilde{b}_{11}x + \widetilde{b}_{21}x^2) + \widetilde{b}_{02}y^2 + \widetilde{Q}_{12}(x,y), \end{cases} \tag{3.32}$$

where $\widetilde{Q}_{1i}(x,y) = O(|x,y|^4)$, $(i = 1, 2)$, and

$$\begin{aligned} &\widetilde{a}_{20} = \frac{-2c^3m^3 - 3c^2m^2r_2 + r_2^3}{9ac^2m}, \quad \widetilde{a}_{30} = -\frac{\delta^4(2cm - r_2)}{54a^2c^4m^2}, \quad \widetilde{a}_{11} = \frac{\delta^2}{6ac^2m}, \\ &\widetilde{a}_{21} = -\frac{\delta^3(2cm - r_2)}{36a^2c^4m^2}, \quad \widetilde{b}_{30} = -\frac{\delta^4(4cm + r_2)(2cm - r_2)}{162a^2c^4m^2}, \\ &\widetilde{b}_{11} = \frac{r_2\delta^2}{6ac^2m}, \quad \widetilde{b}_{21} = -\frac{\delta^3(4cm + r_2)(2cm - r_2)}{108a^2c^4m^2}, \quad \widetilde{b}_{02} = \frac{\delta(2cm - r_2)}{12ac^2m}. \end{aligned}$$

Thirdly, we use the following near-identity transformation

$$u = x, \quad v = y + \widetilde{a}_{20}x^2 + \widetilde{a}_{30}x^3 + y(\widetilde{a}_{11}x + \widetilde{a}_{21}x^2) + \widetilde{Q}_{11}(x,y)$$

and if we change u, v into x, y, we obtain

$$\begin{cases} \dot{x} &= y, \\ \dot{y} &= -\hat{b}_{30}x^3 + y(\hat{b}_{11}x - \hat{b}_{21}x^2) + y^2\hat{Q}_{12}(x,y), \end{cases} \tag{3.33}$$

where

$$\hat{b}_{30} = \frac{\delta^4(2cm - r_2)^2}{81a^2c^4m^2}, \ \hat{b}_{11} = -\frac{\delta^2(8cm - 7r_2)}{18ac^2m}, \ \hat{b}_{21} = \frac{\delta^3(2cm - r_2)(4cm + 7r_2)}{108a^2c^4m^2}.$$

If we make a rescaling of coordinates and time by

$$X = \frac{\hat{b}_{21}}{\sqrt{\hat{b}_{30}}}x, \quad Y = \frac{\hat{b}_{21}^2}{\hat{b}_{30}^{\frac{3}{2}}}y, \quad \tau = \frac{\hat{b}_{30}}{\hat{b}_{21}}t$$

and rewrite X, Y, τ into x, y, t, system (4.35) becomes

$$\begin{cases} \dot{x} &= y, \\ \dot{y} &= -x^3 + bxy - x^2y + y^2Q_{12}(x,y), \end{cases} \tag{3.34}$$

where $b = \frac{7r_2 - 8cm}{2(2cm - r_2)}$.

It follows from the classification criteria for the nilpotent singularity in [127, 128], we have that if $\frac{24\sqrt{2}-8}{17}cm < r_2 < 2cm$, then $b > 2\sqrt{2}$, S^* is a nilpotent elliptic point of codimension 3. It is a nilpotent point of focus type of codimension 3 when $0 < b < 2\sqrt{2}$ or $(\frac{8}{7}cm < r_2 < \frac{24\sqrt{2}-8}{17}cm)$. If $r_2 = \frac{8}{7}cm$ $(b = 0)$ or $r_2 = \frac{24\sqrt{2}-8}{17}cm$ $(b = 2\sqrt{2})$, it is a nilpotent singularity of codimension ≥ 4. □

In Figure 3.5, we simulate and present the 3 types of nilpotent singularity classified in Theorem 3.3.4 with parameters selected for each of the cases. Figure 3.5(a) and 3.5(b) represent the two cases of nilpotent focus, nilpotent elliptic point of codimension 3 is presented in Figure 3.5(c), and the most degenerate case of nilpotent focus of codimension 4 is presented in Figure 3.5(d)).

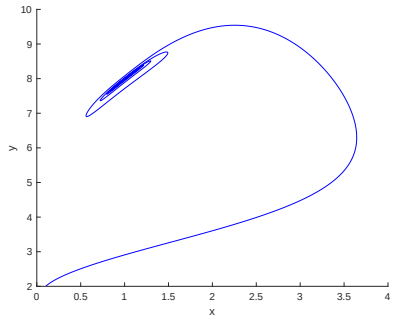

(a) Nilpotent focus($b < 0$)

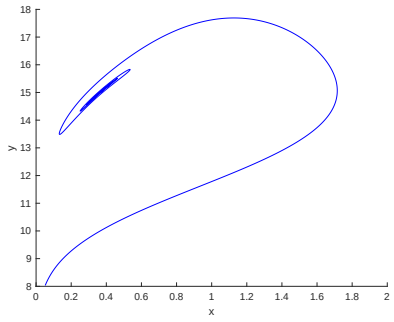

(b) Nilpotent focus($0 < b < 2\sqrt{2}$)

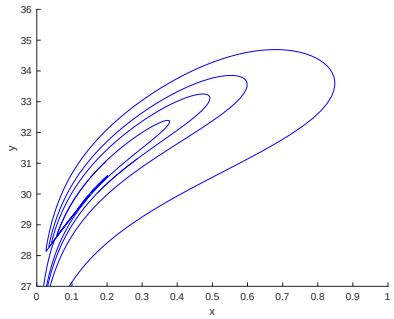

(c) Nilpotent elliptic point ($b > 2\sqrt{2}$)

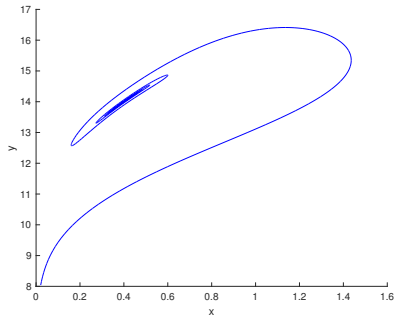

(d) Nilpotent point of codimension at least 4

Figure 3.5: The phase portrait of different type of nilpotent singularity when fixed $a = 1, c = 1, m = 1$. (a) Nilpotent focus of codimension 3 ($b < 0$): $r_2 = 0.5$, $K_1 = 5, K_2 = 4, r_1 = 5$; (b) Nilpotent focus of codimension 3 ($0 < b < 2\sqrt{2}$): $r_2 = 1.2$, $K_1 = 3.0909, K_2 = 12.2727, r_1 = 12.4667$; (c) Nilpotent elliptic point of codimension 3 ($b > 2\sqrt{2}$): $r_2 = 1.6$, $K_1 = 2.3333, K_2 = 27.6923, r_1 = 27.7334$; (d) Nilpotent focus of codimension 4 ($b = 0$), $r_2 = \frac{8}{7}$,$K_1 = 3.2, K_2 = 11.2, r_1 = \frac{80}{7}$.

It is worth pointing out that the most degenerate case occurs when $r_2 = \frac{8}{7}cm$, and

then the system (3.1) localized at S^* is topologically equivalent to

$$\begin{cases} \dot{x} &= y, \\ \dot{y} &= -x^3 - x^2 y. \end{cases} \tag{3.35}$$

System (3.35) is the 3-jet of nilpotent focus of codimension 4. This is also the cubic Liénard equations. In the work of Khibnik et al. [130], they called it doubly degenerate Bogdanov-Takens point with no quadratic terms in the normal form. There are different type of unfolding of this nilpotent singularity of codimension 4, which is analyzed by the Dangelmayr and Guckenheimer (1987) [129] and Khibnik et al. (1998) [130]. From their analysis, we can obtain that three different types of codimension 3 bifurcation, Cusp type Bogdanov-Takens bifurcations of codimension 3, focus type and elliptic type of nilpotent singularity of codimension 3 can bifurcate from this nilpotent singularity of codimension 4. This nilpotent focus of codimension 4 serves as an organizing center for the complex dynamics of the system (3.1).

We summary the above bifurcation analysis in the table 3.1.

As in the available bifurcation studies [78, 79, 76] where K_1 and K_2 were commonly used as bifurcation parameters, here we will add r_1 as the third parameter, namely we will study system (3.1) for parameters (K_1, K_2, r_1) in a neighborhood of (K_1^*, K_2^*, r_1^*) to explore the complex dynamics which can be bifurcated from the codimension 3 nilpotent singularity S^*.

Table 3.1: The summary of different type of bifurcations in system (3.1)

Conditions	Types of bifurcation	codimension
Pest free equilibrium $S_{01}(0, K_1)$,		
$K_2 = \frac{r_1 a}{m}$;	Saddle-node	1
$K_2 = \frac{r_1 a}{m}$, $K_1 = \frac{r_2 a}{r_2 - cm}(r_2 > cm)$;	Saddle-node	2
Coexistence equilibrium $\overline{S}(\overline{E}, \overline{M})$,		
$U(\overline{E}) = 0, k_1 = k_2, T(J(\overline{S}))) \neq 0$;	Saddle-node	1
$U(\overline{E}) = 0, k_1 = k_2, U''(\overline{E}) = 0, T(J(\overline{S})) \neq 0$;	Saddle-node	2
$U(\overline{E}) = 0, T(J(\overline{S})) = 0, D(J(\overline{S})) > 0$;	Hopf	≥ 1
$U(\overline{E}) = 0, k_1 = k_2, T(J(\overline{S})) = 0$;	Bogdanov-Takens	2
$U(\overline{E}) = 0, k_1 = k_2, T(J(\overline{S})) = 0, T'(J(\overline{S})) = 0$;	Cusp type Bogdanov-Takens	3
$U(\overline{E}) = 0, k_1 = k_2, U''(\overline{E}) = 0, T(J(\overline{S})) = 0$,	Nilpotent singularity	≥ 3
$r_2 \in (\frac{24\sqrt{2}-8}{17}cm, 2cm)$;	Elliptic type	3
$r_2 \in (0, \frac{8}{7}cm) \cup (\frac{8}{7}cm, \frac{24\sqrt{2}-8}{17}cm)$;	Focus type	3
$r_2 = \frac{8}{7}cm$;	Focus type	4
$r_2 = \frac{24\sqrt{2}-8}{17}cm$;	Elliptic type	≥ 4

Let

$$K_1 = K_1^* + \epsilon_1,\ K_2 = K_2^* + \epsilon_2,\ r_1 = r_1^* + \epsilon_3,$$

where $\epsilon = (\epsilon_1, \epsilon_2, \epsilon_3)$ and $|\epsilon|$ is sufficiently small. Then we will study the bifurcation of the following unfolding system

$$\begin{cases} \dfrac{dE}{dt} &= (r_1^* + \epsilon_3)\, E\left(1 - \dfrac{E}{K_1^* + \epsilon_1}\right) - \dfrac{mEM}{a+E}, \\ \dfrac{dM}{dt} &= r_2 M\left(1 - \dfrac{M}{K_2^* + \epsilon_2}\right) + \dfrac{cmEM}{a+E}. \end{cases} \tag{3.36}$$

Theorem 3.3.5. *For parameters $|\epsilon|$ sufficiently small and any other positive parameters a, c, m, system* (3.36) *is a generic unfolding of the codimension 3 nilpotent singularity of elliptic type when $\frac{24\sqrt{2}-8}{17}cm < r_2 < 2cm$, of focus type when $0 < r_2 < \frac{8}{7}cm$ and $\frac{8}{7}cm < r_2 < \frac{24\sqrt{2}-8}{17}cm$.*

Proof. It has been shown by Dumortier et al. [127] that a generic unfolding with the parameters (μ_1, μ_2, μ_3), of codimension 3 nilpotent singularity is C^∞ equivalent to

$$\begin{cases} \dot{x} &= y, \\ \dot{y} &= \mu_1 + \mu_2 x - x^3 + y(\mu_3 + bx - x^2 + O(x^3)) + y^2 Q(x,y). \end{cases} \tag{3.37}$$

We will show that system (3.36), with parameters $\epsilon = (\epsilon_1, \epsilon_2, \epsilon_3)$, is also a generic unfolding of codimension 3 singularity by showing that there exist smooth coordinate change which take (3.36) into (3.37) with $\frac{D(\mu_1,\mu_2,\mu_3)}{D(\epsilon_1,\epsilon_2,\epsilon_3)}|_{\epsilon=(0,0,0)} \neq 0$.

When $\epsilon = 0$, the system (3.1) has a nilpotent equilibrium $S^*(E^*, M^*)$. Let $x =$

$E - E^*$, $y = M - M^*$. When $|\epsilon|$ is sufficient small, the system (3.36) becomes

$$\begin{cases} \dot{x} &= L_{11}(x) + yL_{12}(x), \\ \dot{y} &= L_{21}(x) + yL_{22}(x) + Q_2 y^2, \end{cases} \tag{3.38}$$

where

$$\begin{aligned} L_{11}(x) =& \frac{a(2cm - r_2)\big(2\delta^2\epsilon_1 + 18acm\epsilon_3 + 3\delta\epsilon_1\epsilon_3\big)}{3\delta\big(\epsilon_1\delta + a(8cm - r_2)\big)} \\ &+ \frac{6\delta^2\epsilon_1 + 3a(4cm + r_2)\epsilon_3 + 3\delta\epsilon_1\epsilon_3 + 2a\delta(8cm - r_2)}{3\big(\epsilon_1\delta + a(8cm - r_2)\big)}x \\ &+ \frac{4\delta^4\epsilon_1 - 9acm(2cm - r_2)\delta\epsilon_3 - 2a\delta^2(8cm - r_2)(cm - 2r_2)}{9acm(2cm - r_2)\big(\epsilon_1\delta + a(8cm - r_2)\big)}x^2 \\ &- \frac{4\delta^4}{27a^2c^2m^2(2cm - r_2)}x^3 + O(x^4), \end{aligned}$$

$$\begin{aligned} L_{12}(x) =& -\frac{2cm - r_2}{3c} - \frac{\delta^2}{9ac^2m}x + \frac{\delta^3}{27a^2c^3m^2}x^2 - \frac{\delta^4}{81a^3c^4m^3}x^3 + O(x^4), \\ L_{21}(x) =& \frac{8ac^2m\delta^2\epsilon_2}{18ac^2mr_2 + (2cm - r_2)\delta\epsilon_2} + \frac{4c\delta^2}{3(2cm - r_2)}x - \frac{4\delta^3}{9am(2cm - r_2)}x^2 \\ &+ \frac{4\delta^4}{27a^2cm^2(2cm - r_2)}x^3 + O(x^4), \\ L_{22}(x) =& \frac{-36ac^2mr_2\delta + 2(2cm - r_2)\delta^2\epsilon_2}{54ac^2mr_2 + 3(2cm - r_2)\delta\epsilon_2} + \frac{\delta^2}{9acm}x + \frac{-\delta^3}{27a^2c^2m^2}x^2 \\ &+ \frac{\delta^4}{81a^3c^4m^3}x^3 + O(x^4), \\ Q_2 =& \frac{-r_2(2cm - r_2)\delta}{18ac^2mr_2 + (2cm - r_2)\delta\epsilon_2}. \end{aligned}$$

Then, we make the following transformation

$$x_1 = x, \quad y_1 = L_{11}(x) + yL_{12}(x).$$

System (3.38) can be transformed into

$$\begin{cases} \dot{x_1} &= y_1, \\ \dot{y_1} &= \overline{L}_{21}(x_1) + y_1\overline{L}_{21}(x_1) + y_1^2\overline{Q}_2(x_1), \end{cases} \tag{3.39}$$

where

$$\begin{aligned} \overline{L}_{21}(x_1) =& d_{00} + d_{10}x_1 + d_{20}x_1^2 + d_{30}x_1^3 + O(x_1^4), \\ \overline{L}_{22}(x_1) =& d_{01} + d_{11}x_1 + d_{21}x_1^2 + d_{31}x_1^3 + O(x_1^4), \end{aligned}$$

with

$$\begin{aligned} d_{00} =& \frac{4(2cm - r_2)\delta^2}{27cr_2(8cm - r_2)} \left[3cr_2\epsilon_1 - (8cm - r_2)\epsilon_2 + \frac{27ac^2mr_2}{\delta^2}\epsilon_3 + O(|\epsilon|^2)\right], \\ d_{10} =& \frac{2\delta^3}{27acmr_2(8cm - r_2)}\Big[r_2(14cm - r_2)\epsilon_1 - 2m(8cm - r_2)\epsilon_2 + \frac{54ac^2m^2r_2}{\delta^2}\epsilon_3 \\ & + O(|\epsilon|^2)\Big], \\ d_{20} =& \frac{\delta^4(2cm - r_2)^2}{81a^2c^3m^2r_2(8cm - r_2)(2cm - r_2)}\Big[\frac{2cr_2(26c^2m^2 - 2cmr_2 - r_2^2)}{(2cm - r_2)^2}\epsilon_1 \\ & + (8cm - r_2)\epsilon_2 - \frac{27ac^2mr_2}{\delta^2}\epsilon_3 + O(|\epsilon|^2)\Big], \quad d_{30} = -\frac{4\delta^4}{81a^2c^2m^2} + O(|\epsilon|), \\ d_{01} =& \frac{(2cm - r_2)^2\delta^2}{27ac^2mr_2(8cm - r_2)}\left[\frac{18c^2mr_2}{2cm - r_2}\epsilon_1 + (8cm - r_2)\epsilon_2 - \frac{27ac^2mr_2}{\delta^2}\epsilon_3 + O(|\epsilon|^2)\right], \\ d_{11} =& -\frac{(8cm - 7r_2)\delta^2}{9acm(2cm - r_2)} + O(|\epsilon|), \quad d_{21} = -\frac{(4cm + 7r_2)\delta^3}{27a^2c^2m^2(2cm - r_2)} + O(|\epsilon|), \\ d_{31} =& -\frac{(8cm + 11r_2)\delta^4}{81a^3c^3m^3(2cm - r_2)} + O(|\epsilon|). \end{aligned}$$

Then, we reduce the $\overline{L}_{21}(x_1)$ to $-x_1^3 + u_2x_1 + u_1$[60]. Note that for ϵ sufficiently small, $d_{30}(\epsilon) = \frac{\partial^3\overline{L}_{21}}{\partial x_1^3}(0) = -\frac{4(cm+r_2)^4}{81a^2c^2m^2} + O(|\epsilon|) \neq 0$, we make the translation

$$x_2 = x_1 + \frac{d_{20}}{3d_{30}}, \quad y_2 = y_1$$

which brings the system into

$$\begin{cases} \dot{x_2} &= y_2, \\ \dot{y_2} &= \widetilde{L}_{21}(x_2) + y_2\widetilde{L}_{22}(x_2) + y_2^2\widetilde{Q}_2(x_2), \end{cases} \tag{3.40}$$

where

$$\begin{aligned} \widetilde{L}_{21}(x_2) =& \widetilde{d}_{00} + \widetilde{d}_{10}x_2 - \widetilde{d}_{30}x_2^3 + O(x_2^4), \\ \widetilde{L}_{22}(x_2) =& \widetilde{d}_{01} + \widetilde{d}_{11}x_2 + \widetilde{d}_{21}x_2^2 + O(x_2^3), \end{aligned}$$

Then, if we rescale y_2 and time t using

$$x_3 = x_2, \quad y_3 = \frac{y_2}{\sqrt{\widetilde{d}_{30}}}, \quad \widetilde{t} = \sqrt{\widetilde{d}_{30}}t$$

the coefficient of x_3^3 becomes $1 + O(|\epsilon_2|)$. We have

$$\begin{cases} \dot{x_3} &= y_3, \\ \dot{y_3} &= \widetilde{\widetilde{L}}_{21}(x_3) + y_3\widetilde{\widetilde{L}}_{22}(x_3) + y_3^2\widetilde{\widetilde{Q}}_2(x_3), \end{cases} \tag{3.41}$$

where

$$\begin{aligned} \widetilde{\widetilde{L}}_{21}(x_3) =& \widetilde{\widetilde{d}}_{00} + \widetilde{\widetilde{d}}_{10}x_3 - x_3^3 + O(x_3^4), \\ \widetilde{\widetilde{L}}_{22}(x_3) =& \widetilde{\widetilde{d}}_{01} + \widetilde{\widetilde{d}}_{11}x_3 - \widetilde{\widetilde{d}}_{21}x_3^2 + O(x_3^3), \end{aligned}$$

with

$$\widetilde{\widetilde{d}}_{00} = \frac{3a^2cm^2(2cm-r_2)}{r_2(8cm-r_2)\delta^2}\left[3cr_2\epsilon_1-(8cm-r_2)\epsilon_2+\frac{27ac^2mr_2}{\delta^2}\epsilon_3+O(|\epsilon|^2)\right],$$

$$\widetilde{\widetilde{d}}_{10} = \frac{3acm}{2r_2(8cm-r_2)\delta}\Big[r_2(14cm-r_2)\epsilon_1-2m(8cm-r_2)\epsilon_2+\frac{54ac^2m^2r_2}{\delta^2}\epsilon_3$$
$$+O(|\epsilon|^2)\Big],$$

$$\widetilde{\widetilde{d}}_{01} = \frac{1}{24cr_2(8cm-r_2)}\Big[-\frac{2cr_2(64c^3m^3-54c^2m^2r_2-30cmr_2^2+7r_2^3)}{(2cm-r_2)^2}\epsilon_1$$
$$+(8cm-r_2)^2\epsilon_2-\frac{27ac^2mr_2^2}{\delta^2}\epsilon_3+O(|\epsilon|^2)\Big],$$

$$\widetilde{\widetilde{d}}_{11} = \frac{7r_2-8cm}{2(2cm-r_2)}+O(|\epsilon|), \quad \widetilde{\widetilde{d}}_{21} = \frac{(4cm+7r_2)\delta}{6acm(2cm-r_2)}+O(|\epsilon|).$$

Using the Malgrange preparation theorem, we can reduce the $\widetilde{\widetilde{L}}_{21}(x_3)$ to $\widetilde{\widetilde{d}}_{00}+\widetilde{\widetilde{d}}_{10}x_3-x_3^3$.

For system (3.41), $\widetilde{\widetilde{d}}_{21}(0) = \frac{(4cm+7r_2)\delta}{6acm(2cm-r_2)} > 0$. Thus, we reduce the $\widetilde{\widetilde{L}}_{22}(x_3)$ to $u_3+bx_3-x_3^2+O(x_3^3)$ by rescaling the x_3, y_3, $\widetilde{t}$ using $x_4 = \widetilde{\widetilde{d}}_{21}x_3$, $y_4 = \widetilde{\widetilde{d}}_{21}^2y_3$, $\tau = \frac{1}{\widetilde{\widetilde{d}}_{21}}\widetilde{t}$.

Now if we rewrite x_4 ,y_4 ,τ into x, y, t, then the system becomes

$$\begin{cases} \dot{x} &= y, \\ \dot{y} &= \hat{d}_{00}+\hat{d}_{10}x-x^3+y[\hat{d}_{01}+\hat{d}_{11}x-x^2+O(x^3)]+y^2\hat{Q}_2(x), \end{cases} \tag{3.42}$$

where

$$\hat{d}_{00} = \frac{(4cm+7r_2)^3\delta}{72ac^2mr_2(8cm-r_2)(2cm-r_2)^2}\Big[3cr_2\epsilon_1 - (8cm-r_2)\epsilon_2 + \frac{27ac^2mr_2}{\delta^2}\epsilon_3 + O(|\epsilon|^5)\Big],$$

$$\hat{d}_{10} = \frac{(4cm+7r_2)^2\delta}{36acmr_2(8cm-r_2)(2cm-r_2)^2}\Big[r_2(14cm-r_2)\epsilon_1 - 2m(8cm-r_2)\epsilon_2 + \frac{54ac^2m^2r_2}{(\delta^2}\epsilon_3 \quad + O(|\epsilon|^4)\Big],$$

$$\hat{d}_{01} = \frac{(4cm+7r_2)\delta}{144ac^2mr_2(8cm-r_2)(2cm-r_2)}\Big[(8cm-r_2)^2\epsilon_2 - \frac{27ac^2mr_2^2}{\delta^2}\epsilon_3 - \frac{2cr_2(64c^3m^3-54c^2m^2r_2-30cmr_2^2+7r_2^3)}{(2cm-r_2)^2}\epsilon_1 + O(|\epsilon|^3)\Big],$$

$$\hat{d}_{11} = \frac{7r_2-8cm}{2(2cm-r_2)} + O(|\epsilon|).$$

Then, if we denote $\hat{d}_{00} = \mu_1(\epsilon_1,\epsilon_2,\epsilon_3)$, $\hat{d}_{10} = \mu_2(\epsilon_1,\epsilon_2,\epsilon_3)$, $\hat{d}_{01} = \mu_3(\epsilon_1,\epsilon_2,\epsilon_3)$, $\hat{d}_{11} = b(\epsilon_1,\epsilon_2,\epsilon_3)$, since $r_2 < 2cm$, we can verify that

$$\left|\frac{\partial(\mu_1,\mu_2,\mu_3)}{\partial(\epsilon_1,\epsilon_2,\epsilon_3)}\right|_{\epsilon=0} = \frac{\delta(4cm+7r_2)^6}{2304a^2c^3m^2r_2(8cm-r_2)(2cm-r_2)^4} > 0. \tag{3.43}$$

Thus, the transformation of parameters is nonsingular. The system (3.36) with parameters $\epsilon = (\epsilon_1,\epsilon_2,\epsilon_3)$, is a generic family unfolding the codimension 3 nilpotent singularity. □

3.3.5 Bifurcation diagram

Based on the bifurcation analysis of Dumortier et al. [127], we present the bifurcation diagrams in the following two figures, Figure 3.6 and 3.7. The bifurcation set is a topo-

logical cone with vertex at $0 \in \mathbb{R}^3$, composed of surfaces and lines which are transversal to the spheres $\mathbb{S} = \{(\mu_1, \mu_2, \mu_3 | \mu_1^2 + \mu_2^2 + \mu_3^2) = \sigma^2, 0 < \sigma \ll 1\}$ by removing one point outside the bifurcation set, on the hemisphere $\mu_2 < 0$. The vertical coordinate is μ_3; the horizontal coordinate is μ_1 oriented to the left.

In the bifurcation diagrams shown in Figure 3.6 and 3.7, there are three points labeled as Cusp for cusp point, BT for Bogdanov-Takens point and DH for degenerate Hopf bifurcation point. The bifurcation curves presented include the curves of saddle-node bifurcations (SN), Hopf bifurcations (H), Homoclinic bifurcation (Hom) and saddle-node bifurcation of limit cycles (SN_{lc}).

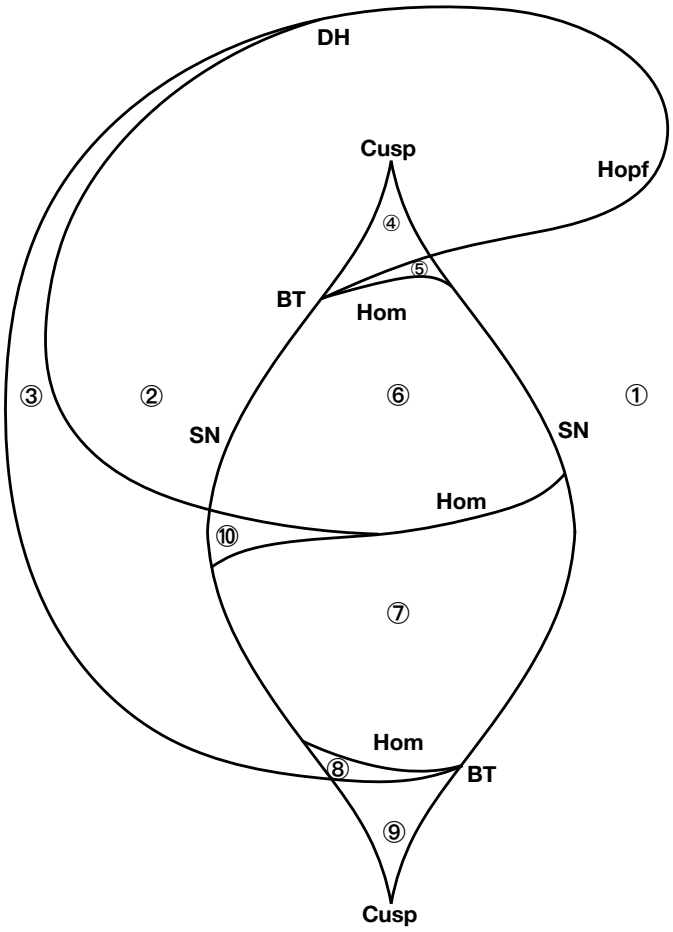

Figure 3.6: The bifurcation diagram of focus type nilpotent singularity of codimension 3.

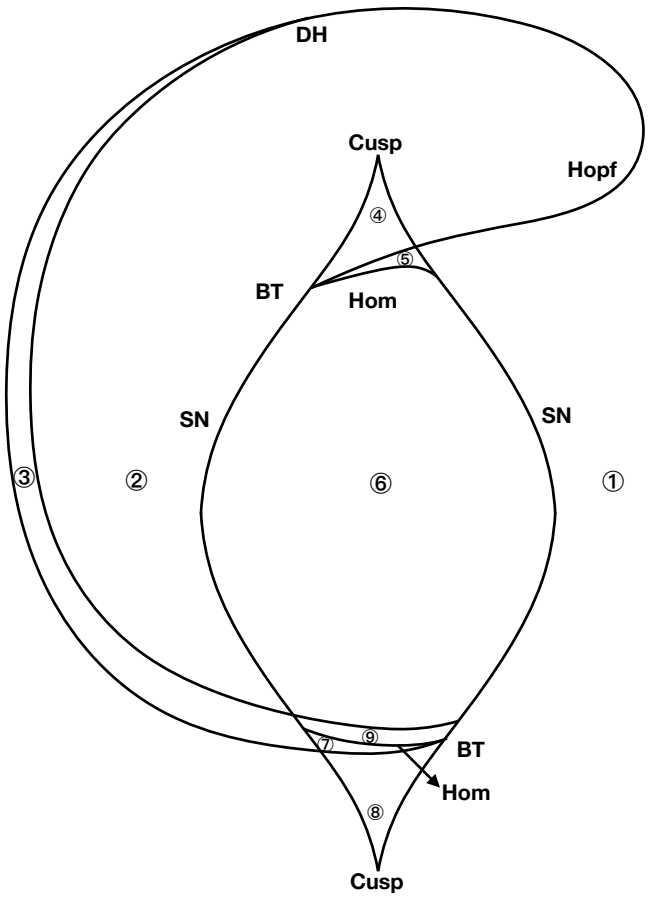

Figure 3.7: The bifurcation diagram of elliptic type nilpotent singularity of codimension 3.

In order to understand the dynamics for the interaction of the two species in different sizes of tea garden, we will numerically investigate and present the bifurcation diagrams in (K_1, K_2) plane with different value of r_1 for both the focus and elliptic cases.

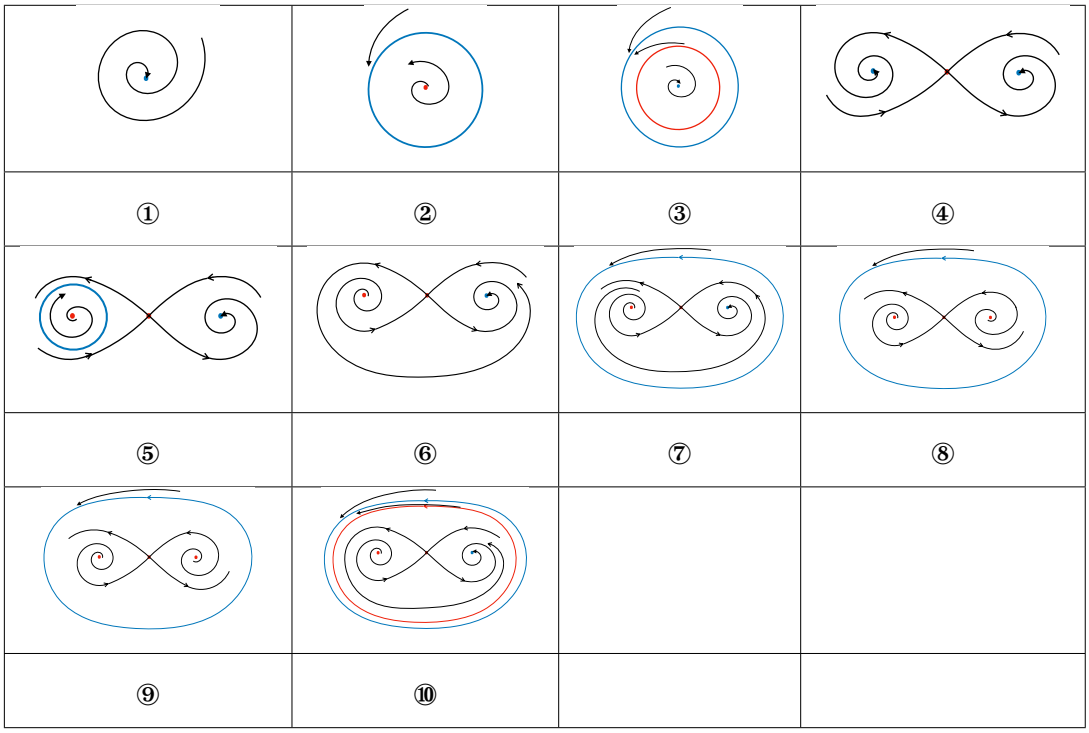

Table 3.2: Collections of phase portraits for the system in the elliptic case when the parameters vary in subregions , referring to Figure 3.6.

Focus type From the Theorem (3.3.4), we know that the nilpotent singularity of codimension 3 is focus type when we fix four parameters $a = 1, c = 1, m = 1$ and $r_2 = 0.5$. Then, we plot the bifurcation diagram in (K_1, K_2) plane with different r_1 by choosing $r_2 = 0.5$. From Figure 3.8(a) - 3.8(e), we can see the changing trend of relative position between the Hopf bifurcation curve and saddle-node bifurcation curve. When r_1 decreases from 6 to 4, the Hopf curve moves toward rightward from the outside of saddle-node bifurcation curve to the inside, without changing the structure in Figure 3.8(a).

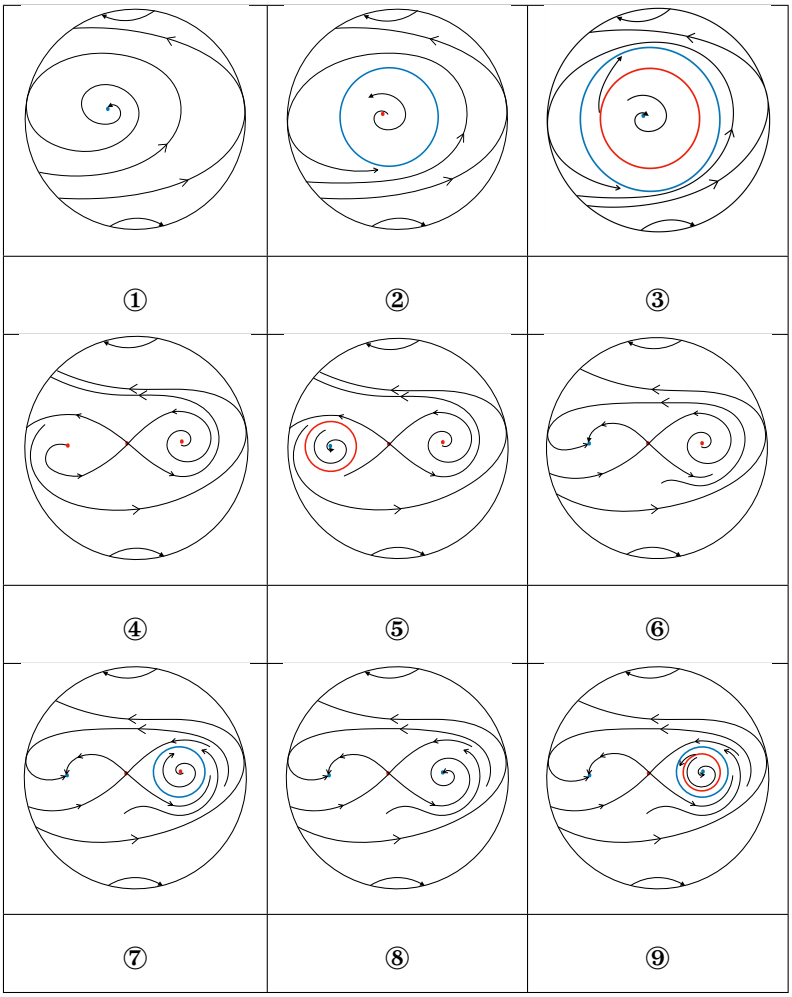

Table 3.3: Collections of phase portraits for the system in the elliptic case when the parameters vary in subregions, referring to Figure 3.7.

When r_1 keeps decreasing, the Hopf bifurcation curve changes the shape as show in Figure 3.8(e).

The saddle-node bifurcation curve is composed of the upper part, the lower part and the intersection point cusp point, while the Bogdanov-Takens point separates the

saddle-node bifurcation curve into two part with stable saddle-node bifurcation curve and unstable bifurcation curve. The Hopf bifurcation curve is tangent to the lower part of saddle-node bifurcation curve in Figure 3.8(e) ($r_1 = 3.5$) and 3.8(d) ($r_1 = 4$), while the Hopf bifurcation curve is tangent to the upper part of saddle-node bifurcation curve in Figure 3.8(a) and 3.8(b) ($r_1 = 6$). In Figure 3.8(c) ($r_1 = 5$), the parameters satisfy the condition (3.29) in Theorem 3.3.4 at which the nilpotent point of codimension 3 occurs when cusp point and Bogdanov-Takens point of codimension 2 coincide. In this case, the Hopf bifurcation curve is tangent to both stable saddle-node bifurcation curve and unstable saddle-node bifurcation curve. Also, the number of degenerate Hopf point is changed from 0 to 2 when r_1 changes from 3.5 to 6 pass through $r_1 = r_1^* = 5$. We simulate the bifurcation curve of saddle-node bifurcation of limit cycle near the degenerate Hopf bifurcation point. In the region c between the bifurcation curve of subcritical Hopf and saddle-node of limit cycle, the system (3.1) can have two limit cycle, one stable and the other is unstable, which is verified by the numerical simulations as whow in Figure 3.12(c).

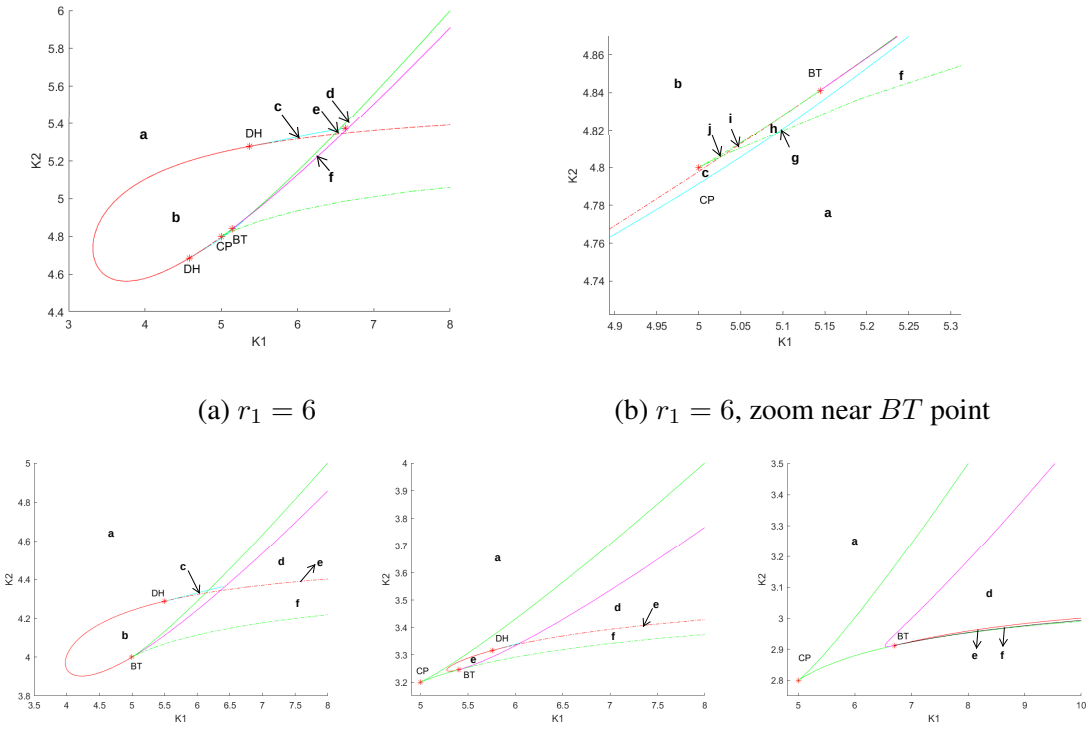

(a) $r_1 = 6$

(b) $r_1 = 6$, zoom near BT point

(c) $r_1 = 5$

(d) $r_1 = 4$

(e) $r_1 = 3.5$

Figure 3.8: Bifurcation diagram for the nilpotent focus of codimension 3 in (K_1, K_2) plane with different r_1 when $a, c, m = 1$ and $r_2 = 0.5$. The green solid and dot lines are the stable and unstable saddle-node bifurcation respectively; red solid and dot line represents the supercritical and subcritical Hopf bifurcation; cyan line stands for the saddle-node of limit cycle; magenta line is neutral saddle curve not the bifurcation curve. DH is the degenerate Hopf point; CP is the cusp point; BT is the Bogdanov-Takens point.

Elliptic type As the same with focus type, we fix four parameters $a = 1, c = 1, m = 1$ and $r_2 = 1.6$, and the nilpotent singularity of codimension 3 is of elliptic type according to the Theorem (3.3.4). Then, we plot the bifurcation diagram in (K_1, K_2) plane with different r_1. Compare to focus type we can see the similar changing trend of relative position between the Hopf bifurcation curve and saddle-node bifurcation curve and the number of degenerate Hopf point, from Figure 3.9(a)- 3.9(e). The Hopf curve moves rightward with decreasing r_1, and it finally changes the shape. However, the most part of parameters are in the region $K_2 > \frac{r_1 a}{m}$ where S_1 is in the negative quadrant in Figure 3.9(d) and Figure 3.9(e). In order to show the moving trend of Hopf curve, we still present the bifurcation diagram which contains the parameters in the region $K_2 > \frac{r_1 a}{m}$.

Another difference is that the Hopf bifurcation curve is tangent to the upper part of saddle-node bifurcation curve when $r_1 < r_1^*$ instead of the lower part of saddle-node bifurcation curve in focus type. Whereas $r_1 > r_1^*$, the Hopf bifurcation curve is tangent to the lower part of saddle-node bifurcation curve. We did not present it in Figure 3.9 due to the redundancy. Also, in elliptic type bifurcation diagram in (K_1, K_2) plane, there are two Bogdanov-Takens points, we omit the one in the region of $K_2 > \frac{r_1 a}{m}$.

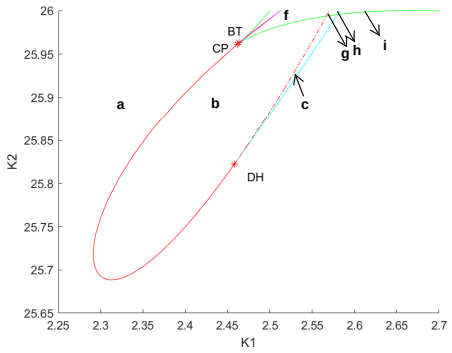

(a) $r_1 = 26$

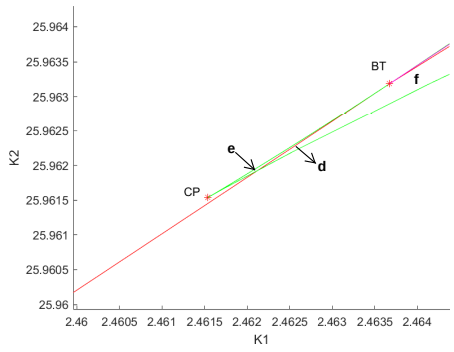

(b) $r_1 = 26$, zoom near BT point

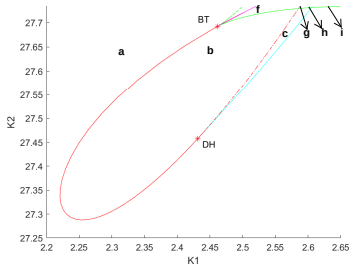

(c) $r_1 = 27.73333334$

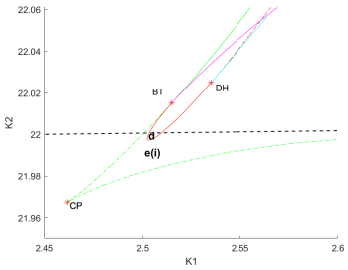

(d) $r_1 = 22$

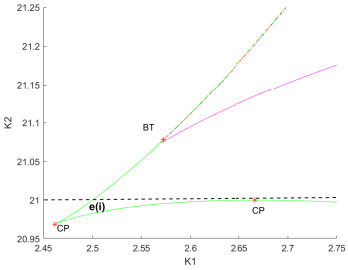

(e) $r_1 = 21$

Figure 3.9: Bifurcation diagram of the codimension 3 nilpotent elliptic point in (K_1, K_2) plane with different r_1 and $a = c = m = 1$, $r_2 = 1.6$. The line colors and points explanation are the same as in Figure 3.8.

Next, we plot the one-parameter bifurcation diagram to explain the model dynamics. First, we present bifurcation diagram in (E, K_1) plane with different K_2 as shown in Figure 3.10 and bifurcation diagram in (E, K_2) plane with different K_1 as shown in Figure 3.11. In general, reducing the carrying capacity of *E. onukii* population in the tea

plantation to a certain low level, the low level of *E. onukii* population state can be stable under different carrying capacities of *A. baccarum*, and pest suppression is possible. With the decreasing of carrying capacity of *E. onukii*, one can see that the system may go through a stable state of high *E. onukii* to the gradual excitation of oscillations around the unique equilibrium, and a stable state of low *E. onukii* (Figure 3.10(a)). For an environment that is not suitable for *E. onukii*, the pest *E. onukii* can be effectively controlled, yet this may not always work. For some level of the capacity for *A. baccarum*, the *E. onukii* population can still outbreak even though the capacity of *E. onukii* is reduced when the initial capacity of *E. onukii* is relatively high (Figure 3.10(b) - Figure 3.10(f)). Also, the initial condition plays an important role. Different initial states can lead to different equilibrium states, low level of *E. onukii* or the large-amplitude oscillation of *E. onukii* population (Figure 3.10(f)).

When we fixed the carrying capacity of *E. onukii*, increasing the capacity of *A. baccarum* may be effective to control *E. onukii* (Figure 3.11(d), Figure 3.11(h)). However, in other cases, increasing the capacity of *A. baccarum* may not be effective from the beginning. On the contrary, it may induce a large amplitude oscillation of *E. onukii* population. Small increases in the carrying capacity of *A. baccarum* may lead to an opposite effect. The initial state of the *E. onukii* is also important for the pest control (Figure 3.11(d)).

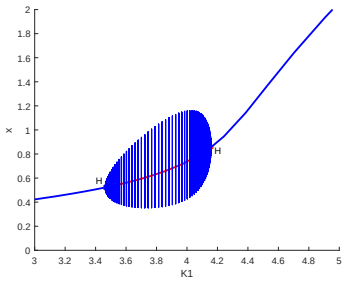

(a) $K_2 = 4.6$

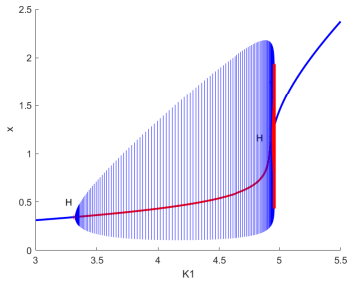

(b) $K_2 = 4.78$

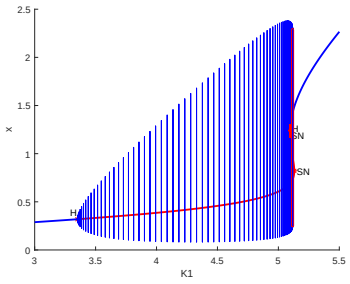

(c) $K_2 = 4.826$

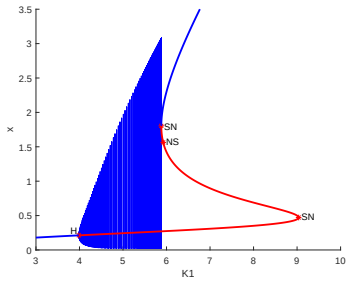

(d) $K_2 = 5.1$

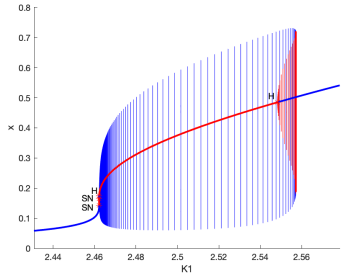

(e) $K_2 = 25.962$

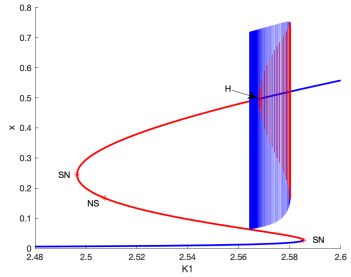

(f) $K_2 = 25.996$

Figure 3.10: Bifurcation diagrams in (E, K_1) plane shown different scenarios of changing K_2. We fixed $a = 1, c = 1, m = 1$, and (a)-(d) $r_2 = 0.5, r_1 = 6$ (focus type), (e)-(f) $r_2 = 1.6, r_1 = 26$ (elliptic type). H is the Hopf point; SN is the saddle node; NS is the neutral saddle point. The blue and red color represent the equilibrium is stable and unstable, respectively.

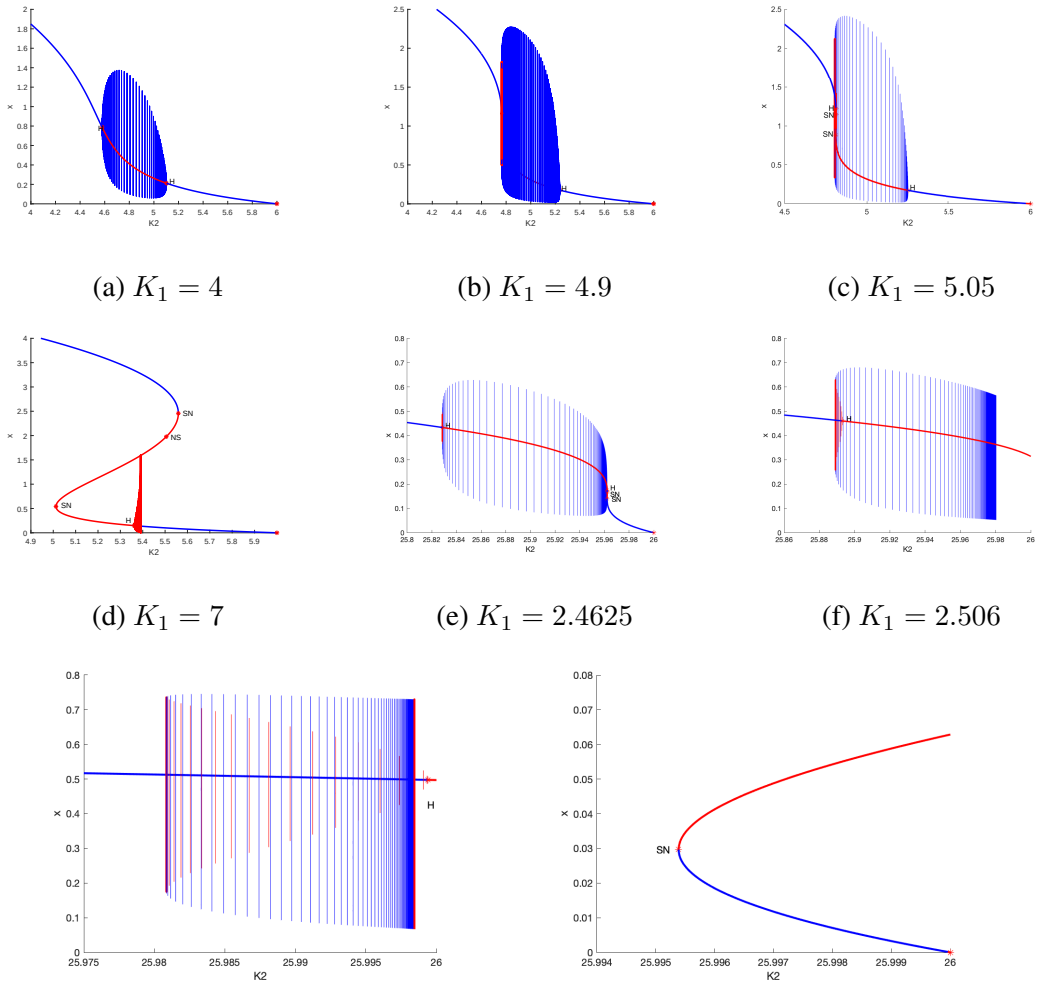

(a) $K_1 = 4$ (b) $K_1 = 4.9$ (c) $K_1 = 5.05$

(d) $K_1 = 7$ (e) $K_1 = 2.4625$ (f) $K_1 = 2.506$

(g) $K_1 = 2.57$ (h) $K_1 = 2.58$

Figure 3.11: Bifurcation diagram in (E, K_2) plane with different K_1. We fixed $a = 1, c = 1, m = 1$, and (a)-(d) $r_2 = 0.5, r_1 = 6$ (focus type), (e)-(h) $r_2 = 1.6, r_1 = 26$ (elliptic type). H is the Hopf point; SN is the saddle node; NS is the neutral saddle point. The blue and red color represent the equilibrium is stable and unstable, respectively. Note that we did not present the cases of elliptic type which is similar to focus type due to redundancy.

3.4 Numerical simulations and existence of three limit cycles

In this section, we will carry out numerical simulations and plot phase portraits by choosing different parameter values in the subregion of bifurcation diagram to explain the complexity of the dynamics.

Focus type When the parameters (K_1, K_2) in region from a to j in Figure 3.8, all the phase portraits are presented in Figure 3.12. It contains all the possible solutions of system (3.1) when the nilpotent singularity of codimension 3 is of focus type.

In the case 3.12(a) to 3.12(c) , the system has one unique positive equilibrium, and it goes through from a stable node to an unstable node through a Hopf bifurcation, then becomes a stable node again. The system (3.1) has three equilibria in case 3.12(d) to 3.12(j) which happens when the parameter (K_1, K_2) are in the inside of saddle-node bifurcation curve. The S_3 is always stable while S_1 changes from stable node to unstable node through a Hopf bifurcation as shown in the case 3.12(d) to 3.12(f). In the case 3.12(h) to 3.12(j) , S_1 is always an unstable node while S_3 goes through stable node to unsatble node, and the system always has a large amplitude stable limit cycle outside the three equilibrium points.

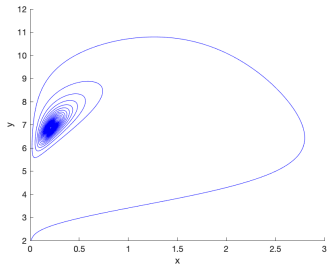

(a) $K_1 = 3.9, K_2 = 5.1$ (①)

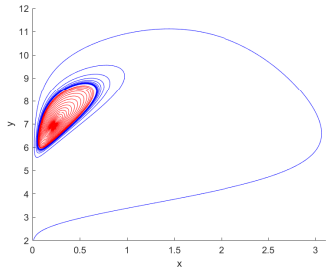

(b) $K_1 = 4.2, K_2 = 5.1$ (②)

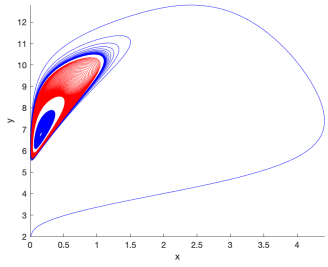

(c) $K_1 = 5.713, K_2 = 5.303$ (③)

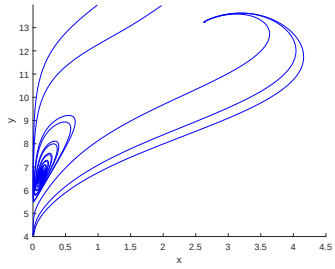

(d) $K_1 = 6.7, K_2 = 5.4$ (④)

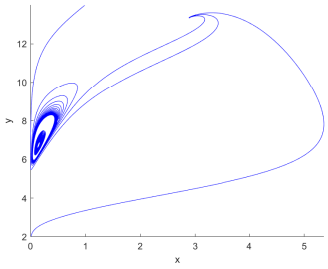

(e) $K_1 = 6.74, K_2 = 5.36$ (⑤)

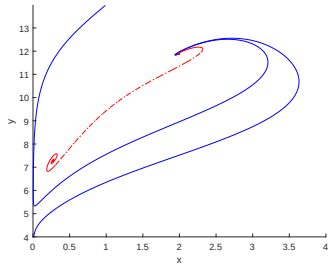

(f) $K_1 = 5.9, K_2 = 5.1$ (⑥)

Figure 3.12: The phase portrait of system (3.1) with a nilpotent singularity of focus type. Here when fixed $r_2 = 0.5, r_1 = 6$ in the generic regions of parameters (K_1, K_2). The regions $(a)-(j)$ correspond to the regions of bifurcation diagram in Figure 3.8. The blue line represents that the solution is stable, while the red line stands for unstable solution. Also, we use red dot line to clarify the situation that S_1 is unstable and S_3 is stable.

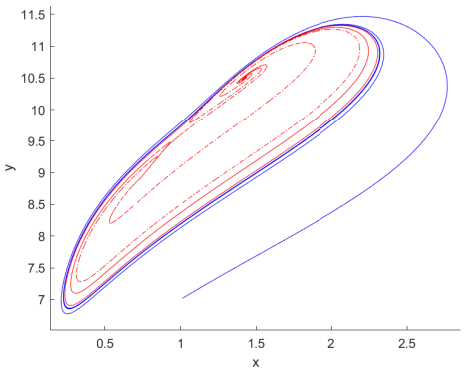

(g) $K_1 = 5.116, K_2 = 4.826$ (⑦)

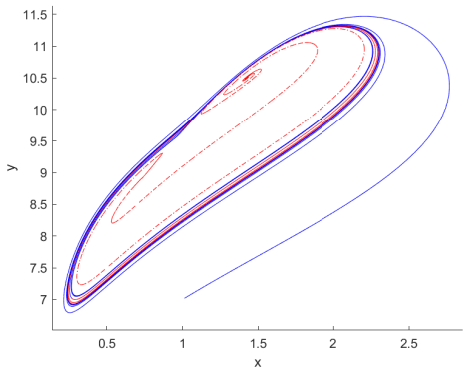

(h) $K_1 = 5.117, K_2 = 4.826$ (⑩)

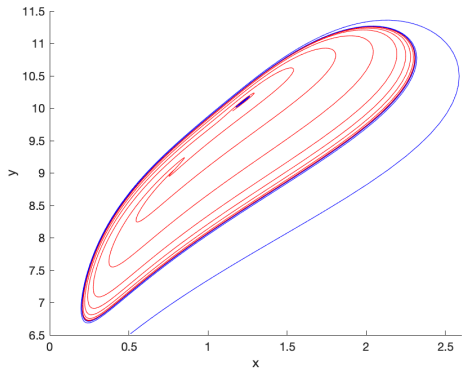

(i) $K_1 = 5.05, K_2 = 4.8125$ (⑧)

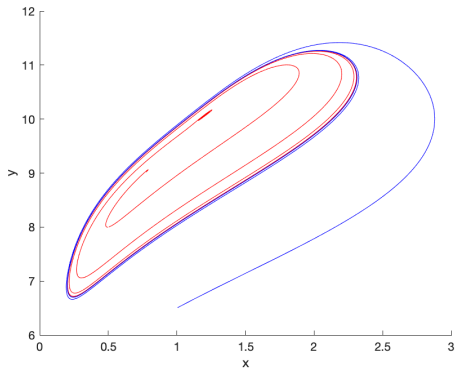

(j) $K_1 = 5.05, K_2 = 4.8128$ (⑨)

Figure 3.12: (Continued) The phase portrait of system (3.1) with a nilpotent singularity of focus type. Here when fixed $r_2 = 0.5, r_1 = 6$ in the generic regions of parameters (K_1, K_2). The regions $(a) - (j)$ correspond to the regions of bifurcation diagram in Figure 3.8. The blue line represents that the solution is stable, while the red line stands for unstable solution. Also, we use red dot line to clarify the situation that S_1 is unstable and S_3 is stable.

Elliptic type For system (3.1) with a nilpotent singularity of elliptic type, we present the phase portraits when the parameters are in the corresponding regions from a to i in Figure 3.9. In the case 3.13(a) to 3.13(c), the phase portrait of the system shows the same structure as in focus type.

The system has one unique positive equilibrium, and it has one stable limit cycle in Figure 3.13(b) and two limit cycles in Figure 3.13(c). The system (3.1) has three equilibria in the case 3.13(d) to 3.13(i) which happens when the parameter (K_1, K_2) are in the inside of saddle-node bifurcation curve. The S_1 is always stable while S_3 changes from a stable node to an unstable node through a Hopf bifurcation, then to a stable node again in the case 3.13(e) to 3.13(i). But we did not find the large amplitude stable limit cycle outside the three equilibrium points in the elliptic type, which also proved in the studies of Dumortier et al. [127].

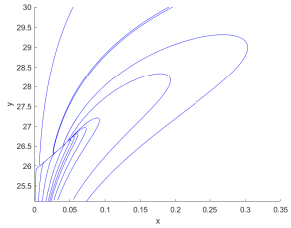

(a) $K_1 = 2.1, K_2 = 25.89$ (①)

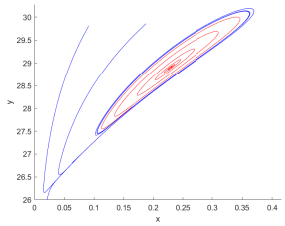

(b) $K_1 = 2.4, K_2 = 25.89$ (②)

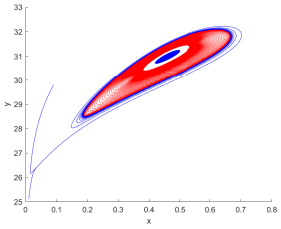

(c) $K_1 = 2.506, K_2 = 25.892$ (③)

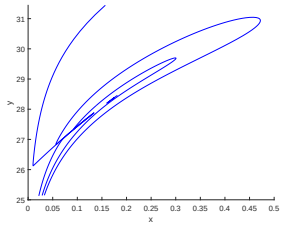

(d) $K_1 = 2.46219, K_2 = 25.962$(⑧)

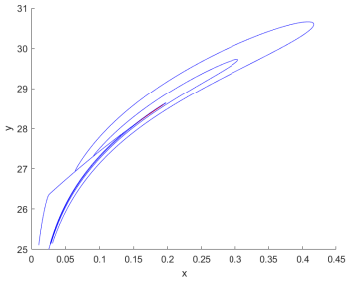

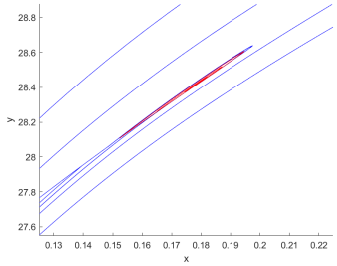

(e) $K_1 = 2.4625, K_2 = 25.9622$(⑦)

Figure 3.13: The phase portrait of system (3.1) with a nilpotent elliptic singularity when fixed $r_2 = 1.6, r_1 = 26$ in the generic regions of parameters (K_1, K_2). The regions $(a) - (i)$ are correspond to the regions of bifurcation diagram in Figure 3.9. The blue line represents that the solution is stable, while the red line stands for unstable solution. Also, we use red dot line to clarify the situation that S_1 is stable and S_3 is unstable. In case (e) and (i), the S_1 and S_3 are stable.

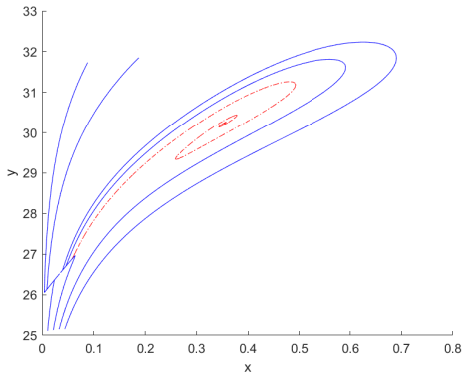

(f) $K_1 = 2.506, K_2 = 25.985$ (⑥)

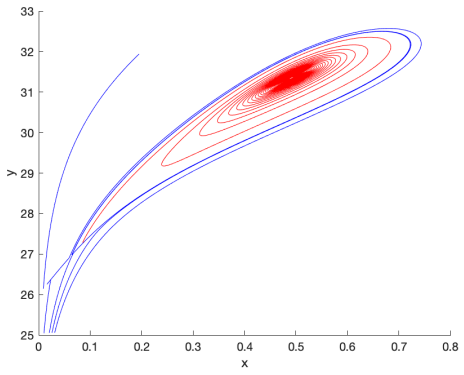

(g) $K_1 = 2.5655, K_2 = 25.996$ (⑦)

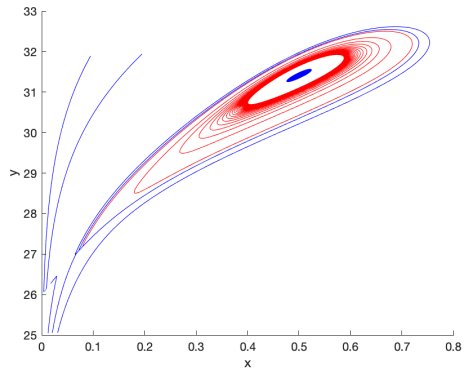

(h) $K_1 = 2.57, K_2 = 25.996$ (⑨)

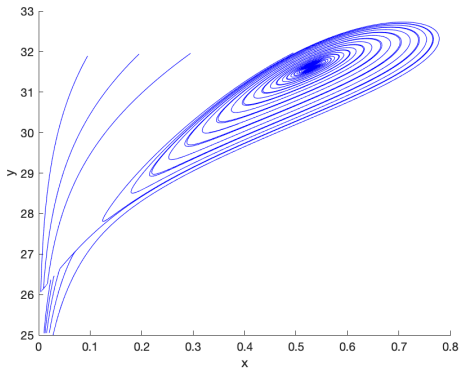

(i) $K_1 = 2.585, K_2 = 25.996$ (⑧)

Figure 3.13: (Continued) The phase portrait of system (3.1) with a nilpotent elliptic singularity when fixed $r_2 = 1.6, r_1 = 26$ in the generic regions of parameters (K_1, K_2). The regions $(a) - (i)$ are correspond to the regions of bifurcation diagram in Figure 3.9. The blue line represents that the solution is stable, while the red line stands for unstable solution. Also, we use red dot line to clarify the situation that S_1 is stable and S_3 is unstable. In case (e) and (i), the S_1 and S_3 are stable.

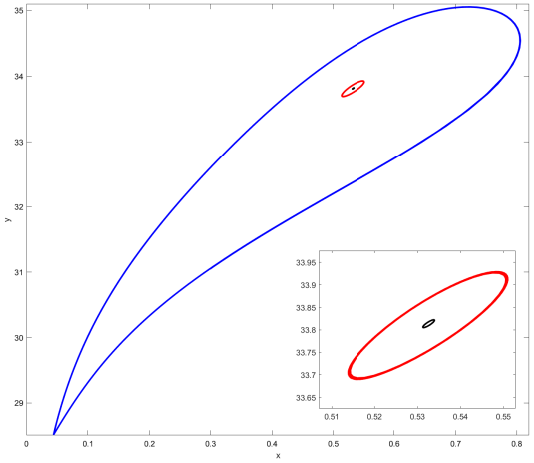

(a) Phase portrait of 3 limit cycles

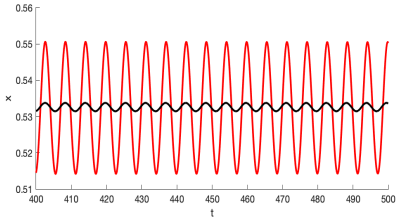

(b) 2 limit cycles with small amplitude

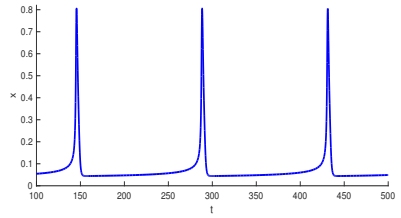

(c) 1 limit cycle with large amplitude

Figure 3.14: The most special case that the system have three limit cycles when $K_1 = 2.5868, K_2 = 27.78, r_1 = 27.783333334$, and $r_2 = 1.6, a = 1, c = 1, m = 1$. The initial conditions for solution curves in black, red and blue are $(x_0, y_0) = (0.5316, 33.81)$; $(0.5164, 33.69)$ and $(x_0, y_0) = (0.2931, 31.01)$, respectively.

Three limit cycles in the system with singularity of elliptic type We want to point out is that we find a special case that for the system (3.1) with a nilpotent elliptic equilibrium, the system can have three distinct limit cycles when $K_1 = 2.5868, K_2 = 27.78, r_1 = 27.78333334$, $r_2 = 1.6$, $a = 1$, $c = 1$, $m = 1$, a case corresponds to the region c in Figure 3.9(c). The largest limit cycle shows that the slow-fast pattern. And the period is around 150 days which is close to the life span of the *A. baccarum* (81-114

days [27], varied with local climate).

This case of three limit cycles may occur in parameters between the homoclinic bifurcation and the limit point of limit cycle bifurcation, a case similar to Shan et. al (2016) [137], where they numerically showed the existence of the three limit cycles when the system has three positive equilibrium in the most degenerate case of nilpotent singularity. The existence of three limit cycles also is presented in the global analysis of the cubic Liénard equation in Khibnik et al. (1998) [130]. Also, the number of limit cycle in system (3.1) may be at least 4 when consider the bifurcation of the most degenerate case $r_2 = \frac{8}{7}cm$, the nilpotent focus of codimension 4 [130]. As for the exact number of limit cycles which can be bifurcated from the nilpotent focus of codimension 4 in the system, it still remains an open problem which is associated with the bifurcation of a Liénard systems and even with the famous Hilbert sixteenth problem for planar polynomial systems. This existence of three limit cycles also manifests that the complexity of the dynamics of the generalist predator *A. baccarum* and prey *E. onukii* in tea plantation can be much more complicated with bi-stability and even tri-stability.

3.5 Conclusion and discussion

In this chapter, we establish a predator-prey model for the tea green leafhopper pest *E. onukii* and their predatory mite *A. baccarum* as a generalist predator. The euryphagous nature is crucial for the predator to survival in nature, and it is a very important character-

istic of the species which leads to easier coexistence of the two species. The look-simple two dimension model exhibits very complex dynamics. Through bifurcation analysis, we have shown that there can be different equilibrium states (see Figs. 3.12 and 3.13) when the parameters vary in tea plantations, and the associated bifurcations and dynamics of these equilibria reveal the possible scenarios.

The eradication of the pest *E. onukii* is difficult. Even though when the carrying capacity of the predatory mite *A. baccarum* is high enough ($K_2 > \frac{r_1 a}{m}$), the pest-free equilibrium is locally stable. But it still exists the stable equilibrium state of high *E. onukii* population. The pest eradication also depends on the initial condition of *E. onukii* population, as observed in Seo and Wolkowicz (2020) [78]. Hence, it is plausible to suppress the pest rather than eradicate it. The analysis of the coexistence equilibrium is also crucial for the pest suppression strategy.

It turns out that the co-existence of these two species is always possible. We can classify the phase portraits of the system (3.1) when (K_1, K_2) is in different regions while r_1 is varied. By the local stability and bifurcation analysis of all the equilibrium states, we summarize the different possible types equilibrium state in Table 3.4, varying from single equilibrium, single limit cycle, two equilibria, two equilibria and limit cycle, equilibrium and limit cycle with the number of 1 , 2, even 3. And it may have more types of coexistence state when the growth rate of generalist predator (r_2) varied. There are many different combinations and types of coexistence of the two species *E. onukii*

and *A. baccarum* when the external condition changes. Also, it is possible to have a stable coexistence of *E. onukii* and *A. baccarum* in different states for the same external conditions.

Table 3.4: The classification of the phase portraits of the system (3.1) with a nilpotent singularity

	Equilibrium state	Focus type	Elliptic type
Monostablity	Single equilibrium	Figure 3.12(a), 3.12(f)	Figure 3.13(a), 3.13(f)
	Single limit cycle	Figure 3.12(b), 3.12(j) (surrounding 3 singularity)	Figure 3.13(b)
Bistability	Two stable equilbria	Figure 3.12(d)	Figure 3.13(d), 3.13(i)
	Equilibrium and 1 limit cycle	Figure 3.12(e), 3.12(g) (surrounding 3 singularity)	Figure 3.13(e), 3.13(g)
	Equilibrium and 2 limit cycles	Figure 3.12(c), 3.12(h) (2 surrounding 3 singularity), Figure 3.12(i) (1 surrounding 3 singularity)	Figure 3.13(c)
	Equilibrium and 3 limit cycles		Figure 3.14
Tristability	Two stable equilibria and 2 limit cycles		Figure 3.13(h)

Mathematically there are several different types of multi-stability. When the parameters are all fixed, the system can have two stable fixed points, a stable fixed point and a

stable limit cycle, two stable fixed point and a stable limit cycle, a stable fixed point and two stable limit cycles. Also, biologically the behavior of the system is much different in the case of two stable equilibria, equilibrium and a limit cycle. This result is different from the finding of Colling et.al (1990) [138] due to the existence of a large amplitude periodic solution in our model. Moreover, the phenomenon is much more complicated with the *A. baccarum* as a generalist predator. The phenomenon of two different stable states has been well studied [49, 138], however, as far as we know that it is not common to see the existence of three different stable states, or triple-stability in a biological system. When the reproduction rate r_2 varies in the interval $\frac{24\sqrt{2}-8}{17}cm < r_2 < 2cm$, the system can have three different stable states for the same parameters, two stable fixed point and one stable limit cycle (Figure 3.15).

As we described in the introduction, the different phenomena are observed in the field study. Hence, it is possible that there are different coexistence states of *A. baccarum* and *E. onukii* in different levels of population sizes. In addition to the growth and development rules of *A. baccarum* itself, the extensive appetite of *A. baccarum* may generate that there are a variety of possible coexistence phenomena between *A. baccarum* and *E. onukii*, which may correspond to many stable states presented in the model.

We claim that S_1 is the equilibrium with low *E. onukii* and low *A. baccarum* population, while S_3 is the equilibrium with high *E. onukii* and high *A. baccarum* population. The multistability allows the system to model the *E. onukii* population outbreak in re-

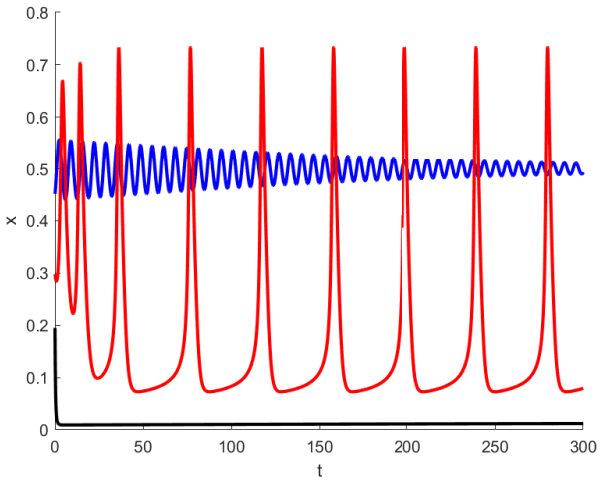

(a) The trajectory of x with respect to time t

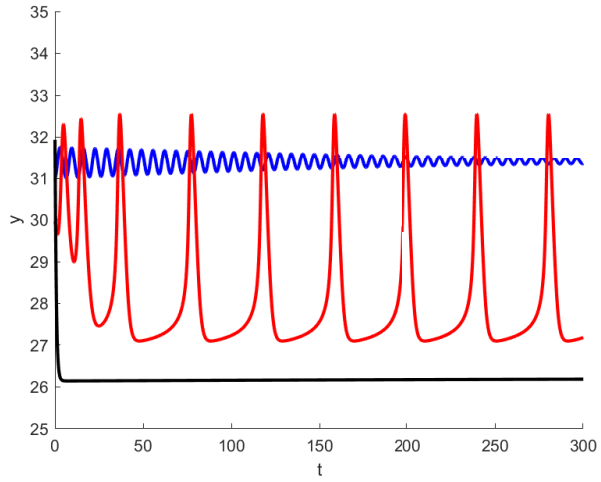

(b) The trajectory of y with respect to time t

Figure 3.15: The different stable states under different initial condition with parameter fixed at $K_1 = 2.57, K_2 = 25.996, r_1 = 26, r_2 = 1.6, a = 1, c = 1, m = 1$. The black line: $(x_0, y_0) = (0.2, 32)$; the red line: $(x_0, y_0) = (0.3, 30)$; the blue line: $(x_0, y_0) = (0.45, 31)$.

sponse to population perturbations, like the increase in predator by artificially releasing or the deceasing caused by the pesticide. If the populations are at a stable state with high *E. onukii* and high *A. baccarum* population, the population perturbations will force the populations to move to the state with low *E. onukii* and low *A. baccarum* population. The release of predator and the application of pesticide can effectively take control of *E. onukii* population. However, it can also cause the populations to jump to the oscillations that the *A. baccarum* can not effectively control *E. onukii*. Even worse, the population perturbations may lead the populations to move from low *E. onukii* and *A. baccarum* population to high *E. onukii* and *A. baccarum* population, which make the problem worse. But the introduction of *A. baccarum* always reduces the abundance of *E. onukii* below the carrying capacity and may have some effects on pest suppression.

Referring to different tea plantations, where K_1, K_2 and r_1 are all fixed, the system may have different biological behaviors as different growth rates of *A. baccarum* (r_2). Increasing r_2 may also be helpful to control *E. onukii*. Mathematically, different r_2 manifests themselves as different types of degenerate singularities, the focus type and the elliptic type and more degenerate focus case. With the increase of r_2, the type of degenerate equilibrium changes from the focus ($0 < r_2 < \frac{8}{7}cm, \frac{8}{7}cm < r_2 < \frac{24\sqrt{2}-8}{17}cm$) to elliptic ($\frac{24\sqrt{2}-8}{17}cm, 2cm$), and the large amplitude oscillation of *E. onukii* population may disappear. We may observe the slow-fast oscillation of *E. onukii* population. When the growth rate of *A. baccarum* is relatively high, the abundance of *E. onukii* may maintain

a low level the most of time. Even though when the *E. onukii* increase significantly in a short time, the *A. baccarum* will increase fast and then control the *E. onukii* (Figure 3.14). This shows the possibility of pest suppression by using the generalist predatory mite, *A. baccarum*.

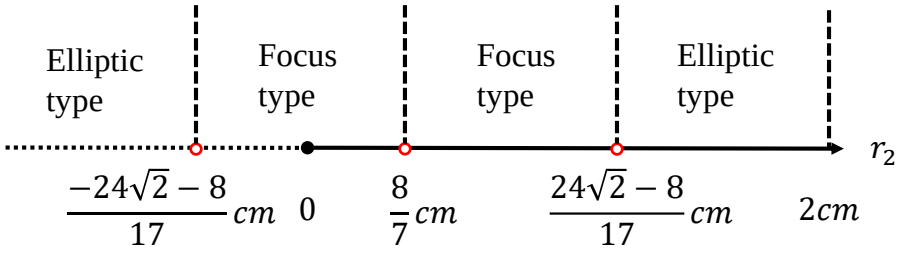

Figure 3.16: The type of nilpotent singularity when r_2 varied.

Also, we notice that our analysis can extend to when the predator is a specialist predator with intraspecific competition, the system (3.3) ($r_2 < 0$, Figure 3.16). All types of coexistence states analyzed in our study can also occur between specialist predators and prey. Competition within the predator may be more conducive to the coexistence of predator and prey.

In this chapter, we close by noting that the dynamical behavior of this generalist predator-prey system is complicated. We analyze the change of dynamics using four different parameters. The nilpotent focus of of codimension 4 serves as an organizing center for the complex dynamics of the model. We find that it can have three limit cycles around one of the positive equilibrium and even 4 limit cycles. Moreover, various coexistence phenomena can happen. Not only the bistability, but also the tri-stability can

happen too.

4 The dynamics of predatory mite and the pest leafhopper with stage structure

This work has been conducted in collaboration with Dr. Zhu, H. I have collaborated in constructing the models, theoretical analyses and numerical simulations.

4.1 Introduction

The control of *E. onukii* by natural enemies has been an important topic as seen in our fields studies [121, 122]. In chapter 3, we analyze the dynamics of the two-dimensional predator-prey model with a generalist predator, *A. baccarum*. As presented in chapter 3, Seo and Wolkowicz [78] and Xiang et al. [79], the rich dynamics in the system (3.1) include saddle node bifurcation of codimension 1 and 2, Hopf bifurcation, Bogdanov-Takens bifurcation and bifurcations of nilpotent singularities. And the pest eradication and control using the generalist predator is not easy and need further investigation.

In the natural world, each species usually has its own life cycle with different stages.

The predator adults may have higher predation ability. In comparison, the adults of prey may have a higher ability to avoid predation and the immature pest may be protected by their eggshells. In a tea garden, the development of *A. baccarum* goes through stages of egg, prelarva, larva, nymph and adult. Once they progress to the larvae stage, they become active and can feed on suitable prey [26]. For *E. onukii*, it grows up through the stages of egg, nymph and adult, and the nymph stage is composed of five instars. Eggs are usually laid beneath the phloem of tender tea shoots to avoid natural enemies [139]. Naturally one would hope to build a model to include all stages of the two species. However, it is not easy to deal with the complexity of higher dimension systems with multiple nonlinear interactions across stages.

The predator-prey systems with stage structure for the prey received much attention in recent years and two types of questions were well studied. One is about the permanence of the system, like the periodic predator-prey system with different functional response of Holling type I [140], Holling type II and III [141], Holling type IV [61], Beddington–DeAngelis type [64], Crowley–Martin type [66] and general functional response [142]. The other studies usually focus on the existence and stability of Hopf bifurcations in the systems with stage structure for prey. The periodic phenomena can be observed when incorporating the time delay of birth to maturity about the prey in the predator-prey system with the functional response of Beddington–DeAngelis type [143], Holling type II [144] and Leslie–Gower predator-prey model [145]. The chaotic dynamics were also

observed in a simple predator-prey model with a discrete delay between the capture of the prey and its conversion to viable biomass [146, 147]. Recently, Beay et al. (2020) considered a Rosenzweig-MacArthur specialist predator-prey model with stage-structure in prey that can exhibit Hopf bifurcation [71]. To the best of our knowledge, there are rigorous bifurcation analysis for the generalist predator-prey model with a stage structure yet due to the technical complexity.

The reproduction and development stage contribute most to the adult population of *E. onukii*, and the control of non-adult *E. onukii* is difficult which requires different strategy, hence we choose to start with a simpler case by considering two stages of *E. onukii* first. We will use $E_1(t)$ and $E_2(t)$ to denote the density of eggs and hatched individuals (nymphs and adults) of *E. onukii* at time t respectively. If we still use $M(t)$ to denote the density of *A. baccarum*, then, in a given tea plantation, the assumptions of the two species population are given by following:

(A1) The *E. onukii* eggs population $E_1(t)$. The birth rate of *E. onukii* eggs population is proportional to the existing hatched individuals (nymphs and adults) with a proportionality $r_1 = \overline{r}_1 g_1$, where g_1 is the ratio of adults with spawning ability in the hatched individuals (nymphs and adults) of *E. onukii*. $\overline{r}_1$ is oviposition rate of the adults of *E. onukii* with spawning ability. Also, we neglect the natural death rate by considering the growth rate as the net growth rate. We denote α as the successful hatching rate of *E. onukii* eggs.

(A2) The *E. onukii* hatched individuals (nymphs and adults) population $E_2(t)$. κ_1 is the intra-specific competition rate of the hatched individuals (nymphs and adults) of *E. onukii*. The natural death rate of hatched individuals (nymphs and adults) is neglected.

(A3) The *A. baccarum* population $M(t)$. r_2 is net birth rate of *A. baccarum*, and κ_2 is the intra-specific competition rate of the *A. baccarum* population. *A. baccarum* can prey on hatched individuals (nymphs and adults) of *E. onukii* with the functional response of Holling type II [30]. a is half saturation amount of *A. baccarum*. m is maximum amount of hatched individuals (nymphs and adults) eaten by *A. baccarum*. c is the rate of converting *E. onukii* hatched individuals (nymphs and adults) into *A. baccarum*.

Hence, we build the following system

$$\begin{cases} \dfrac{dE_1}{dt} &= r_1 E_2 - \alpha E_1, \\ \dfrac{dE_2}{dt} &= \alpha E_1 - \kappa_1 E_2^2 - \dfrac{mE_2 M}{a + E_2}, \\ \dfrac{dM}{dt} &= r_2 M - \kappa_2 M^2 + \dfrac{cmE_2 M}{a + E_2}. \end{cases} \tag{4.1}$$

where all the parameters $r_1, r_2, \alpha, \kappa_1, \kappa_2, a, c, m$ are positive.

There are a total of 8 parameters in the model (4.1). If we rescale the state variables

and time by letting

$$E_1(t) = aX_1(t), \quad E_2(t) = aX_2(t), \quad M(t) = acY(t), \quad t = \frac{1}{cm}\tau,$$

and we replace τ with t, and change X_1, X_2, Y into E_1, E_2 and M, then system (4.1) can be rewritten as

$$\begin{cases} \dfrac{dE_1}{dt} &= \hat{r}_1 E_2 - \hat{\alpha} E_1, \\ \dfrac{dE_2}{dt} &= \hat{\alpha} E_1 - \hat{\kappa}_1 E_2^2 - \dfrac{E_2 M}{1+E_2}, \\ \dfrac{dM}{dt} &= \hat{r}_2 M - \hat{\kappa}_2 M^2 + \dfrac{E_2 M}{1+E_2}, \end{cases} \tag{4.2}$$

where $\hat{r}_1 = \frac{r_1}{cm}$, $\hat{r}_2 = \frac{r_2}{cm}$, $\hat{\alpha} = \frac{\alpha}{cm}$, $\hat{\kappa}_1 = \frac{a\kappa_1}{cm}$, and $\hat{\kappa}_2 = \frac{a\kappa_2}{m}$. Hence we have a system with only 5 free parameters. We will select $\alpha, r_1, r_2, \kappa_1, \kappa_2$ as bifurcation parameters, with a focus on α, the hatching rate, to explore the dynamics of the generalist predator-prey model with stage structure of prey.

The model (4.1) exhibits three boundary equilibria and up to three coexistence equilibria. The bifurcation and associated complex dynamics involve the saddle-node bifurcation of codimension 1 and 2, Hopf bifurcation, degenerate Hopf bifurcation, Bogdanov-Takens bifurcation, nilpotent singularities of codimension 3 with focus type, elliptic type and cusp type and their bifurcations. Comparing with the system (3.1), we find that the hatching rate α can be used to organize the bifurcations of the nilpotent singularities of focus, elliptic and cusp type in system (4.1). The periodic oscillation of population can be observed when α varies through some critical value and the amplitude of periodic solution may decrease with a smaller α. This observation will help to identify the time

window for developing a plausible control mechanism for the leafhopper pest *E. onukii* in the tea plantation.

In addition, we summarize the general classification of nilpotent singularity. We follow the terms and classifications given by Dumortier et al. [127] and in Zhu and Rousseau [128], and distinguish the BT point and nilpotent singularity according to the value of quadratic term in the normal form. For the nilpotent singularity S with following normal form

$$\begin{cases} \dot{x} &= y, \\ \dot{y} &= b_{20}x^2 + b_{11}xy + b_{30}x^3 + y^2O(x,y) + O(|x,y|^4). \end{cases} \tag{4.3}$$

- If $b_{20} \neq 0$, $b_{11} \neq 0$, S is a cusp point of codimension 2. The system will undergo the BT bifurcation.

- If $b_{20} \neq 0$, $b_{11} = 0$, S is a cusp point of at least codimension 3. The system will undergo the cusp type BT bifurcation at least codimension 3.

- If $b_{20} = 0$, $b_{30} \neq 0$, $b_{11} \neq 0$, S is a nilpotent singularity of at least codimension 3.

  – if $sign(b_{30}) < 0$,

    (1) when $|b_{11}| > 2\sqrt{2}$, S is a codimension 3 nilpotent sigularity of elliptic type.

    (2) when $0 < |b_{11}| < 2\sqrt{2}$, S is a codimension 3 nilpotent singularity of focus type.

(3) when $b_{11} = \pm 2\sqrt{2}$, S is nilpotent point of elliptic type at least codimension 4.

– if $sign(b_{30}) > 0$, S is codimension 3 nilpotent point of saddle type.

• If $b_{20} = 0$, $b_{30} \neq 0$, $b_{11} = 0$, S is a nilpotent focus of codimension at least 4.

Most importantly, the most degenerate singularity in system (3.1) and (4.1) both have a 3-jet which is C^∞ -equivalent to

$$\begin{cases} \dot{x} &= y, \\ \dot{y} &= -x^3 - x^2 y. \end{cases} \tag{4.4}$$

A candidate for a four-parameter unfolding of (4.4) is

$$\begin{cases} \dot{x} &= y, \\ \dot{y} &= -(x^3 + rx^2 + nx + m) + y(b - x^2), \end{cases} \tag{4.5}$$

which was discussed in Dangelmayr and Guckenheimer (1987) [129]. They considered a two-parameter family of two dimensional slices in the parameter space and observed four type of codimension 3 bifurcations, including the degenerate Takens-Bogdanov bifurcation [129] that is the cusp type of BT bifurcation of codimension 3 analyzed in the Dumortier et al. (1987) [148]. Khibnik et al. (1998) presented another candidate for the universal unfolding of (4.4) [130],

$$\begin{cases} \dot{x} &= y, \\ \dot{y} &= \mu_1 + \mu_2 x + \mu_3 y + \mu_4 xy - x^3 - x^2 y. \end{cases} \tag{4.6}$$

They studied the global bifurcations and the full four-parameter unfolding (4.6) that is analyzed by varying μ_4 in (μ_1, μ_2, μ_3) space. They found that the bifurcation diagram for large μ_4 ($\mu_4 \gg 0$) is the same as for the nilpotent focus [127]. The case of elliptic type nilpotent point was not clear then. Zhu and Rousseau (2002) [128] analyzed the finite cyclicity of the nilpotent singularity of elliptic type, which occurs when $\mu_4 > 2\sqrt{2}$ [127]. Also, there are another two candidates of four-parameter unfolding of (4.4)

$$\begin{cases} \dot{x} &= y, \\ \dot{y} &= \mu_1 + \mu_2 x^2 + \mu_3 y + \mu_4 xy - x^3 - x^2 y, \end{cases} \tag{4.7}$$

$$\begin{cases} \dot{x} &= y, \\ \dot{y} &= \mu_1 + \mu_2 x + \mu_3 x^2 + \mu_4 xy - x^3 - x^2 y. \end{cases} \tag{4.8}$$

One can find that these four different universal unfoldings can be transformed to each other by the appropriate transformation under certain conditions. But the details of the universal unfolding of the codimension 4 nilpotent singularity is not clear yet. In our model, this nilpotent singularity of codimension 4 can serve as the organizing center of complex dynamics of the system.

This chapter is organized as the following. In section 2, we begin our analysis by presenting the existence and types of equilibria and local stability. In section 3, we study the bifurcations and complex dynamics including saddle-node bifurcation, Hopf bifurcations, BT bifurcations, and bifurcations of nilpotent elliptic point and focus of

codimension 3. We give a full classification of the nilpotent singularities and their bifurcations. The selected bifurcation diagram near the nilpotent focus and elliptic point of codimension 3 are discussed. To reveal the impact of stage of *E. onukii*, we will present the dynamics using the hatching rate as parameter. We summarize our results in section 4 and compare the generalist predator prey model with and without stage structure. The importance of stage structure and the possible pest control applications are discussed. Some of the calculations were assisted by the use of Maple [132]. The phase portraits and one and two-parameter bifurcation diagrams were produced by the Matlab [133].

4.2 Equilibrium states and local stability

We will use κ_1 and κ_2 as parameters to discuss the number of non-negative equilibria.

4.2.1 Existence and number of boundary and interior equilibria

One can get the equilibria by setting the right hand sides of system (4.1) equal to zero. It always has a equilibrium point at origin $S_0(0,0,0)$. The system also has a non-negative predator-extinction equilibrium $S_{10}(p_1K_1, K_1, 0)$ with $K_1 = \frac{r_1}{\kappa_1}$, and $p_1 = \frac{r_1}{\alpha}$ that represents the abundance ratio of eggs and hatched individuals (nymphs and adults) of *E. onukii* at equilibrium state. Similarly, the pest-free equilibrium $S_{01}(0,0,K_2)$ exists with $K_2 = \frac{r_2}{\kappa_2}$. Here K_1 and K_2 are referred as the carrying capacity for *E. onukii* hatched individuals (nymphs and adults) and *A. baccarum* respectively for the given tea garden.

For the co-existence equilibrium state $\overline{S}(\overline{E_1}, \overline{E_2}, \overline{M})$, if exists, is the intersection of the following two curves in E_2M subspace

$$\begin{aligned} U_1(E_2) &= \frac{\alpha E_1 - \kappa_1 E_2^2}{E_2} \frac{(a+E_2)}{m}, \\ U_2(E_2) &= \frac{1}{\kappa_2}(r_2 + \frac{cmE_2}{a+E_2}), \end{aligned} \tag{4.9}$$

where $E_1 = p_1 E_2$ and its E_2 coordinate satisfies

$$\begin{aligned} U(E_2) =& E_2^3 - (\frac{r_1}{\kappa_1} - 2a)E_2^2 + \left[a^2 - 2a\frac{r_1}{\kappa_1} + \frac{m(cm+r_2)}{\kappa_1\kappa_2}\right] E_2 \\ &+ \frac{a^2 r_1}{\kappa_1\kappa_2}\left[\frac{mr_2}{ar_1} - \kappa_2\right] = 0. \end{aligned} \tag{4.10}$$

The cubic equation (4.10) has at most 3 positive roots. Note that when

$$\kappa_2 = \overline{\kappa}_2 = \frac{r_2 m}{r_1 a}, \tag{4.11}$$

it has a solution $E_2 = 0$ which is associated with the pest-free equilibrium $S_{01}(0, 0, K_2)$.

Also, if $\kappa_2 < \overline{\kappa}_2$, the equation (4.10) has at most 2 positive roots. Hence, system (4.1) can have up to 6 non-negative equilibria.

To decide the number of positive roots of $U(E_2)$, we calculate its discriminant with respect to E_2. Let Δ_0 be the discriminant, then we have

$$\Delta_0 = \Delta_0(\kappa_2) = \frac{3m^2}{\kappa_1^4\kappa_2^3}[a_2(\kappa_1)\kappa_2^2 + a_1(\kappa_1)\kappa_2 + a_0(\kappa_1)],$$

where

$$a_2(\kappa_1) = 4ac(a\kappa_1 + r_1)^3,$$

$$a_1(\kappa_1) = a^2(8c^2m^2 - 20cmr_2 - r_2^2)\kappa_1^2 - 2ar_1\delta_1(10cm + r_2)\kappa_1 - r_1^2\delta_1^2,$$

$$a_0(\kappa_1) = 4m\delta_1^3\kappa_1,$$

with $\delta_1 = r_2 + cm$. For convenience, we denote

$$f(\kappa_1) = a_2(\kappa_1)\kappa_2^2 + a_1(\kappa_1)\kappa_2 + a_0(\kappa_1),$$

then the real roots of (4.10) is determined by the sign of the function $f(\kappa_1)$. Let $\Delta_1(\kappa_1)$ be the discriminant of $f(\kappa_1)$ with respect to κ_2, then

$$\Delta_1(\kappa_1) = (a\kappa_1 r_2 + r_1\delta_1)(r_1\delta_1 - a\kappa_1\delta_2)^3,$$

with $\delta_2 = 8cm - r_2$. If we denote the unique positive root of $\Delta_1(\kappa_1) = 0$ as

$$\kappa_1^* = \frac{r_1\delta_1}{a\delta_2},$$

then, when $0 < \kappa_1 < \kappa_1^*$, $\Delta_0(\kappa_2) = 0$ may have two positive roots

$$\kappa_2 = \kappa_2^-(\kappa_1) = \frac{-a_1(\kappa_1) - \sqrt{\Delta_1(\kappa_1)}}{2a_2(\kappa_1)}, \quad \kappa_2 = \kappa_2^+(\kappa_1) = \frac{-a_1(\kappa_1) + \sqrt{\Delta_1(\kappa_1)}}{2a_2(\kappa_1)}.$$

If we substitute κ_1^* into $\Delta_0(\kappa_2) = 0$, then we have

$$\kappa_2^* = \frac{\delta_1^2\delta_2}{27r_1ac^2m}.$$

Similarly, with $\Delta_0(\overline{\kappa}_2) = 0$, we get correspondingly

$$\overline{\kappa}_1 = \frac{r_1(r_2 - cm)}{r_2 a}(r_2 > cm).$$

For the existence of positive equilibrium, summarizing the above we have the following proposition.

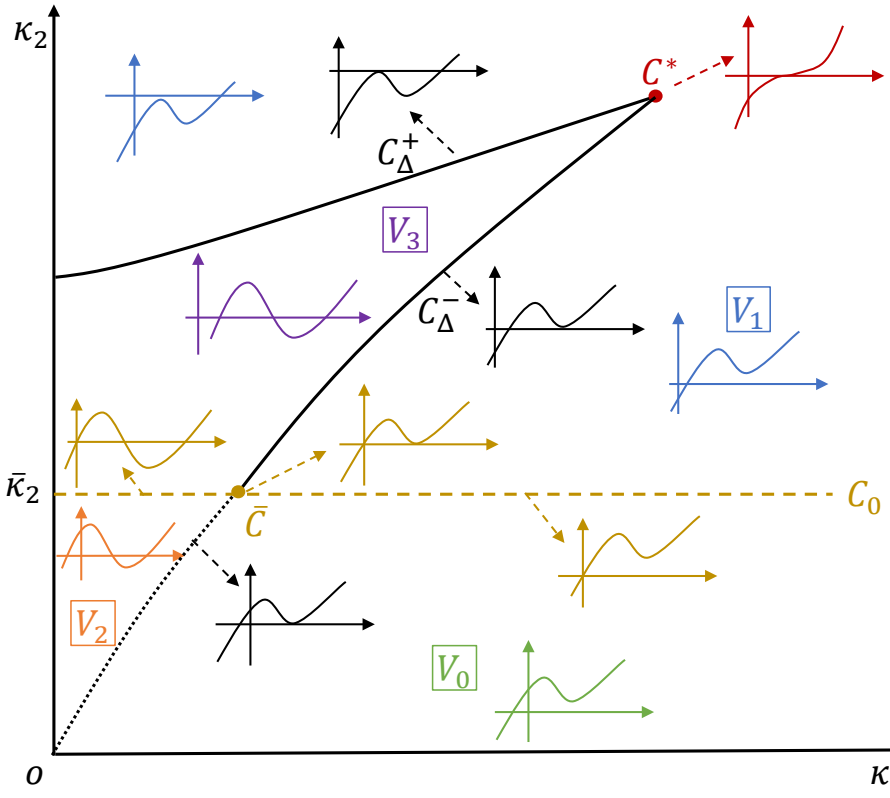

Figure 4.1: Existence of positive equilibria (number and position) of system (4.1) with κ_1 and κ_2 as parameters. There exist 0, 1, 2 and 3 positive equilibria in regions V_0, V_1, V_2, and V_3, respectively. A saddle-node bifurcation occurs when parameters across $C_\Delta^\pm$, and a transcritical bifurcation occurs when C_0 is crossed.

Proposition 4.2.1. *In the (κ_1, κ_2) plane, three curves*

$$C_0 : \kappa_2 = \overline{\kappa}_2, \quad \kappa_1 > 0,$$

$$C_\Delta^- : \kappa_2 = \kappa_2^-(\kappa_1), \quad 0 < \kappa_1 < \kappa_1^*, \kappa_2 > 0,$$

$$C_\Delta^+ : \kappa_2 = \kappa_2^+(\kappa_1), \quad 0 < \kappa_1 < \kappa_1^*, \kappa_2 > 0,$$

divide the region $\kappa_1 > 0, \kappa_2 > 0$ into 4 subregions V_0, V_1, V_2, and V_3 (see Figure 4.1*):*

$$V_0 = \{(\kappa_1, \kappa_2) | \kappa_1 > 0, \kappa_2 < \kappa_2^-(\kappa_1) \cap \kappa_2 < \overline{\kappa}_2\},$$

$$V_1 = \{(\kappa_1, \kappa_2) | \kappa_1 > 0, \kappa_2 > \overline{\kappa}_2\} \setminus V_3,$$

$$V_2 = \{(\kappa_1, \kappa_2) | \kappa_1 > 0, \kappa_2^-(\kappa_1) < \kappa_2 < \overline{\kappa}_2\},$$

$$V_3 = \{(\kappa_1, \kappa_2) | 0 < \kappa_1 < \kappa_1^*, \kappa_2^-(\kappa_1) < \kappa_2 < \kappa_2^+(\kappa_1) \cap \kappa_2 > \overline{\kappa}_2\}.$$

In regions V_0, V_1, V_2, V_3, system (4.1) *has 0,1,2 and 3 positive equilibria, respectively. S_1, S_2 and S_3 denote the three simple co-existence equilibria whenever they exist, where corresponding $\overline{E_2}$ coordinate satisfy $\overline{E_2}(S_1) < \overline{E_2}(S_2) < \overline{E_2}(S_3)$. If exists, S_{12} denote the positive equilibrium where S_1 and S_2 coalesce. The similar definitions may be adapted to S_{23} and S_{123}. For system* (4.1)*,*

(1) along C_0, where $\overline{C} = (\overline{\kappa}_1, \overline{\kappa}_2)$

- *if $\kappa_1 > \overline{\kappa}_1$, there is no co-existence equilibria;*
- *if $\kappa_1 = \overline{\kappa}_1$, there is a co-existence equilibrium of multiplicity 2, S_{23};*

- *if* $\kappa_1 < \overline{\kappa}_1$*, there are two co-existence equilibria,* S_2 *and* S_3*.*

(2) along C_Δ^+*, there is a simple co-existence equilibrium* S_3 *and a co-existence equilibrium of multiplicity 2,* S_{12}*.*

(3) along C_Δ^-*,*

- *if* $\kappa_2 > \overline{\kappa}_2$*, there is a simple co-existence equilibrium* S_1 *and a co-existence equilibrium of multiplicity 2,* S_{23}*;*

- *if* $\kappa_2 \leq \overline{\kappa}_2$*, there is a co-existence equilibrium of multiplicity 2,* S_{23}*.*

(4) at the point $C^*(\kappa_1^*, \kappa_2^*) = (\frac{r_1\delta_1}{a\delta_2}, \frac{\delta_1^2\delta_2}{27r_1ac^2m})$*, there is a co-existence equilibrium of multiplicity 3,* $S_{123} = (\frac{r_1a\delta_3}{\delta_1\alpha}, \frac{a\delta_3}{\delta_1}, \frac{18r_1ac^2m}{\delta_1\delta_2})(0 < r_2 < 2cm)$.

As shown in Figure 4.1, the system (4.1) may have 1 simple coexistence equilibrium S_1 or S_3, or 1 degenerate coexistence equilibrium S_{23} or S_{123}, or 2 coexistence equilibria S_1, S_{23} or S_{12}, S_3 or S_2, S_3, or 3 coexistence equilibria S_1, S_2 and S_3 simultaneously.

4.2.2 Local stability of equilibria

System (4.1) has three boundary equilibria, $S_0(0, 0, 0)$, predator-extinction equilibrium $S_{10}(p_1K_1, K_1, 0)$ and pest-free equilibrium $S_{01}(0, 0, K_2)$.

The Jacobian matrix of system (4.1) is

$$J = \begin{pmatrix} -\alpha & r_1 & 0 \\ \alpha & -2\kappa_1 E_2 - MP'(E_2) & -P(E_2) \\ 0 & cMP'(E_2) & r_2 - 2\kappa_2 M + cP(E_2) \end{pmatrix} \tag{4.12}$$

where $P(E_2) = \frac{mE_2}{a+E_2}$. Using the Jacobian matrix, one can verify the equilibrium point $S_0(0,0,0)$ is a saddle with 2 positive eigenvalues and 1 negative eigenvalue.

The characteristic equation of system (4.1) at $S_{10}(p_1K_1, K_1, 0)$ is

$$\big[(r_1 + \kappa_1 a)\lambda - (r_2\kappa_1 a + r_1 r_2 + cmr_1)\big]\big[\lambda^2 + (2r_1 + \alpha)\lambda + r_1\alpha\big] = 0. \tag{4.13}$$

One can verify that two roots of the equation (4.13) are negative and the third one is $r_2 + \frac{cmr_1}{r_1+\kappa_1 a} > 0$. Hence, the predator-extinction equilibrium S_{10} is always unstable.

For the pest-free equilibrium point $S_{01}(0, 0, K_2)$, its characteristic equation is

$$(\lambda + r_2)\big[\lambda^2 + (\alpha + \frac{mr_2}{a\kappa_2})\lambda + \alpha(\frac{mr_2}{a\kappa_2} - r_1)\big] = 0. \tag{4.14}$$

One eigenvalue is $-r_2$, the other two are decided by a quadratic equation. With (4.11), one can verify that the pest-free equilibrium S_{01} is locally asymptotically stable if $\kappa_2 < \overline{\kappa}_2 = \frac{r_2 m}{r_1 a}$ and it is unstable if $\kappa_2 > \overline{\kappa}_2$.

To discuss the local stability of coexistence equilibria, by using $U_1(E_2)$ and $U_2(E_2)$

we rewrite the system (4.1) as

$$\begin{cases} \dfrac{dE_1}{dt} &= r_1E_2 - \alpha E_1, \\ \dfrac{dE_2}{dt} &= P(E_2)[U_1(E_2) - M], \\ \dfrac{dM}{dt} &= \kappa_2 M[U_2(E_2) - M]. \end{cases} \tag{4.15}$$

We calculate the Jacobian matrix and evaluate it at coexistence equilibrium point $\overline{S}$

$$J(\overline{S}) = \begin{pmatrix} -\alpha & r_1 & 0 \\ \alpha & P(\overline{E_2})U_1'(\overline{E_2}) & -P(\overline{E_2}) \\ 0 & \kappa_2\overline{M}U_2'(\overline{E_2}) & -\kappa_2\overline{M} \end{pmatrix} \tag{4.16}$$

The characteristic equation of system (4.15) at the coexistence equilibrium $\overline{S}$ is of the form

$$\lambda^3 + A_2\lambda^2 + A_1\lambda + A_0 = 0, \tag{4.17}$$

where

$$\begin{aligned} A_2 &= \alpha + \kappa_2\overline{M} - P(\overline{E_2})U_1'(\overline{E_2}), \\ A_1 &= \alpha[\kappa_2\overline{M} - P(\overline{E_2})U_1'(\overline{E_2})] + P(\overline{E_2})\kappa_2\overline{M}[U_2'(\overline{E_2}) - U_1'(\overline{E_2})] - r_1\alpha, \\ A_0 &= \alpha\kappa_2\overline{M}P(\overline{E_2})[U_2'(\overline{E_2}) - U_1'(\overline{E_2})] - r_1\alpha\kappa_2\overline{M}. \end{aligned} \tag{4.18}$$

A straightforward calculation finds that $A_2 > 0$. And the trace of $J(\overline{S})$ is

$$T(\overline{S}) = -A_2 = -\alpha - \kappa_2\overline{M} + P(\overline{E_2})U_1'(\overline{E_2}) < 0,$$

Then, there always is a negative eigenvalue. The determinant of $J(\overline{E})$ is

$$D(\overline{S}) = -A_0 = -\alpha\kappa_2\overline{M}\{P(\overline{E_2})[U_2'(\overline{E_2}) - U_1'(\overline{E_2})] - r_1\}.$$

The $J(\overline{S})$ has 1 zero eigenvalue when $A_0 = 0$, $U_2'(\overline{E_2}) - U_1'(\overline{E_2}) = \frac{r_1}{P(\overline{E_2})}$, which differs the condition of $U_2'(\overline{E_2}) - U_1'(\overline{E_2}) = 0$ in system (3.1) 3.

Since we only discuss the positive equilibrium point of the system, which tell us that $\overline{E_2} > 0, \overline{M_2} > 0$, and the parameters $\alpha, \kappa_2 > 0$. So the sign of the $D(\overline{E})$ is defined by the slope difference of the curve $U_1(E_2)$ and $U_2(E_2)$ at equilibrium point. We define $k_1 = U_1'(\overline{E_2})$, $k_2 = U_2'(\overline{E_2})$ and $\overline{k} = \frac{r_1}{P(\overline{E_2})}$.

Proposition 4.2.2. *For system* (4.1)*,*

(1) the predator-extinction equilibrium S_{10} is a hyperbolic saddle.

(2) the pest-free equilibrium S_{01} is

- *if $\kappa_2 > \overline{\kappa}_2$: a hyperbolic saddle;*
- *if $\kappa_2 = \overline{\kappa}_2$: a saddle-node of codimension 1;*
- *if $\kappa_2 < \overline{\kappa}_2$: a locally stable node.*

(3) For the co-existence equilibria,when exist,

- *S_1 and S_3 is an anti-saddle;*
- *S_2 is a hyperbolic saddle;*
- *if $T(J(S_{12(23)})) \neq 0$, $S_{12(23)}$ is a saddle-node of codimension 1;*
- *if $T(S_{1(3)}) = 0$ and $D(S_{1(3)}) > 0$, $S_{1(3)}$ is a Hopf bifurcation point;*
- *if $T(J(S_{12(23)})) = 0$, $S_{12(23)}$ is a BT point;*

4.3 Bifurcations and complex dynamics

4.3.1 Saddle-node bifurcation

Theorem 4.3.1. *For the system* (4.1)*, if* $T(J(S_{12(23)})) \neq 0$*, the co-existence equilibrium* S_{12} *or* S_{23}*,*

(1) when exists, it is an saddle node of codimension 1. When $\kappa_2 = \kappa_2^{\pm}(\kappa_1)$*, the system undergoes a saddle-node bifurcation.*

(2) if $\kappa_1 = \kappa_1^*$*, and* $\kappa_2 = \kappa_2^*$ *which occurs at* $S_{12} = S_{23} = S_{123}$*, it is a saddle node of codimension 2, and the system undergoes a cusp bifurcation.*

The unfolding of the semi-hyperbolic point of codimension 2 is given in the bifurcation diagram of Figure 4.1 *using* κ_1, κ_2 *as parameters.*

Proof. Follow the Prop. 4.2.2, the co-existence equilibrium S_{12} or S_{23} is saddle-node of codimension 1. For simplicity, we use $(\overline{E_1}, \overline{E_2}, \overline{M})$ to denote the coordinates at S_{12} or S_{23}. The straightforward calculation of $k_2 - k_1 = \overline{k}$ obtains the condition, that is

$$\kappa_2 = \widetilde{\kappa}_2 = \frac{acm^2}{(a + \overline{E_2})^2(r_1 a - \kappa_1 - 2\kappa_1 \overline{E_2})}$$

Also, one can find that $\widetilde{\lambda}_1, 0, \widetilde{\lambda}_3$ are the three eigenvalues of $J(\overline{S})$, with associated eigen-

vectors $\widetilde{V}_{1|E_2=\overline{E_2}}$, $\widetilde{V}_{2|E_2=\overline{E_2}}$, $\widetilde{V}_{3|E_2=\overline{E_2}}$, where

$$\widetilde{V}_1 = \begin{pmatrix} \frac{r_1}{\alpha+\widetilde{\lambda}_1} \\ 1 \\ \frac{\widetilde{\kappa}_2\overline{M}k_2}{\widetilde{\kappa}_2\overline{M}+\widetilde{\lambda}_1} \end{pmatrix}, \quad \widetilde{V}_2 = \begin{pmatrix} \frac{r_1}{\alpha} \\ 1 \\ k_2 \end{pmatrix}, \quad \widetilde{V}_3 = \begin{pmatrix} \frac{r_1}{\alpha+\widetilde{\lambda}_3} \\ 1 \\ \frac{\widetilde{\kappa}_2\overline{M}k_2}{\widetilde{\kappa}_2\overline{M}+\widetilde{\lambda}_3} \end{pmatrix},$$

and

$$\widetilde{\lambda}_1 = \frac{-\widetilde{A}_2 - \sqrt{\widetilde{A}_2^2 - 4\widetilde{A}_1}}{2}, \quad \widetilde{\lambda}_3 = \frac{-\widetilde{A}_2 + \sqrt{\widetilde{A}_2^2 - 4\widetilde{A}_1}}{2},$$
$$\widetilde{A}_2 = \frac{2\overline{E_2}^2\kappa_1 + (a\kappa_1 + \delta_1 + \alpha)\overline{E_2} + a(r_1 + r_2 + \alpha)}{a + \overline{E_2}},$$
$$\widetilde{A}_1 = \frac{2\alpha\kappa_1\overline{E_2}^2 + ((a\kappa_1 + \delta_1 - r_1)\alpha + r_1\delta_1)\overline{E_2} + ar_2(r_1 + \alpha)}{a + \overline{E_2}}.$$

Then, we derive the normal form on the one dimensional center manifold as follows. Firstly, we bring the equilibrium S_{12} or S_{23} to the origin by the transformation $X_1 = E_1 - \overline{E_1}, X_2 = E_2 - \overline{E_2}, Y = M - \overline{M}$ and expand system (4.1) in the neighborhood of the new origin. Under the following transformation,

$$\begin{pmatrix} X_1 \\ X_2 \\ Y \end{pmatrix} = T \begin{pmatrix} x_1 \\ x_2 \\ y \end{pmatrix}, \quad T = (\widetilde{V}_1, \widetilde{V}_2, \widetilde{V}_3).$$

and $|T| \neq 0$, then we have

$$\begin{cases} \dot{x_1} &= \widetilde{\lambda}_1 x_1 + \sum\limits_{i,j,k\in\mathbb{N}}^{i+j+k=2} \overline{a}_{ijk} x_1^i x_2^j y^k + O(|x_1, x_2, y|^3), \\ \dot{x_2} &= \sum\limits_{i,j,k\in\mathbb{N}}^{i+j+k=2,3} \overline{b}_{ijk} x_1^i x_2^j y^k + O(|x_1, x_2, y|^4), \\ \dot{y} &= \widetilde{\lambda}_3 y + \sum\limits_{i,j,k\in\mathbb{N}}^{i+j+k=2} \overline{c}_{ijk} x_1^i x_2^j y^k + O(|x_1, x_2, y|^3), \end{cases} \tag{4.19}$$

where

$$\overline{b}_{020} = \frac{\alpha(r_2 a + \delta_1 \overline{E_2})}{\widetilde{A}_1 (a + \overline{E_2})^3 [(\delta_1 - \alpha)\overline{E_2} + a(r_2 - \alpha)]} (q_3 \overline{E_2}^3 + q_2 \overline{E_2}^2 + q_1 \overline{E_2} + q_0),$$

$$q_3 = -\kappa_1(\delta_1 - \alpha),$$

$$q_2 = -\kappa_1 a(\delta_1 + r_2 - 2\alpha) + (\delta_1 + \widetilde{\lambda}_1)(\delta_1 + \widetilde{\lambda}_3),$$

$$q_1 = -a[\kappa_1 a(r_2 - \alpha) - 2r_2^2 - 2r_2(cm + \widetilde{A}_2) + cm\widetilde{A}_2 - 2\widetilde{A}_1],$$

$$q_0 = a^2(r_2 + \widetilde{\lambda}_1)(r_2 + \widetilde{\lambda}_3).$$

For simplicity, we choose not to present all the coefficients here. For $x_2 \sim 0$, there exists a center manifold

$$x_1 = -\frac{\overline{a}_{020}}{\widetilde{\lambda}_1} x_2^2 + O(|x_2|^3), \quad y = -\frac{\overline{c}_{020}}{\widetilde{\lambda}_3} x_2^2 + O(|x_2|^3), \tag{4.20}$$

The system (4.19) reduced on the one dimensional center manifold (4.20) is given by

$$\dot{x_2} = \overline{b}_{020} x_2^2 + O(|x_2|^3).$$

We can verify that $\overline{b}_{020} = 0$ if $\kappa_1 = \kappa_1^*, \kappa_2 = \kappa_2^*$, which occurs at $S_{12} = S_{23} = S_{123}$ and then co-existence equilibrium $S_{12} = S_{23}$ is a saddle node of codimension 2. □

Theorem 4.3.2. *For the system* (4.1)*, the pest-free equilibrium* S_{01}*,*

(1) if $\kappa_2 = \overline{\kappa}_2$*, it is an saddle node of codimension 1. Along the curve* C_0*, the system undergoes a saddle-node bifurcation.*

(2) if $\kappa_2 = \overline{\kappa}_2$ *and* $\kappa_1 = \overline{\kappa}_1$*,which occurs at* $S_{01} = S_{12}$*, it is a saddle node of codimension 2, and system undergoes a cusp bifurcation.*

Proof. When $\kappa_2 = \overline{\kappa}_2$, then $S_{01} = (0, 0, \frac{r_1 a}{m})$, and the equation (4.14) becomes

$$(\lambda + r_2)\left[\lambda^2 + (\alpha + r_1)\lambda\right] = 0. \tag{4.21}$$

We can easily find that $D(J(S_{01})) = 0$, and $0, -r_2, -\alpha - r_1$ are the three eigenvalues of $J(S_{01})$. Translate pest-free equilibrium S_{01} into the origin by letting $X_1 = E_1, X_2 = E_2, Y = M - \frac{r_1 a}{m}$, and make the transformation

$$\begin{pmatrix} X_1 \\ X_2 \\ Y \end{pmatrix} = \hat{T} \begin{pmatrix} x_1 \\ x_2 \\ y \end{pmatrix}, \quad \hat{T} = (\hat{V}_1, \hat{V}_2, \hat{V}_3).$$

where

$$\hat{V}_1 = \begin{pmatrix} -1 \\ 1 \\ \frac{cr_1}{r_2 - r_1 - \alpha} \end{pmatrix}, \quad \hat{V}_2 = \begin{pmatrix} \frac{r_1}{\alpha} \\ 1 \\ \frac{cr_1}{r_2} \end{pmatrix}, \quad \hat{V}_3 = \begin{pmatrix} 0 \\ 0 \\ 1 \end{pmatrix}.$$

and $|\hat{T}| \neq 0$, then we have

$$\begin{cases} \dot{x_1} &= (-\alpha - r_1)x_1 + \sum\limits_{i,j,k\in\mathbb{N}}^{i+j+k=2} \bar{\bar{a}}_{ijk} x_1^i x_2^j y^k + O(|x_1, x_2, y|^3), \\ \dot{x_2} &= \sum\limits_{i,j,k\in\mathbb{N}}^{i+j+k=2,3} \bar{\bar{b}}_{ijk} x_1^i x_2^j y^k + O(|x_1, x_2, y|^4), \\ \dot{y} &= -r_2 y + \sum\limits_{i,j,k\in\mathbb{N}}^{i+j+k=2} \bar{\bar{c}}_{ijk} x_1^i x_2^j y^k + O(|x_1, x_2, y|^3) \end{cases} \tag{4.22}$$

where

$$\bar{\bar{b}}_{020} = \frac{\alpha[r_1(r_2 - cm) - \kappa_1 r_2 a]}{r_2 a(r_1 + \alpha)}.$$

Other coefficients are not presented here. For $x_2 \sim 0$, there exists a center manifold

$$x_1 = \frac{\bar{\bar{a}}_{020}}{\alpha + r_1} x_2^2 + O(|x_2|^3), \quad y = \frac{\bar{\bar{c}}_{020}}{r_2} x_2^2 + O(|x_2|^3), \tag{4.23}$$

The system (4.22) reduced on the one dimensional center manifold (4.23) is given by

$$\dot{x_2} = \bar{\bar{b}}_{020} x_2^2 + O(|x_2|^3).$$

We can verify that $\bar{\bar{b}}_{020} = 0$ if $\kappa_1 = \overline{\kappa}_1 (r_2 > cm)$, which occurs at $S_{12} = S_{01}$. Hence, the pest free equilibrium $S_{12} = S_{01}$ is a semi-hyperbolic point of codimension 2. □

4.3.2 Hopf bifurcations

Following the Prop. 4.2.2, the co-existence equilibrium S_1 or S_3, when exists, may undergo a Hopf bifurcation if $T(S_i) = 0$ and $D(S_i) > 0$ $(i = 1, 3)$. Here, we still use $\overline{E_2}$ to

denote the E_2-coordinate at S_1 or S_3. It follows from (4.17) that for Hopf bifurcation to occur, we have

$$A_0 = A_1 A_2, \quad A_1 > 0,$$

and the equation (4.17) becomes

$$(\lambda + A_2)(\lambda^2 + A_1) = 0. \tag{4.24}$$

Hence, if we define and collect the expression in terms of α, we get

$$H(\alpha) = A_0 - A_1 A_2 = h_2\alpha^2 + h_1\alpha + h_0, \tag{4.25}$$

where

$$\begin{aligned}
h_0 =& -\frac{\delta_1\overline{E_2} + ar_2}{\kappa_2(a+\overline{E_2})^5}\left[2\kappa_1\overline{E_2}^2 + (a\kappa_1+\delta_1)\overline{E_2} + a(r_1+r_2)\right]\Big[2\kappa_1\kappa_2\overline{E_2}^4 + 5a\kappa_1\kappa_2\overline{E_2}^3 \\
&+ a(4a\kappa_1\kappa_2 + \kappa_2 r_1)\overline{E_2}^2 + a(a^2\kappa_1\kappa_2 + 2a\kappa_2 r_1 + cm^2)\overline{E_2} + a^3\kappa_2 r_1\Big], \\
h_1 =& \frac{1}{(a+\overline{E_2})^2}\{-4\kappa_1^2\overline{E_2}^4 + \Big[(2r_1 - 4\delta_1)\kappa_1 - 4a\kappa_1^2\Big]\overline{E_2}^3 - \Big[a^2\kappa_1^2 + (2cm + r_1 + 6r_2)a\kappa_1 \\
&+ \delta_1^2\Big]\overline{E_2}^2 - \Big[(r_1+2r_2)a^2\kappa_1 + a(2r_1\delta_1 + 2r_2\delta_1 - r_1^2)\Big]\overline{E_2} - (2r_1+r_2)a^2 r_2\}, \\
h_2 =& \frac{-2\kappa_1\overline{E_2}^2 + (-a\kappa_1 - \delta_1 + r_1)\overline{E_2} - ar_2}{a+\overline{E_2}}.
\end{aligned}$$

Let Δ_h be the discriminant of $H(\alpha)$ with respect to α, and we have

$$\begin{aligned}\Delta_h =& h_1^2 - 4h_0h_2 \\ =& \frac{1}{(a+\overline{E_2})^4}\Big[4\kappa_1^2\overline{E_2}^4 + (4a\kappa_1^2 - 2\kappa_1 r_1)\overline{E_2}^3 + (a^2\kappa_1^2 + ar_1\kappa_1 - \delta_1^2)\overline{E_2}^2 + a(a\kappa_1 r_1 \\ & - 2r_2\delta_1 - r_1^2)\overline{E_2} - a^2 r_2^2\Big]^2 - \frac{4am^2c\overline{E_2}(\delta_1\overline{E_2} + ar_2)}{(a+\overline{E_2})^6\kappa_2}\Big[2\kappa_1\overline{E_2}^2 + (a\kappa_1 + \delta_1)\overline{E_2} + a(r_1 \\ & + r_2)\Big]\Big[2\kappa_1\overline{E_2}^2 + (a\kappa_1 + \delta_1 - r_1)\overline{E_2} + ar_2\Big].\end{aligned}$$

The equation $H(\alpha) = 0$ may have at most two roots if $\Delta_h > 0$, and two potential positive roots are

$$\alpha^- = \frac{-h_1 - \sqrt{\Delta_h}}{2h_2}, \quad \alpha^+ = \frac{-h_1 + \sqrt{\Delta_h}}{2h_2}.$$

And if $\Delta_h = 0$, then the equation $H(\alpha) = 0$ has one unique solution, which is

$$\begin{aligned}\alpha = \alpha^* =& -\frac{h_1}{2h_2} \\ =& \frac{1}{2(a+\overline{E_2})[-\overline{E_2}\kappa_1(a+2\overline{E_2}) + (r_1 - \delta_1)\overline{E_2} - ar_2]}\{\overline{E_2}^2(a+2\overline{E_2})^2\kappa_1^2 + \Big[(2\delta_1 \\ & - r_1)\overline{E_2} + (r_1 + 2r_2)a\Big](a+2\overline{E_2})\overline{E_2}\kappa_1 + \delta_1^2\overline{E_2}^2 + a(2r_1\delta_1 + 2r_2\delta_1 - r_1^2)\overline{E_2} \\ & + (2r_1 + r_2)a^2 r_2\}.\end{aligned}$$

Also, from $A_1 > 0$, we can derive $\kappa_2 < \hat{\kappa}_2$, with

$$\hat{\kappa}_2 = \frac{cm^2 a\overline{E_2}(\delta_1\overline{E_2} + ar_2)}{(a+\overline{E_2})^2(\widetilde{q}_3\overline{E_2}^3 + \widetilde{q}_2\overline{E_2}^2 + \widetilde{q}_1\overline{E_2} + \widetilde{q}_0)},$$

$$\widetilde{q}_3 = -2\kappa_1(\delta_1 + \alpha,$$

$$\widetilde{q}_2 = -[\kappa_1(cm + 3\alpha + 3r_2)a + (\delta_1 - r_1)\alpha],$$

$$\widetilde{q}_1 = -a[\kappa_1(r_2 + \alpha)a + (cm - r_1 + 2r_2)\alpha + \delta_1 r_1],$$

$$\widetilde{q}_0 = -a^2 r_2(r_1 + \alpha).$$

Next, we verify the transversality condition. Let $\hat{\lambda}_1, \hat{\lambda}_2, \hat{\lambda}_3$ be the three eigenvalues of $\overline{S}$. From the previous analysis, we know that there is always a negative eigenvalue, then we can assume that $\hat{\lambda}_1 < 0$, and $\hat{\lambda}_2 + \hat{\lambda}_3 = -A_2 - \hat{\lambda}_1$. Let γ be the real part of $\hat{\lambda}_2$ and $\hat{\lambda}_3$ that satisfy the Eq.(4.17) and we get

$$\frac{\partial\gamma}{\partial\alpha}_{|\alpha=\alpha^{\pm}} = \frac{-\overline{E_2}(\delta_1\overline{E_2} + r_2 a)[\kappa_2(a+\overline{E_2})^2(2\kappa_1\overline{E_2} + a\kappa_1 - r_1) + acm^2]}{(\overline{q}_3\overline{E_2}^3 + \overline{q}_2\overline{E_2}^2 + \overline{q}_1\overline{E_2} + \overline{q}_0)(a+\overline{E_2})^2\kappa_2 - acm^2(\delta_1\overline{E_2} + r_2 a)\overline{E_2}},$$

where

$$\overline{q}_3 = 2(\alpha^{\pm} + \delta_1)\kappa_1,$$

$$\overline{q}_2 = (3a\kappa_1 + \delta_1 - r_1)\alpha^{\pm} + a\kappa_1(3r_2 + cm),$$

$$\overline{q}_1 = (a\kappa_1 - r_1 + 2r_2 + cm)\alpha^{\pm} + r_1\delta_1 + a\kappa_1 r_2,$$

$$\overline{q}_0 = r_2(r_1 + \alpha^{\pm}).$$

Note that $\frac{\partial\gamma}{\partial\alpha}_{|\alpha=\alpha^{\pm}} = 0$ if and only if $r_1 = \kappa_1(a + 2\overline{E_2}) + \frac{acm^2}{(a+\overline{E_2})^2\kappa_2}$, which occurs only $\overline{S} = S_{12}$ or $\overline{S} = S_{23}$ or $\overline{S} = S_{123}$. Hence, $\frac{\partial\gamma}{\partial\alpha}_{|\alpha=\alpha^{\pm}} \neq 0$, which means the transversality

condition is satisfied. Therefore, we have the following proposition about the existence of Hopf bifurcation.

Proposition 4.3.3. *For system* (4.1)*, if* $\kappa_2 < \hat{\kappa}_2$*, the co-existence equilibrium* S_1 *or* S_3*, when exists, and*

(1) if $\alpha = \alpha^-$*, or* $\alpha = \alpha^+$*, the system undergoes a Hopf bifurcation;*

(2) if $\alpha = \alpha^*$*, the system undergoes a Hopf bifurcation which can be degenerate.*

Prop. 4.3.3 gives the necessary conditions for the existence of Hopf bifurcation. Due to the complexity of the system, we are not able to decide the codimension of the Hopf bifurcation without knowing the first and higher order of Lyapunov coefficients. However, the codimension of the Hopf bifurcation can be at least 2 from the existence of the codimension 3 nilpotent singularities [127]. From the Figure 4.2 - 4.4, we numerically present the existence of degenerate Hopf bifurcation. As the α varies, the system has one stable equilibrium, 2 limit cycles and 1 limit cycle. As shown in Figure 4.5, we present two examples of two limit cycles bifurcated from the degenerate Hopf bifurcation when the parameters are near the focus and elliptic type of nilpotent singularities of codimension 3.

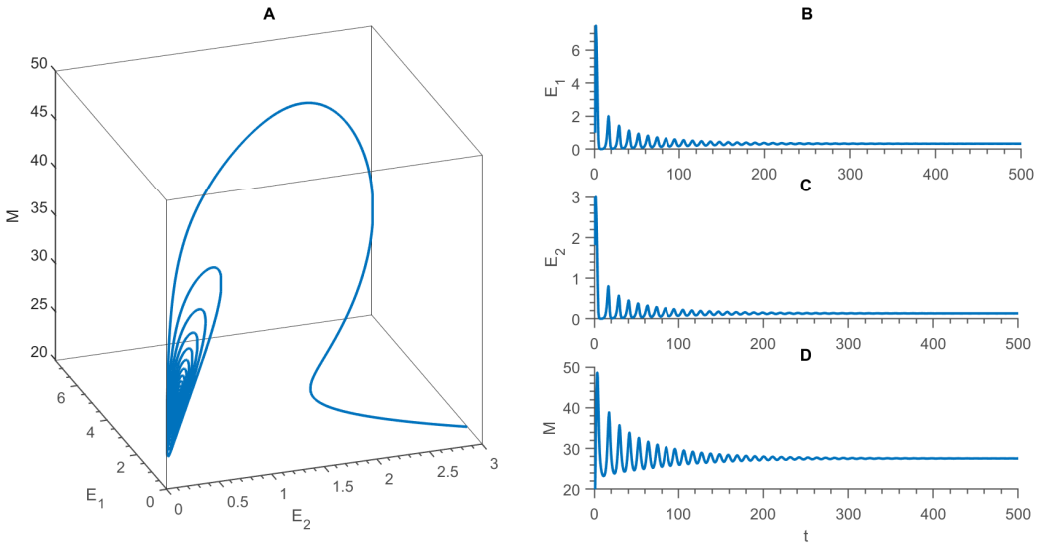

Figure 4.2: The phase portrait and solution plot of system (4.1) when $\alpha = 10$, where $\kappa_2 = 0.0225, \kappa_1 = 5.5, r_1 = 25, r_2 = 0.5, a = 1, c = 1, m = 1$.

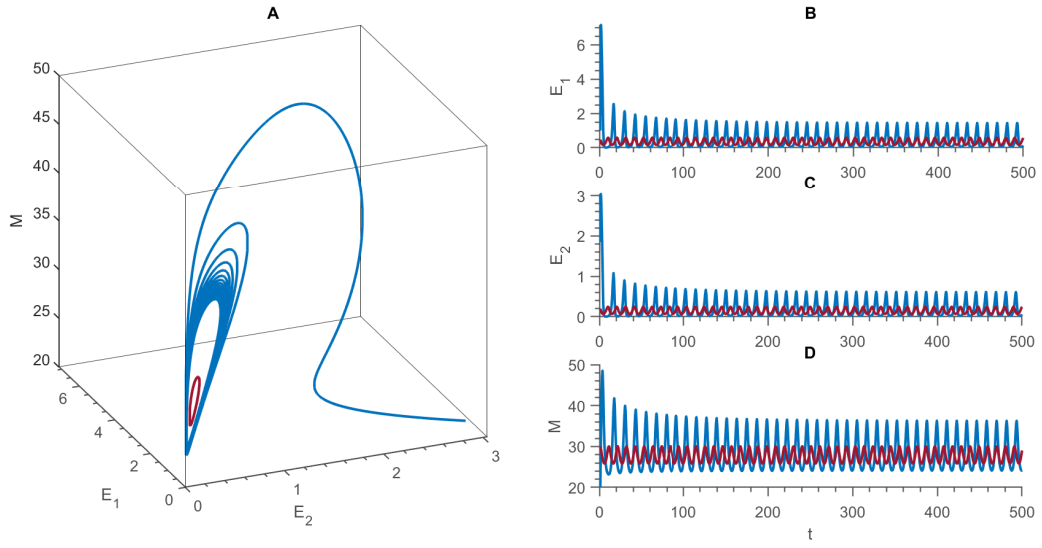

Figure 4.3: The phase portrait and solution plot of system (4.1) when $\alpha = 10.58$, where $\kappa_2 = 0.0225, \kappa_1 = 5.5, r_1 = 25, r_2 = 0.5, a = 1, c = 1, m = 1$. The blue and red color represent the equilibrium is stable and unstable, respectively.

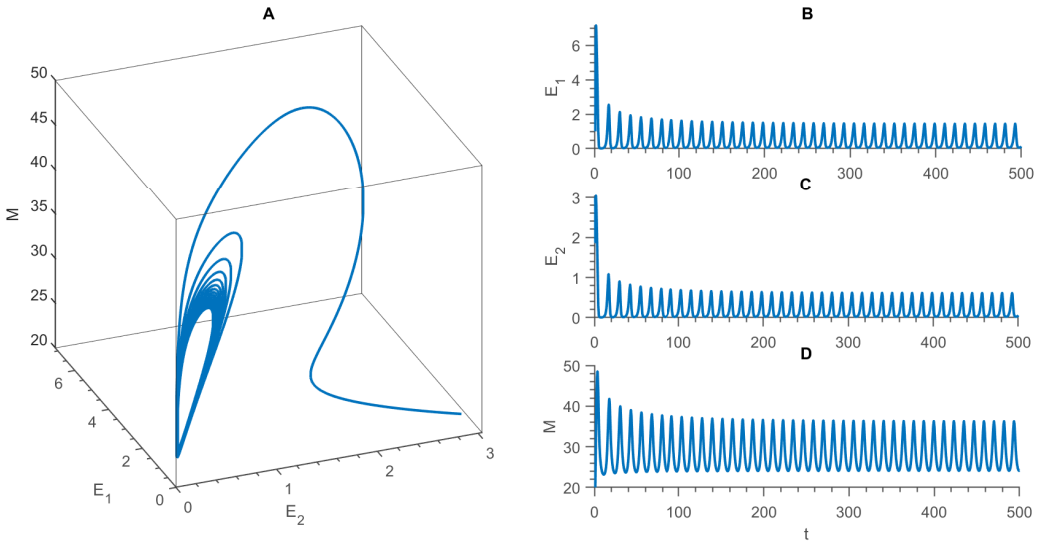

Figure 4.4: The phase portrait and solution plot of system (4.1) when $\alpha = 11$, where $\kappa_2 = 0.0225, \kappa_1 = 5.5, r_1 = 25, r_2 = 0.5, a = 1, c = 1, m = 1$.

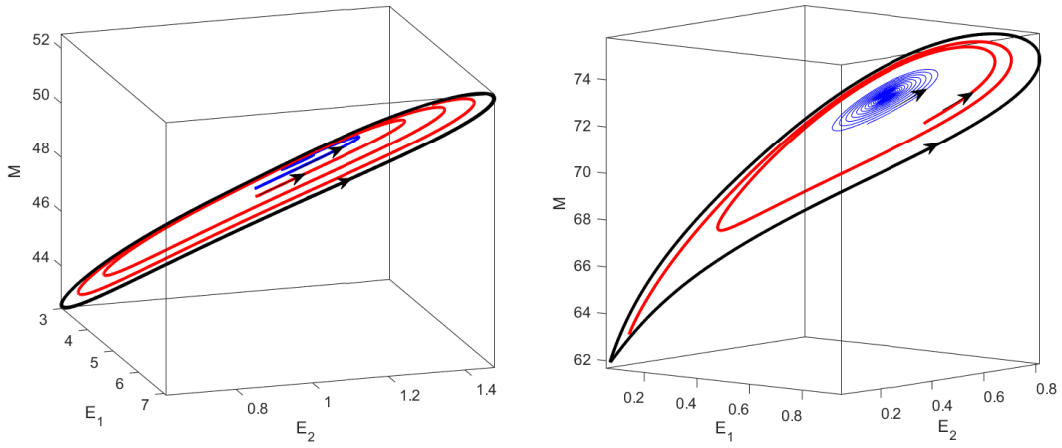

(a) Focus type

(b) Elliptic type

Figure 4.5: Existence of two limit cycles in the case when the parameters are taken near the nilpotent focus and elliptic point of codimension 3. The black color represents the stable limit cycle, and the unstable limit cycles occur between the blue and red curves. $a = 1, c = 1, m = 1$ and (a) $r_2 = 0.5, \alpha = 6.25, r_1 = 30, \kappa_1 = 5.9953, \kappa_2 = 0.02083$, (b) $r_2 = 1.6, \alpha = 51.57, r_1 = 60, \kappa_1 = 23.15, \kappa_2 = 0.026671$.

4.3.3 Cusp point and Bogdanov-Takens bifurcation

Bogdanov-Takens bifurcation occurs in the 2 dimensional version of the system (4.1) in chapter 3, it is reasonable to expect the existence of BT bifurcation in the stage structure model. But the BT bifurcation was not well presented due to the complex expression of the cusp point.

Theorem 4.3.4. *For the system* (4.1)*, the coexistence equilibrium* S_{12} *or* S_{23} *exists if*

$$\kappa_2 = \widetilde{\kappa}_2 = \frac{acm^2}{(a+\overline{E_2})^2(r_1 a - \kappa_1 - 2\kappa_1\overline{E_2})},$$
$$r_1 = \overline{r}_1 = \frac{\alpha(2\kappa_1\overline{E_2}^2 + a\kappa_1\overline{E_2} + \delta_1\overline{E_2} + ar_2)}{\alpha\overline{E_2} - \delta_1\overline{E_2} - ar_2},$$

where $\overline{E_2}$ *is the* E_2*-coordinate of* S_{12} *and* S_{23}*, then* S_{12} *and* S_{23} *are cusp points when exists, and system* (4.1) *localized at has a 2 dimensional center manifold on which the system is topologically equivalent to*

$$\begin{cases} \dot{x} &= y, \\ \dot{y} &= m_{20}x^2 + m_{11}xy + O(|x_2, y|^3). \end{cases} \tag{4.26}$$

Proof. Here, we still use $(\overline{E_1}, \overline{E_2}, \overline{M})$ to denote the coordinates at S_{12} or S_{23} as we can not get the explicit coordinates of S_{12} or S_{23}. Firstly, we bring the co-existence equilibrium point S_{12} or S_{23} to the origin by the translation $X_1 = E_1 - \overline{E_1}, X_2 = E_2 - \overline{E_2}, Y = M - \overline{M}$ and following transformation

$$\begin{pmatrix} X_1 \\ X_2 \\ Y \end{pmatrix} = \overline{P} \begin{pmatrix} x_1 \\ x_2 \\ y \end{pmatrix}, \quad \overline{P} = (\overline{V}_1, \overline{V}_2, \overline{V}_3).$$

where

$$\overline{V}_1 = \begin{pmatrix} \frac{r_1}{\alpha+\overline{\lambda}_1} \\ 1 \\ \frac{k_2\kappa_2\overline{M}}{\kappa_2\overline{M}+\overline{\lambda}_1} \end{pmatrix}, \quad \overline{V}_2 = \begin{pmatrix} \frac{r_1}{\alpha} \\ 1 \\ k_2 \end{pmatrix}, \quad \overline{V}_3 = \begin{pmatrix} \frac{r_1}{\alpha}(\frac{1}{\kappa_2\overline{M}} - \frac{1}{\alpha}) \\ \frac{1}{\kappa_2\overline{M}} \\ 0 \end{pmatrix}.$$

$\overline{\lambda}_1 = \widetilde{A}_2$ and $|\overline{P}| \neq 0$, then we have

$$\begin{cases} \dot{x_1} &= \overline{\lambda}_1 x_1 + \sum\limits_{i,j,k\in\mathbb{N}}^{i+j+k=2} a_{ijk} x_1^i x_2^j y^k + O(|x_1, x_2, y|^3), \\ \dot{x_2} &= y + \sum\limits_{i,j,k\in\mathbb{N}}^{i+j+k=2,3} b_{ijk} x_1^i x_2^j y^k + O(|x_1, x_2, y|^4), \\ \dot{y} &= \sum\limits_{i,j,k\in\mathbb{N}}^{i+j+k=2,3} c_{ijk} x_1^i x_2^j y^k + O(|x_1, x_2, y|^4), \end{cases} \tag{4.27}$$

where

$$b_{020} = \frac{-\overline{E_2}(\delta_1\overline{E_2} + r_2 a)[\overline{p}_5\overline{E_2}^5 + \overline{p}_4\overline{E_2}^4 + \overline{p}_3\overline{E_2}^3 + \overline{p}_2\overline{E_2}^2 + \overline{p}_1\overline{E_2} + \overline{p}_0]}{(a+\overline{E_2})^2(p_3\overline{E_2}^3 + p_2\overline{E_2}^2 + p_1\overline{E_2} - a^2 r_2^2)^2},$$

$$c_{011} = \frac{\alpha\{\overline{\overline{p}}_3\overline{E_2}^3 + \overline{\overline{p}}_2\overline{E_2}^2 + \overline{\overline{p}}_1\overline{E_2} + \overline{\overline{p}}_0\}}{(a+\overline{E_2})(p_3\overline{E_2}^3 + p_2\overline{E_2}^2 + p_1\overline{E_2} - a^2 r_2^2)},$$

$$c_{020} = \frac{\alpha\overline{E_2}(\delta_1\overline{E_2} + r_2 a)}{(a+\overline{E_2})^2(p_3\overline{E_2}^3 + p_2\overline{E_2}^2 + p_1\overline{E_2} - a^2 r_2^2)}\{\kappa_1(3\delta_1 - \alpha)\overline{E_2}^2 + [(\delta_1 - a\kappa_1)\alpha$$

$$+ a\kappa_1(2cm + 5r_2)]\overline{E_2} + r_2 a(2\kappa_1 a + \alpha)\},$$

with

$$p_1 = \kappa_1 a^2(\alpha - r_2) + a(\alpha^2 - 2r_2\delta_1), \quad p_2 = \kappa_1 a[3\alpha - (cm + 3r_2)] + \alpha^2 - \delta_1^2,$$

$$p_3 = 2\kappa_1(\alpha - \delta_1), \quad \overline{p}_5 = 6\kappa_1^2(\alpha - \delta_1)^2,$$

$$\overline{p}_4 = \Big[17\alpha^2 - 12(2cm + 3r_2)\alpha + (7cm + 19r_2)\delta_1\Big]a\kappa_1^2 + (4\alpha - 3\delta_1)(\alpha^2 - \delta_1^2)\kappa_1,$$

$$\overline{p}_3 = \Big[17\alpha^2 - 3(5cm + 13r_2)\alpha + 2(c^2m^2 + 9cmr_2 + 11r_2^2)\Big]a^2\kappa_1^2 + \Big[10\alpha^3 - (4cm$$

$$+ 7r_2)\alpha^2 - 8\delta_1(cm + 2r_2)\alpha + (2cm + 11r_2)\delta_1^2\Big]a\kappa_1 + \alpha^4 - 2\delta_1^2\alpha^2 + \delta_1^3\alpha,$$

$$\overline{p}_2 = \Big[7\alpha^2 - 3(cm + 6r_2)\alpha + r_2(4cm + 11r_2)\Big]a^3\kappa_1^2 + \Big[8\alpha^3 - (cm + 5r_2)\alpha^2$$
$$- (3c^2m^2 + 22cmr_2 + 23r_2^2)\alpha + 3r_2\delta_1(2cm + 5r_2)\Big]a^2\kappa_1 + 2a\alpha^4 - 2\delta_1(cm$$
$$+ 3r_2)a\alpha^2 + 3r_2\delta_1^2 a\alpha,$$
$$\overline{p}_1 = (\alpha^2 - 3\alpha r_2 + 2r_2^2)a^4\kappa_1^2 + \Big[2\alpha^3 - r_2\alpha^2 - 2r_2(3cm + 7r_2)\alpha + 3r_2^2(2cm$$
$$+ 3r_2)\Big]a^3\kappa_1 + a^2\alpha^4 - 2a^2r_2(2cm + 3r_2)\alpha^2 + 3a^2r_2^2\delta_1\alpha,$$
$$\overline{p}_0 = (2r_2 - 3\alpha)a^4r_2^2\kappa_1 + a^3r_2^2\alpha(r_2 - 2\alpha), \quad \overline{\overline{p}}_3 = 2\kappa_1(3\delta_1 - \alpha),$$
$$\overline{\overline{p}}_2 = 2(\delta_1 - a\kappa_1)\alpha + 4(cm + 3r_2)\kappa_1 a, \quad \overline{\overline{p}}_1 = r_2a(7a\kappa_1 + 3\alpha), \quad \overline{\overline{p}}_0 = r_2a^2(a\kappa_1 + \alpha).$$

Other coefficients are very complex and we do not present here. For $x_2, y \sim 0$, there exists a center manifold $x_1 = O(|x_2, y|^2)$ on which we have

$$\begin{cases} \dot{x_2} &= y + b_{020}x_2^2 + b_{011}x_2y + b_{002}y^2 + O(|x_2, y|^3), \\ \dot{y} &= c_{020}x_2^2 + c_{011}x_2y + c_{002}y^2 + O(|x_2, y|^3). \end{cases} \tag{4.28}$$

Then we use the following near-identity transformation

$$u = x_2, \quad v = y + b_{020}x_2^2 + b_{011}x_2y + b_{002}y^2 + O(|x_2, y|^3).$$

and if we change u, v into x, y, we obtain

$$\begin{cases} \dot{x} &= y, \\ \dot{y} &= m_{20}x^2 + m_{11}xy + O(|x_2, y|^3). \end{cases} \tag{4.29}$$

where

$$
\begin{aligned}
m_{20} =& c_{020} \\
=& \frac{\alpha\overline{E_2}(\delta_1\overline{E_2}+r_2a)}{(a+\overline{E_2})^2(p_3\overline{E_2}^3+p_2\overline{E_2}^2+p_1\overline{E_2}-a^2r_2^2)}\{\kappa_1(3\delta_1-\alpha)\overline{E_2}^2+[(\delta_1-a\kappa_1)\alpha \\
&+a\kappa_1(2cm+5r_2)]\overline{E_2}+r_2a(2\kappa_1a+\alpha)\}, \\
m_{11} =& c_{011}+2b_{020} \\
=& \frac{\widetilde{p}_7\overline{E_2}^7+\widetilde{p}_6\overline{E_2}^6+\widetilde{p}_5\overline{E_2}^5+\widetilde{p}_4\overline{E_2}^4+\widetilde{p}_3\overline{E_2}^3+\widetilde{p}_2\overline{E_2}^2+\widetilde{p}_1\overline{E_2}+\widetilde{p}_0}{(a+\overline{E_2})^2(p_3\overline{E_2}^3+p_2\overline{E_2}^2+p_1\overline{E_2}-a^2r_2^2)^2},
\end{aligned}
$$

with

$$
\begin{aligned}
\widetilde{p}_7 =& 4\kappa_1^2(3\delta_1^2-\alpha^2)(\alpha-\delta_1), \\
\widetilde{p}_6 =& [-14\alpha^3+2(7cm+11r_2)\alpha^2+2\delta_1(11cm+21r_2)\alpha-2(7cm+25r_2)\delta_1^2]a\kappa_1^2 \\
&+(-2\alpha^4+2\delta_1\alpha^3+4\delta_1^2\alpha^2+2\delta_1^3\alpha-6\delta_1^4)\kappa_1, \\
\widetilde{p}_5 =& \Big[-18\alpha^3+6(3cm+8r_2)\alpha^2+4(3c^2m^2+14cmr_2+13r_2^2)\alpha-2\delta_1(2c^2m^2 \\
&+25cmr_2+41r_2^2)\Big]a^2\kappa_1^2+\Big[-6\alpha^4+6(cm+2r_2)\alpha^3+6\delta_1(cm+2r_2)\alpha^2 \\
&+2(3cm+5r_2)\delta_1^2\alpha-4(cm+7r_2)\delta_1^3\Big]a\kappa_1+2\delta_1^3\alpha(\alpha-\delta_1), \\
\widetilde{p}_4 =& \Big[-10\alpha^3+(10cm+53r_2)\alpha^2+(2c^2m^2+15cmr_2+23r_2^2)\alpha-6r_2(2c^2m^2 \\
&+11cmr_2+11r_2^2)\Big]a^3\kappa_1^2+\Big[-6\alpha^4+2(3cm+13r_2)\alpha^3+(2c^2m^2+11cmr_2 \\
&+11r_2^2)\alpha^2+\delta_1(2c^2m^2+17cmr_2+17r_2^2)\alpha-4r_2(4cm+13r_2)\delta_1^2\Big]a^2\kappa_1 \\
&+r_2a\alpha^4+a(2cm+7r_2)\delta_1^2\alpha^2-8r_2a\delta_1^3\alpha,
\end{aligned}
$$

$$\widetilde{p}_3 = \Big[-2\alpha^3 + (2cm + 31r_2)\alpha^2 - r_2(2cm + 3r_2)\alpha - 2r_2^2(6cm + 13r_2)\Big]a^4\kappa_1^2$$
$$+ \Big[-2a^3\alpha^4 + 2a^3(cm + 13r_2)\alpha^3 + a^3\alpha^2 r_2^2 + 2a^3 r_2\delta_1(cm + 5r_2)\alpha$$
$$- 24a^3 r_2^2\delta_1(cm + 2r_2)\Big]\kappa_1 + 3r_2a^2\alpha^4 + 4r_2a^2\delta_1(cm + 2r_2)\alpha^2 - 12a^2r_2^2\delta_1^2\alpha,$$
$$\widetilde{p}_2 = \Big[9r_2\alpha^2 - r_2(cm + 5r_2)\alpha - 4r_2^3\Big]a^5\kappa_1^2 + \Big[12r_2\alpha^3 - r_2(cm + 3r_2)\alpha^2 - r_2(c^2m^2$$
$$+ 4cmr_2 + 2r_2^2)\alpha - 2r_2^3(8cm + 11r_2)\Big]a^4\kappa_1 + 3a^3r_2\alpha^4 - a^3r_2(c^2m^2 - 2r_2^2)\alpha^2$$
$$- 8a^3r_2^3\delta_1\alpha,$$
$$\widetilde{p}_1 = (\alpha - r_2)a^6\alpha r_2\kappa_1^2 + \Big[2a^5r_2\alpha^3 - a^5r_2^2\alpha^2 - 2a^5r_2^2(cm + 2r_2)\alpha - 4a^5r_2^4\Big]\kappa_1$$
$$+ a^4r_2\alpha^4 - 2a^4r_2^2\delta_1\alpha^2 - 2a^4r_2^4\alpha,$$
$$\widetilde{p}_0 = -a^5\alpha r_2^3(\kappa_1 a + \alpha).$$

and rewrite X, Y, τ into x, y, t, the system (4.29) is topologically equivalent to system (4.26). □

From the above theorem, if $m_{20} \neq 0$ and $m_{11} = 0$, S_{12} or S_{23} will be a cusp point and the BT bifurcation will be at least of codimension 3. Huang et al. proved the existence of cusp point of codimension 3 in the generalist predator prey model without stage structure [79]. Also, the existence of cusp type BT bifurcation of codimension 3 has been presented in a small neighborhood of parameter space in the nilpotent focus of codimension 4 [129]. In addition, two BT bifurcation of codimension 2 ($m_{20} \neq 0$, $m_{11} \neq 0$) can occur which is associated with the nilpotent focus of codimension 4. This

is the case called the doubly degenerate BT point with no quadratic term in the normal form ($m_{20} = 0$, $m_{11} = 0$) used in Khibnik et al. (1998) [130].

On the other hand, note that can verify that $m_{20} = 0$ when $\kappa_1 = \kappa_1^*$, $\kappa_2 = \kappa_2^*$, we have that the two cusp points can occur simultaneously to become $S_{12} = S_{23} = S_{123} = S^*$, and the degenerate co-existence equilibrium is a nilpotent singularity of codimension at least 3. The further analysis can be found in the section 4.3.4.

4.3.4 Nilpotent focus and elliptic point, and their bifurcations

From the Prop. 4.2.1, system (4.1) has one unique positive equilibrium $S_{123} = S^*(E_1^*, E_2^*, M^*)$ of multiplicity 3, with

$$E_1^* = \frac{r_1^* a\delta_3}{\delta_1\alpha}, \quad E_2^* = \frac{a\delta_3}{\delta_1}, \quad M^* = \frac{18 r_1^* a c^2 m}{\delta_1\delta_2},$$

where $\delta_3 = 2cm - r_2$ if

$$\kappa_1 = \kappa_1^* = \frac{r_1\delta_1}{a\delta_2}, \quad \kappa_2 = \kappa_2^* = \frac{\delta_1^2\delta_2}{27 r_1 a c^2 m}, \quad r_1 = r_1^* = \frac{2\delta_1\delta_2}{3\delta_3 - \frac{2}{\alpha}\delta_1\delta_2} (\alpha > \frac{2\delta_1\delta_2}{3\delta_3}). \tag{4.30}$$

Theorem 4.3.5. *For system* (4.1) *with all positive parameters and* $(\kappa_1, \kappa_2, r_1)$ *satisfying* (4.30)*, the equilibrium* $S^*(E_1^*, E_2^*, M^*)$ *is a nilpotent singularity of codimension at least 3, and the system* (4.1) *localized at* S^* *has a 2 dimensional center manifold on which the*

system is topologically equivalent to

$$\begin{cases} \dot{x} &= y, \\ \dot{y} &= -x^3 + bxy - x^2y + y^2Q_{12}(x,y). \end{cases} \tag{4.31}$$

where $b = \frac{7r_2 - 8cm}{2\sqrt{\delta_3^2 - \frac{4}{9\alpha^2}\delta_1^2\delta_2\delta_3}}$.

Furthermore, if we fix the parameters a, c, m*, and depending on the value of* r_2 *and* α*, we have* $b = f(r_2, \alpha)$.

(1) When $b > 2\sqrt{2}$ *or* $b < -2\sqrt{2}$*,* S^* *is a codimension 3 nilpotent sigularity of elliptic type.*

(2) When $0 < b < 2\sqrt{2}$ *or* $-2\sqrt{2} < b < 0$*,* S^* *is a nilpotent singularity of the focus type of codimension 3.*

(3) When $b = 0$*,* S^* *is focus type nilpotent point of codimension* 4.

(4) When $b = \pm 2\sqrt{2}$*,* S^* *is elliptic type nilpotent point of codimension* ≥ 4.

Proof. Firstly, we translate the degenerate equilibrium S^* to the origin by $X_1 = E_1 - E_1^*$, $X_2 = E_2 - E_2^*$, $Y = M - M^*$ and expand system (4.1) in the neighborhood of the new

origin, we will have

$$\begin{pmatrix} \dot{X}_1 \\ \dot{X}_2 \\ \dot{Y} \end{pmatrix} = J(S^*) \begin{pmatrix} X_1 \\ X_2 \\ Y \end{pmatrix} + \begin{pmatrix} 0 \\ a_{20}X_2^2 + a_{11}X_2Y + a_{21}X_2^2Y + a_{30}X_2^3 \\ b_{20}X_2^2 + b_{11}X_2Y + b_{02}Y^2 + b_{21}X_2^2Y + b_{30}X_2^3 \end{pmatrix} + Q_1(X_1, X_2, Y), \tag{4.32}$$

where $Q_1(X_1, X_2, Y) = O(|X_1, X_2, Y|^4)$ and

$$J(S^*) = \begin{pmatrix} -\alpha & r_1^* & 0 \\ \alpha & a_{10} & a_{01} \\ 0 & b_{10} & b_{01} \end{pmatrix}, a_{10} = -\frac{6r_1^* cm}{\delta_2}, a_{01} = -\frac{\delta_3}{3c}, b_{10} = \frac{2r_1^* c\delta_1}{\delta_2}, b_{01} = -\frac{2\delta_1}{3},$$

$$a_{11} = -\frac{\delta_1^2}{9amc^2}, a_{20} = \frac{-2r_1^*\delta_1(cm - 2r_2)}{3acm\delta_2}, a_{21} = \frac{\delta_1^3}{27a^2m^2c^3}, a_{30} = -\frac{2r_1^*\delta_1^3}{9a^2c^2m^2\delta_2},$$

$$b_{11} = \frac{\delta_1^2}{9acm}, b_{20} = -\frac{2r_1^*\delta_1^2}{3am\delta_2}, b_{02} = -\frac{\delta_1^2\delta_2}{27ac^2mr_1^*}, b_{21} = -\frac{\delta_1^3}{27a^2c^2m^2},$$

$$b_{30} = \frac{4r_1^*\delta_1^3}{9a^2cm^2\delta_2}.$$

Next we transform the linear part of the system (4.32) to the Jordan canonical form and find $J(S^*)$ is nilpotent. Note that $J(S^*)V_1 = \Lambda V_1$, where $\Lambda = \frac{9\alpha^2\delta_3 - 4\delta_1^2\delta_2}{3(3\alpha\delta_3 - 2\delta_1\delta_2)}$, $V_1 = (\frac{r_1^*}{\alpha+\Lambda}, 1, \frac{U_2'(E_2^*)\kappa_2^*M^*}{\kappa_2^*M^*+\Lambda})$, and the generalized eigenvectors associated with the zero eigenvalues are $V_2 = (\frac{r_1^*}{\alpha}, 1, U_2'(E_2^*))'$, $V_3 = (\frac{r_1^*}{\alpha}(\frac{1}{\kappa_2^*M^*} - \frac{1}{\alpha}), \frac{1}{\kappa_2^*M^*}, 0)'$ which satisfy

$J(S^*)V_2 = 0, J(S^*)V_3 = V_2$. Under the non-singular linear transformation

$$\begin{pmatrix} X_1 \\ X_2 \\ Y \end{pmatrix} = P \begin{pmatrix} x_1 \\ x_2 \\ y \end{pmatrix}, \quad P = (V_1, V_2, V_3),$$

with $|P| = \frac{9c\Lambda}{\alpha\delta_3(3\alpha - 2\delta_1)} > 0$, system (4.32) becomes

$$\begin{cases} \dot{x_1} &= \Lambda x_1 + \sum\limits_{i,j,k\in\mathbb{N}}^{i+j+k=2} \widetilde{a}_{ijk} x_1^i x_2^j y^k + O(|x_1, x_2, y|^3), \\ \dot{x_2} &= y + \sum\limits_{i,j,k\in\mathbb{N}}^{i+j+k=2,3} \widetilde{b}_{ijk} x_1^i x_2^j y^k + O(|x_1, x_2, y|^4), \\ \dot{y} &= \sum\limits_{i,j,k\in\mathbb{N}}^{i+j+k=2,3} \widetilde{c}_{ijk} x_1^i x_2^j y^k + O(|x_1, x_2, y|^4) \end{cases} \tag{4.33}$$

where $\widetilde{c}_{020} = 0$, and we choose not to present other expression of $\widetilde{a}_{ijk}, \widetilde{b}_{ijk}, \widetilde{c}_{ijk}$ here. For $x_2, y \sim 0$, there exists a center manifold. On the center manifold, we have $x_1 = O(|x_2, y|^2)$ and

$$\begin{cases} \dot{x_2} &= y + \widetilde{\widetilde{a}}_{20} x_2^2 + \widetilde{\widetilde{a}}_{11} x_2 y + \widetilde{\widetilde{a}}_{21} x_2^2 y + \widetilde{\widetilde{a}}_{30} x_2^3 + y^2 O(|x_2, y|), \\ \dot{y} &= \widetilde{\widetilde{b}}_{30} x_2^3 + \widetilde{\widetilde{b}}_{11} x_2 y + \widetilde{\widetilde{b}}_{02} y^2 + \widetilde{\widetilde{b}}_{21} x_2^2 y + y^2 O(|x_2, y|). \end{cases} \tag{4.34}$$

Then we use the following near-identity transformation

$$u = x_2, \quad v = y + \widetilde{\widetilde{a}}_{20} x_2^2 + \widetilde{\widetilde{a}}_{11} x_2 y + \widetilde{\widetilde{a}}_{21} x_2^2 y + \widetilde{\widetilde{a}}_{30} x_2^3 + y^2 O(|x_2, y|).$$

and if we change u, v into x, y, we obtain

$$\begin{cases} \dot{x} &= y, \\ \dot{y} &= -\hat{b}_{30} x^3 + y(\hat{b}_{11} x - \hat{b}_{21} x^2) + y^2 \hat{Q}_{12}(x, y). \end{cases} \tag{4.35}$$

where

$$\hat{b}_{30}=\frac{4\alpha^2\delta_1^4\delta_3^2}{9a^2c^2m^2(9\alpha^2\delta_3-4\delta_1^2\delta_2)},\ \ \hat{b}_{11}=\frac{\alpha^2\delta_1^2(7r_2-8cm)}{acm(9\alpha^2\delta_3-4\delta_1^2\delta_2)},$$
$$\hat{b}_{21}=-\frac{4\alpha\delta_1^3(243cm\delta_3^2\alpha^5+\hat{p}_3\alpha^3+\hat{p}_2\alpha^2+\hat{p}_1\alpha+\hat{p}_0)}{3a^2c^2m^2(9\alpha^2\delta_3-4\delta_1^2\delta_2)^3},\quad \alpha\neq\frac{2\delta_1}{3}\sqrt{\frac{\delta_2}{\delta_3}},$$
$$\hat{p}_3=-27\delta_2(16c^2m^2-15cmr_2+5r_2^2)\delta_1^2,\quad \hat{p}_2=9\delta_2(16c^2m^2-36cmr_2+17r_2^2)\delta_1^3,$$
$$\hat{p}_1=-6(8cm-11r_2)\delta_2^2\delta_1^4,\quad \hat{p}_0=16\delta_3\delta_2^2\delta_1^5.$$

If we make a rescaling of coordinates and time by

$$X=\frac{\hat{b}_{21}}{\sqrt{\hat{b}_{30}}}x,\quad Y=\frac{\hat{b}_{21}^2}{\hat{b}_{30}^{\frac{3}{2}}}y,\quad \tau=\frac{\hat{b}_{30}}{\hat{b}_{21}}t$$

and rewrite X,Y,τ into x,y,t. Then we obtain the normal form (4.31), and

$$b=\frac{\hat{b}_{11}}{\sqrt{\hat{b}_{30}}}=\frac{7r_2-8cm}{2\sqrt{\delta_3^2-\frac{4}{9\alpha^2}\delta_1^2\delta_2\delta_3}}.$$

When $b=\pm2\sqrt{2}$, we have the following curve

$$\hat{\alpha}=\alpha(r_2)=\frac{8\sqrt{2}\sqrt{\delta_2\delta_3(64c^2m^2-16cmr_2-17r_2^2)}\delta_1}{3(64c^2m^2-16cmr_2-17r_2^2)},$$
$$(0<r_2<2cm, r_2\neq\frac{24\sqrt{2}-8}{17}cm),$$

which are presented in the Figure 4.7. It follows from the classification criteria for the nilpotent singularity in [127, 128], then we have the classification of nilpotent singularity.

When $r_2=\frac{8}{7}cm$, then we have $b=0$, and

$$\kappa_1^*=\frac{25\alpha cm}{(7\alpha-80cm)a},\kappa_2^*=\frac{5m(7\alpha-80cm)}{343\alpha a},r_1^*=\frac{80\alpha cm}{7\alpha-80cm}(\alpha>\frac{80cm}{7}),$$

and system (4.35) becomes following system

$$\begin{cases} \dot{x} &= y, \\ \dot{y} &= -\hat{\hat{b}}_{30}x^3 - \hat{\hat{b}}_{21}x^2y + y^2\hat{\hat{Q}}_{12}(x,y). \end{cases} \tag{4.36}$$

where

$$\hat{\hat{b}}_{30} = \frac{2500\alpha^2c^2m^2}{49a^2(49\alpha^2 - 800c^2m^2)},$$
$$\hat{\hat{b}}_{21} = \frac{250(-24000c^3m^3 - 22400\alpha c^2m^2 + 2401\alpha^3)cm\alpha}{49a^2(49\alpha^2 - 800c^2m^2)^2}.$$

As $\alpha > \frac{80cm}{7}$, we can easily verify that $\hat{\hat{b}}_{21} > 0$. Then following the same rescaling of coordinates and time, we obtain that

$$\begin{cases} \dot{x} &= y, \\ \dot{y} &= -x^3 - x^2y + y^2\widetilde{\widetilde{Q}}_{12}(x,y). \end{cases} \tag{4.37}$$

We note that the most degenerate equilibrium point of system (4.1) is a codimension 4 nilpotent focus point. This is also observed in our analysis of the generalist predator prey model without stage structure in chapter 3. This most degenerate singularity can serve as the organizing center of the complex dynamics of system (4.1). □

Also, the different types of nilpotent singularities mentioned in Theorem 4.3.5 are present with numerical examples in Figure 4.6. We summarize the above bifurcation analysis in the Table 4.1.

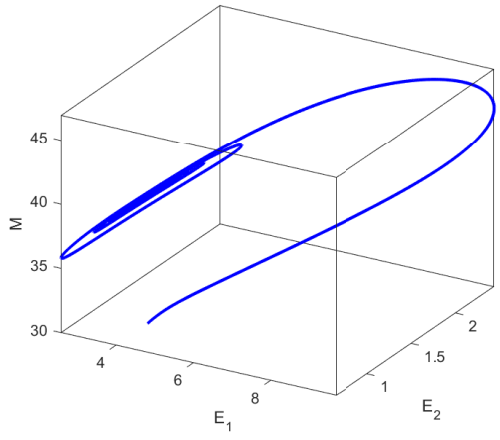

(a) Focus type ($|b| < 2\sqrt{2}$), $r_2 = 0.5, \alpha = 6.25$

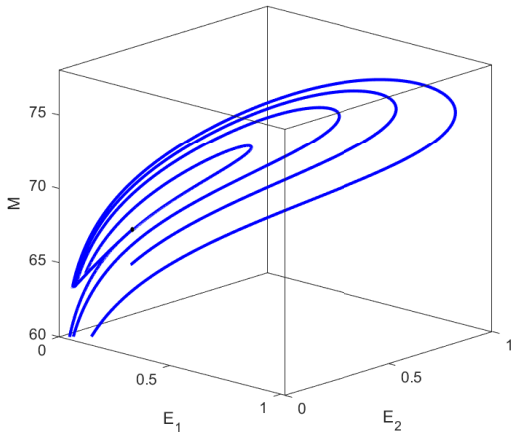

(b) Elliptic type ($|b| > 2\sqrt{2}$), $r_2 = 1.6, \alpha = 50$

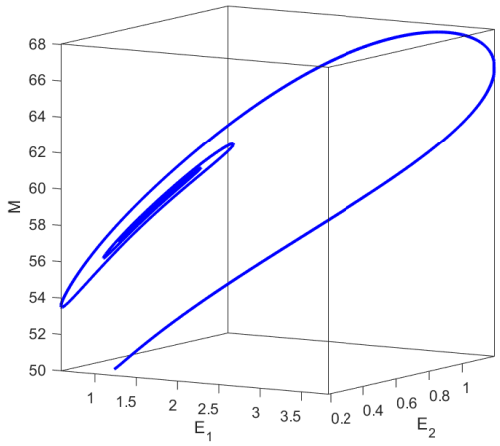

(c) Degenerate focus type ($b = 0$),$r_2 = \frac{8}{7}, \alpha = 15$

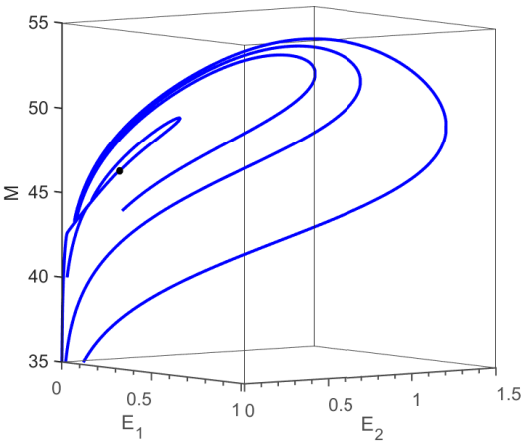

(d) Degenerate elliptic type ($|b| = 2\sqrt{2}$), $r_2 = 1.5243, \alpha = 50$

Figure 4.6: The phase portraits of different type of nilpotent singularities when $\kappa_1 = \kappa_1^*, \kappa_2 = \kappa_2^*, r_1 = r_1^*, a = 1, c = 1, m = 1$.

Table 4.1: The summary of different type of bifurcations in system (4.1)

Conditions	Types of bifurcation	codimension
Pest-free equilibrium $S_{01}(0, 0, \frac{r_2}{\kappa_2})$,		
$\kappa_2 = \frac{r_2 m}{r_1 a}$;	Saddle-node	1
$\kappa_2 = \frac{r_2 m}{r_1 a}$, $\kappa_1 = \frac{r_1(r_2 - cm)}{r_2 a}(r_2 > cm)$;	Saddle-node	2
Coexistence equilibrium $\overline{S}(\overline{E}_1, \overline{E}_2, \overline{M})$,		
$U(\overline{E}) = 0, k_2 - k_1 = \overline{k}, T(J(\overline{S}))) \neq 0$;	Saddle-node	1
$U(\overline{E}) = 0, k_2 - k_1 = \overline{k}, U''(\overline{E}) = 0, T(J(\overline{S})) \neq 0$;	Saddle-node	2
$U(\overline{E}) = 0, T(J(\overline{S})) = 0, D(J(\overline{S})) > 0$;	Hopf	≥ 1
$U(\overline{E}) = 0, k_2 - k_1 = \overline{k}, T(J(\overline{S})) = 0$,	BT	2
$U''(\overline{E}) \neq 0, m_{11} = 0$;	cusp type BT	3
$U''(\overline{E}) = 0$,	Nilpotent singularity	≥ 3
$b = f(r_2, \alpha), \lvert b\rvert < 2\sqrt{2}$;	Focus type	3
$b = f(r_2, \alpha), \lvert b\rvert > 2\sqrt{2}$;	Elliptic type	3
$r_2 = \frac{8}{7}cm$;	Focus type	4
$b = f(r_2, \alpha), \lvert b\rvert = 2\sqrt{2}$;	Elliptic type	≥ 4

Here, we will study system (4.1) for parameters $(\kappa_1, \kappa_2, r_1)$ in a neighborhood of $(\kappa_1^*, \kappa_2^*, r_1^*)$ to explore the complex dynamics which can be bifurcated from the codimen-

sion 3 nilpotent singularity S^*.

Let

$$\kappa_1 = \kappa_1^* + \epsilon_1,\ \kappa_2 = \kappa_2^* + \epsilon_2,\ r_1 = r_1^* + \epsilon_3,$$

where $\epsilon = (\epsilon_1, \epsilon_2, \epsilon_3)$ and $|\epsilon|$ is sufficiently small. Then we will study the bifurcation of the following unfolding system

$$\begin{cases} \dfrac{dE_1}{dt} &= (r_1^* + \epsilon_3)E_2 - \alpha E_1, \\ \dfrac{dE_2}{dt} &= \alpha E_1 - (\kappa_1^* + \epsilon_1)E_2^2 - \dfrac{mE_2M}{a+E_2}, \\ \dfrac{dM}{dt} &= r_2 M - (\kappa_2^* + \epsilon_2)M^2 + \dfrac{cmE_2M}{a+E_2}. \end{cases} \tag{4.38}$$

Theorem 4.3.6. *Denote*

$$\begin{aligned} B_3 =& 54\delta_3^3\alpha^3 - 9(4cm + r_2)(4cm - 3r_2)\delta_1\delta_2\alpha^2 - 6\delta_2(16c^2m^2 - 24cmr_2 + 11r_2^2)\delta_1^2\alpha \\ &+ 16\delta_1^3\delta_2^2\delta_3, \end{aligned}$$

for parameters $|\epsilon|$ sufficiently small and any other positive parameters a, c, m, system (4.38) *is a generic unfolding of the codimension 3 nilpotent singularity of elliptic type when $|b| > 2\sqrt{2}$, of focus type when $|b| < 2\sqrt{2}$, where $b = b(\alpha, r_2) = \frac{7r_2 - 8cm}{2\sqrt{\delta_3^2 - \frac{4}{9\alpha^2}\delta_1^2\delta_2\delta_3}}$, $\alpha > \frac{2\delta_1\delta_2}{3\delta_3}$ and $B_3 \neq 0$.*

Proof. A generic unfolding with the parameters (μ_1, μ_2, μ_3), of codimension 3 nilpotent

singularity is C^∞ equivalent to

$$\begin{cases} \dot{x} &= y, \\ \dot{y} &= \mu_1 + \mu_2 x - x^3 + y(\mu_3 + bx - x^2 + O(x^3)) + y^2 Q(x,y). \end{cases} \tag{4.39}$$

We will show that system (4.38), with parameters $\epsilon = (\epsilon_1, \epsilon_2, \epsilon_3)$, is also a generic unfolding of codimension 3 singularity by showing that there exists smooth coordinate change which take (4.38) into (4.39) with $\frac{D(\mu_1,\mu_2,\mu_3)}{D(\epsilon_1,\epsilon_2,\epsilon_3)}|_{\epsilon=(0,0,0)} \neq 0$.

When $\epsilon = 0$, the system (4.38) has a nilpotent equilibrium $S^*(E_1^*, E_2^*, M^*)$. Let $X_1 = E_1 - E_1^*$,$X_2 = E_2 - E_2^*$, $Y = M - M^*$, and make the transformation

$$\begin{pmatrix} X_1 \\ X_2 \\ Y \end{pmatrix} = P \begin{pmatrix} x_1 \\ x_2 \\ y \end{pmatrix}.$$

When $|\epsilon|$ is sufficient small, the system (4.38) becomes

$$\begin{cases} \dot{x_1} &= l_{000}(\epsilon) + \sum\limits_{i,j,k\in\mathbb{N}}^{i+j+k=1,2} l_{ijk}(\epsilon) x_1^i x_2^j y^k + O(|x_1, x_2, y|^3), \\ \dot{x_2} &= m_{000}(\epsilon) + \sum\limits_{i,j,k\in\mathbb{N}}^{i+j+k=1,2,3} m_{ijk}(\epsilon) x_1^i x_2^j y^k + O(|x_1, x_2, y|^4), \\ \dot{y} &= n_{000}(\epsilon) + \sum\limits_{i,j,k\in\mathbb{N}}^{i+j+k=1,2,3} n_{ijk}(\epsilon) x_1^i x_2^j y^k + O(|x_1, x_2, y|^4) \end{cases} \tag{4.40}$$

When $\epsilon = 0$, then $l_{000}(\epsilon) = 0, m_{000}(\epsilon) = 0, n_{000}(\epsilon) = 0$, and coefficients $l_{ijk}(0), m_{i,j,k}(0)$, $n_{i,j,k}(0)$ are equal to the corresponding coefficients in the system (4.33). Moreover, when $\epsilon = 0$, coefficients in the following computation process should be aligned with those in

each step of the Theorem 4.3.5. Then we compute the center manifold

$$x_1 = h(x_2, y) = \sum_{i,j\in\mathbb{N}}^{0\le i+j\le 2} h_{ij}(\epsilon) x_2^i y^j + O(|x_2, y|^3),$$

and reduce the system to a planar system.

$$\begin{cases} \dot{x_2} &= \widetilde{l}_{00}(\epsilon) + \sum_{i,j\in\mathbb{N}}^{i+j=1,2,3} \widetilde{l}_{ij}(\epsilon) x_2^i y^j + O(|x_2, y|^4), \\ \dot{y} &= \widetilde{m}_{00}(\epsilon) + \sum_{i,j\in\mathbb{N}}^{i+j=1,2,3} \widetilde{m}_{ij}(\epsilon) x_2^i y^j + O(|x_2, y|^4). \end{cases} \tag{4.41}$$

Then, we make the following transformation

$$u = x_2, \quad v = \widetilde{l}_{00}(\epsilon) + \sum_{i,j\in\mathbb{N}}^{i+j=1,2,3} \widetilde{l}_{ij}(\epsilon) x_2^i y^j + O(|x_2, y|^4),$$

and system (4.41) can be transformed into

$$\begin{cases} \dot{u} &= v, \\ \dot{v} &= \widetilde{\widetilde{l}}_{00}(\epsilon) + \sum_{i,j\in\mathbb{N}}^{i+j=1,2,3} \widetilde{\widetilde{l}}_{ij}(\epsilon) u^i v^j + O(|u, v|^4). \end{cases} \tag{4.42}$$

After a sequence of coordinate changes depending on the parameters $(\epsilon_1, \epsilon_2, \epsilon_3)$, we obtain the normal form (4.39) where (μ_1, μ_2, μ_3) is a function of $(\epsilon_1, \epsilon_2, \epsilon_3)$. And we can verify that

$$\left| \frac{\partial(\mu_1, \mu_2, \mu_3)}{\partial(\epsilon_1, \epsilon_2, \epsilon_3)} \right|_{\epsilon=0} = \frac{104976 a^2 c B_1 B_2 B_3 B_4^6}{\alpha \delta_1^4 \delta_3^4 (9\alpha^2\delta_3 - 4\delta_1^2\delta_2)^{18} B_5}. \tag{4.43}$$

where

$$B_1 = 3\alpha\delta_3 - 2\delta_1\delta_2, \quad B_2 = 9\alpha^2\delta_3 - 8\delta_1^2(r_2 + 4cm),$$

$$B_4 = 243cm\delta_3^2\alpha^5 - 27(16c^2m^2 - 15cmr_2 + 5r_2^2)\delta_1^2\delta_2\alpha^3 + 9(16c^2m^2 - 36cmr_2 + 17r_2^2)\delta_1^3\delta_2\alpha^2 - 6(8cm - 11r_2)\delta_1^4\delta_2^2\alpha + 16\delta_1^5\delta_2^2\delta_3,$$

$$B_5 = \sqrt{\frac{\delta_3}{(9\alpha^2\delta_3 - 4\delta_1^2\delta_2)}}, \alpha \neq \frac{2\delta_1}{3}\sqrt{\frac{\delta_2}{\delta_3}}.$$

Thus, the transformation of parameters is nonsingular if $B_1 \neq 0, B_2 \neq 0, B_3 \neq 0, B_4 \neq 0$. The parameters are positive and we know that $\alpha > \frac{2\delta_1\delta_2}{3\delta_3}$ and $0 < r_2 < 2cm$. Then we can easily verify that $B_1 > 0, B_2 > 0, B_4 > 0$. When $B_3 \neq 0$, the system (4.38) with parameters $\epsilon = (\epsilon_1, \epsilon_2, \epsilon_3)$, is a generic family unfolding the codimension 3 nilpotent singularity. □

From the analysis above, we observe that there is no universal unfolding of the codimension 3 nilpotent singularity when $B_3 = 0$. We display the curve of $B_3 = 0$ in the Figure 4.7 given that $\alpha > \frac{2\delta_1\delta_2}{3\delta_3}$, which is equivalent to $B_1 > 0$. Compared with the model without a stage structure, the introduction of α in the model with stage structure results in the change of dynamics of the model. It will affect the classification of nilpotent singularity. Also, we can not unfold the singularity point of codimension 3 along the curve B_3 shown in Figure 4.7. This phenomena is not observed in the model without stage structure which indicates that a model with stages structure may have degenerate singularities with higher codimension and more complex dynamics than the model without stages.

Remark 4.3.7. *For system* (4.1)*, the co-existence equilibrium of multiplicity 3,* S_{123}*,*

- *if* $T(J(S_1 23)) \neq 0$*, it is a saddle node of codimension 2.*
- *if* $T(J(S_1 23)) = 0$*, it occurs at* $S_{123} = S^*$ *and it is a elliptic or focus type nilpotent point of codimension 3 or 4, depending on the value of* r_2 *and* α*.*

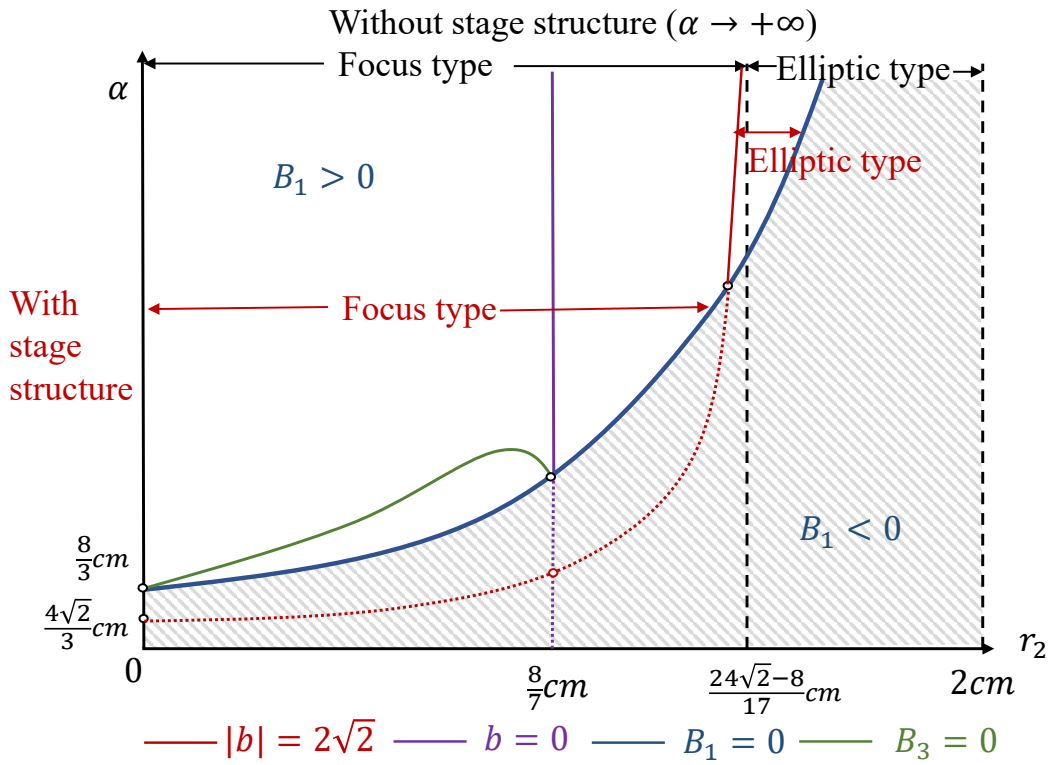

Figure 4.7: The type of nilpotent singularity with varying r_2 and α. The red color represents the situation with stage structure, while the black color represents when there is no stage structure. The area without shadow is the reasonable parameter space. The solid red curve separates the focus type and elliptic type of nilpotent singularity in the model with the stage structure on prey. The blue and green line represent $B_1 = 0$ and $B_3 = 0$. The purple line represents the condition of the nilpotent focus of codimension 4, $b = 0$.

4.3.5 Bifurcation diagram

4.3.5.1 The bifurcation diagram on (κ_1, κ_2) plane near focus and elliptic nilpotent point

The bifurcation diagrams for the focus and elliptic type of nilpotent singularities has been presented in chapter 3. Here, we only present the slice of bifurcation diagram on (κ_1, κ_2) plane near the focus type and elliptic type nilpotent singularities of codimension 3, which are given in Figure 4.8. We fixed $a = 1, c = 1, m = 1, r_1 = r_1^*$, and the coexistence equilibrium point is nilpotent singularity of focus type when $r_2 = 0.5, \alpha = 6.25$ and elliptic type when $r_2 = 1.6, \alpha = 50$, according to the Theorem 4.3.5. Like found in chapter 3, we observed that the curve of Hopf bifurcation and saddle-node bifurcation are tangent at different positions. In the most degenerate focus case of nilpotent singularities, the two branches of saddle node bifurcation curves are tangent to the two branches of Hopf bifurcation curves (Figure 4.8(e)). The BT point separates the Hopf bifurcation curve and the neutral saddle curve while the degenerate Hopf bifurcation point separates the supercritical and subcritical Hopf bifurcation curve. Note that the BT point in the Figure 4.8(a)-4.8(d) should be nilpotent singularity of codimension 3 as here we fix $r_1 = r_1^*$.

4.3.5.2 The effect of hatching rate on the *E. onukii* populations dynamic

We plot the one parameter bifurcation diagram in (α, E_2) plane in Figure 4.9 and present the effect of the hatching rate of *E. onukii* egg (α) on the dynamics of the system. We observe its different performances under different parameter values of intra-specific competition of *E. onukii* hatched individuals (nymphs and adults) (κ_1) and intra-specific competition of *A. baccarum* (κ_2), when the net oviposition rate of *E. onukii* (r_1) and growth rate of *A. baccarum* (r_2) are fixed where the coexistence equilibrium is focus type (Figure 4.9(a) - 4.9(d)) or elliptic type (Figure 4.9(e)) nilpotent singularity of codimension 3, and other parameters are fixed.

When the system has only one coexistence equilibrium (Figure 4.9(b) - 4.9(d)), with the decrease of α, that is, extending the incubation time of the *E. onukii* eggs, the amplitude of the system's limit cycle may gradually decrease, until it finally disappears and becomes a stable coexistence equilibrium (Figure 4.9(b)). Also, it may go through one stable limit cycle to two limit cycles (one stable, one unstable), then to a stable coexistence equilibrium (Figure 4.9(c), 4.9(d)) as the decrease of α. This is also intuitively illustrated by the Figure 4.2, 4.3 and 4.4.

When the system has three coexistence equilibria (Figure 4.9(a), 4.9(e)), the amplitude of stable limit cycle decrease with the decrease of α, while the amplitude of the unstable limit cycle increases with the decrease of α. Then the system will have a sta-

ble coexistence equilibrium with low abundance of *E. onukii* when α decreases to some extent.

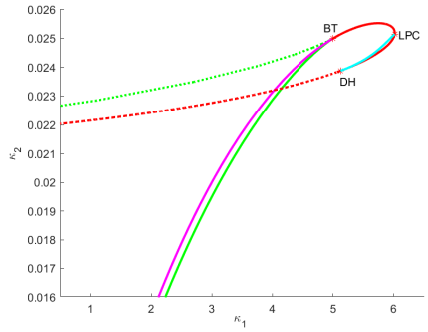

(a) Focus type, $r_2 = 0.5, \alpha = 6.25$

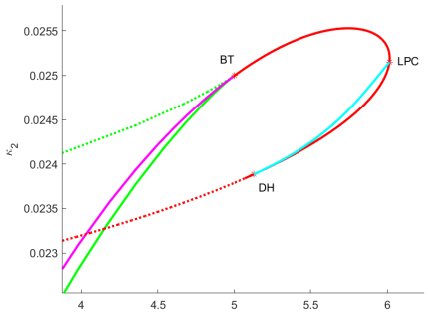

(b) Focus type, zoom plot

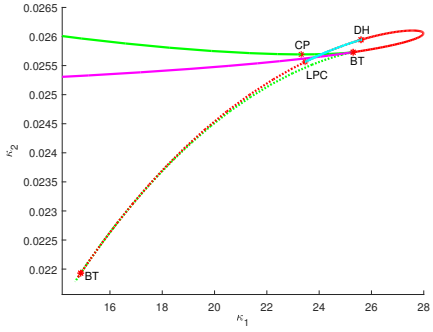

(c) Elliptic type, $r_2 = 1.6, \alpha = 50$

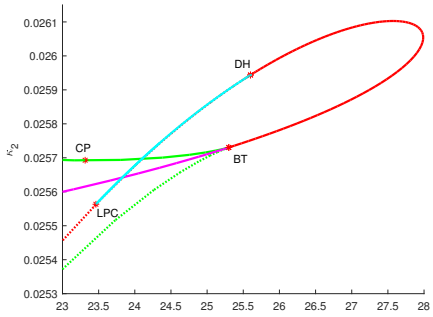

(d) Elliptic type, zoom plot

Figure 4.8: A slice of codimension 3 bifurcation diagram near focus type and elliptic type nilpotent singularities. CP, BT, DH and LPC denote the cusp bifurcation point, the Bogdanov-Takens bifurcation point, degenerate Hopf bifurcation point and limit point of limit cycle, respectively. The green solid and dot lines are the stable and unstable saddle-node bifurcation respectively; red solid and dot line represents the supercritical and subcritical Hopf bifurcation; cyan line stands for the saddle-node of limit cycle; magenta line is neutral saddle curve not the bifurcation curve. $r_1 = r_1^*, a = 1, c = 1, m = 1$.

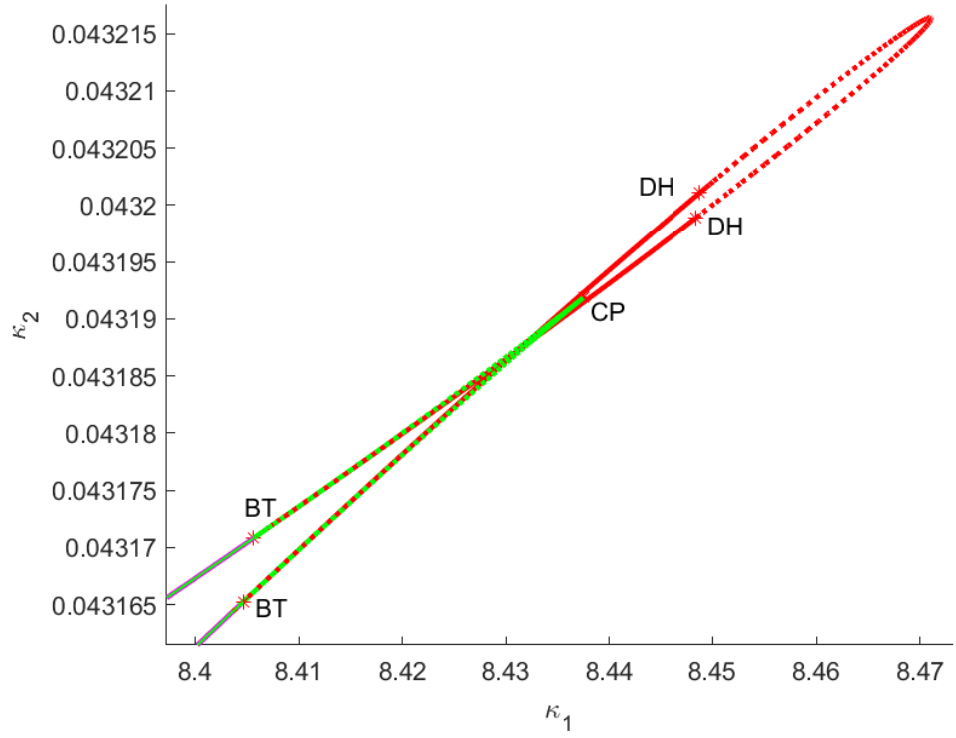

(e) Degenerate focus, $r_2 = \frac{8}{7}, \alpha = 20$

Figure 4.8: (Continued) A slice of codimension 3 bifurcation diagram near focus type and elliptic type nilpotent singularities. CP, BT, DH and LPC denote the cusp bifurcation point, the Bogdanov-Takens bifurcation point, degenerate Hopf bifurcation point and limit point of limit cycle, respectively. The green solid and dot lines are the stable and unstable saddle-node bifurcation respectively; red solid and dot line represents the supercritical and subcritical Hopf bifurcation; cyan line stands for the saddle-node of limit cycle; magenta line is neutral saddle curve not the bifurcation curve. $r_1 = r_1^*, a = 1, c = 1, m = 1$.

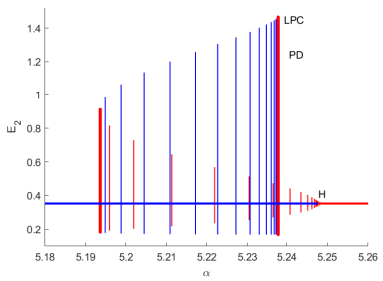

(a) $\kappa_2 = 0.024, \kappa_1 = 4.4386424, r_1 = 25, r_2 = 0.5$

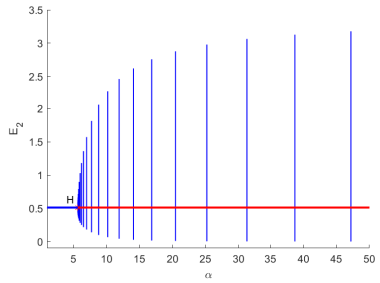

(b) $\kappa_2 = 0.025, \kappa_1 = 5.5, r_1 = 25, r_2 = 0.5$

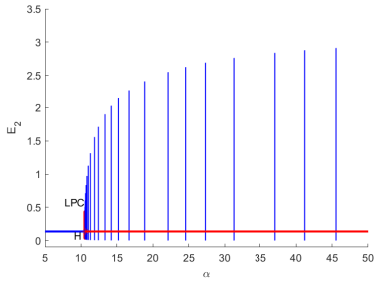

(c) $\kappa_2 = 0.0225, \kappa_1 = 5.5, r_1 = 25, r_2 = 0.5$

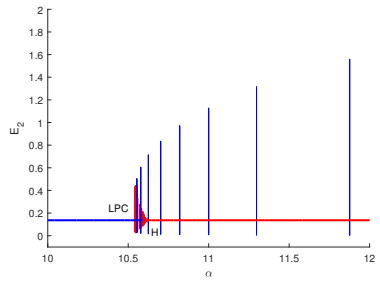

(d) zoom plot of (c)

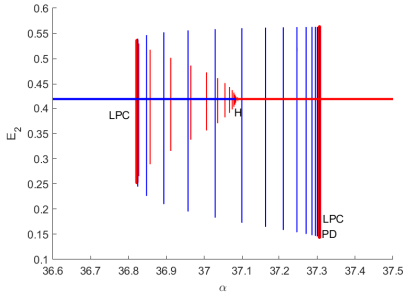

(e) $\kappa_2 = 0.02568, \kappa_1 = 24.5, r_1 = 62.27545, r_2 = 1.6$

Figure 4.9: Bifurcation diagram in (E_2, α) plane with different situations and $a = 1, c = 1, m = 1$. LPC, PD and H represents the limit point of limit cycle, periodic doubling and Hopf bifurcation point. The blue and red color represent the equilibrium is stable and unstable, respectively.

4.4 Discussion

In this chapter, we carry out the bifurcations of this three-dimensional nonlinear system for a generalist predator-prey model with stage structure of prey with Holling type II functional response. We find that the nilpotent singularity of codimension 4 serves as an organizing center for the complex dynamics of the model (4.1). The cusp type of BT bifurcation of codimension 3, focus type of nilpotent singularity of codimension 3, and elliptic type of nilpotent singularity of codimension 3, can occur in system (4.1), which is also observed in chapter 3, and Huang et al. (2020) in the generalist predator prey model without stage structure [79]. These three different codimension 3 bifurcations can can occur from the nilpotent focus of codimension 4. Moreover, we summarize the general classification of nilpotent singularity, and this is also related to the unfolding of the nilpotent focus of codimension 4.

The κ_1, κ_2 describe the crowded effect of the tea plantation with regard to the growth of *E.onukii* and *A. baccarum*. From our analysis, we find when $\kappa_2 < \overline{\kappa}_2$, it is possible to eradicate the pest *E.onukii*. However, if κ_1 is also relatively small, the pest *E.onukii* will either go extinct or outbreak. In this case, pest control heavily depend on the initial abundance of *E. onukii* and *A. baccarum* populations. And there exist the scenarios that the higher abundance of *A. baccarum* will lead to the higher abundance of *E. onukii*. The increase of *A. baccarum* abundance cannot help control *E. onukii*, it may lead to

the outbreak of *E. onukii*. This may also help to explain the field observations in Chen et al [122] that there is no significant decrease of the *E. onukii* abundance though the significant increase of *A. baccarum* abundance was observed. Hence, we need to be more careful when using the generalist predator to control the pest.

Moreover, we compare the system (3.1) and our generalist predator-prey model with stage structure, system (4.1), and the results are presented in Table 4.2. We notice that the condition that the determinant of the Jacobian matrix at co-existence equilibrium is equal to zero is different in the model with and without stage structure, and does not relate to the α. As α goes to ∞, the condition that trace of Jacobian matrix at coexistence equilibrium with multiplicity 3 equals to zero in the model with stage structure is the same with the model without structure. This also can be seen for the coefficient of xy term in the normal form of the system at nilpotent singularity (b). When the incubation time of the *E. onukii* eggs is extremely short, the performance of the model with stage structure is aligned with the model without stage structure.

	without stage structure	with stage structure
D(J($\overline{S}$))=0	$U_2'(\overline{E_2}) - U_1'(\overline{E_2}) = 0$	$U_2'(\overline{E_2}) - U_1'(\overline{E_2}) = \frac{r_1}{P(\overline{E_2})}$
T(J(S_{123}))=0	$r_1^* = \frac{2\delta_1\delta_2}{3\delta_3}$	$r_1^* = \frac{2\delta_1\delta_2}{3\delta_3 - \frac{2}{\alpha}\delta_1\delta_2}$
b	$\frac{7r_2 - 8cm}{2\delta_3}$	$\frac{7r_2 - 8cm}{2\sqrt{\delta_3^2 - \frac{4}{9\alpha^2}\delta_1^2\delta_2\delta_3}}$

Table 4.2: The comparison between the model with and without stage structure.

Furthermore, we find that the hatching rate α has an impact on the dynamics of the system. Different values of α can correspond to different types of nilpotent singularity (Figure 4.7), and the different phase portraits can be observed. In addition, choosing α as a bifurcation parameter, we show that Hopf bifurcations can occur as α crosses some critical values. The system can have periodic solutions. As decreasing the hatching rate, the amplitude of the system's limit cycle may gradually decrease or becomes a stable coexistence equilibrium (Figure 4.9). This also indicates that extending the incubation time of *E. onukii* eggs can be beneficial to pest control. From the biological perspective, the pruning and plucking at the appropriate time are an efficient way to suppress the pest population as the egg of *E.onukii* in the tea tender stem can be taken away, which extend the incubation time of *E. onukii* eggs to ∞.

In addition, it is well-known that the introduction of maturation delay into the predator-prey system can result in the periodic oscillations of populations and complex dynamics,

which has been widely proved in the delay differential equation models [144, 145, 146]. However, our stage structure model by introducing the hatching rate α also reveals this phenomenon, which is not observed in previous ordinary differential equation models.

In this chapter, we investigate the complex dynamics in the generalist predator-prey model with stage structure for prey. The focus type of nilpotent point of codimension 4 serves as the organizing center of all the complex bifurcations that occurred in the system. This most degenerate singularity is also related to the general cubic Liénard equations. Most importantly, we observe that the introduction of stage structure results in the change of dynamics of the generalist predator-prey model. The hatching rate α of *E. onukii* eggs has a great impact on the *E. onukii* and *A. baccarum* populations. The periodic oscillations of the *E. onukii* and *A. baccarum* populations may result from the change of hatching rate of *E. onukii* eggs, which illustrates the importance of incorporating the different life stages of species into the model.

5 Conclusions and future work

5.1 Conclusions

The TGL, *E. onukii*, is one of the most predominant insect pests threatening tea production in many countries [11, 139]. The damage caused by *E. onukii* may result in more fragments, astringent taste and lower quality of made tea, and account for 15-50% total loss of tender tea shoots [5, 11, 149]. However, the control of this pest relies primarily on the heavy use of insecticides which may also increase the insecticide resistance of *E. onukii*. Also, the pesticide residues in the made tea further enlarge the economic losses. Hence, it is essential for the tea economy to develop safe, economic and sustainable control measures to prevent and control *E. onukii*.

A potential biological control agent, the predatory mite *A. baccarum* is an important predator of the leafhopper pest in various agricultural systems, which can prey on *E. onukii* and other insects in tea plantations. Because of its broad feeding habit, the generalist predator is believed to have little advantage in conferring effectiveness in biological control. Nevertheless, the *A. baccarum* have been found that it is beneficial to ecosys-

tems. The role of generalist predators in controlling pests has also been explored in some cropping systems through field experiments. Hence, a good understanding of generalist predatory mite *A. baccarum* and the leafhopper pest *E. onukii* population dynamics is crucial for tea pest suppression. In this dissertation, we aim to understand the population dynamics between *A. baccarum* and *E. onukii*, and then to help achieve the biological control of *E. onukii*.

Firstly, we apply the statistical method to investigate how the relationship of the abundance of the predatory mite and its leafhopper prey is influenced by different treatments, using the field experimental data. We conduct the generalized linear mixed model (GLMM), in particular, zero inflated Poisson mixed models which combine binary logistic and Poisson distributions for the response variable as the monitoring data of both species was strongly overdispersed and had significantly more zero counts than would be expected from a Poisson distribution. We find that the abundance of *A. baccarum* was significantly higher in tea canopies of intercropped treatments than in canopies over natural ground cover and litter samples showed higher abundances of *A. baccarum* when tea was intercropped with *Paspalum notatum* than with natural ground cover, in the first year of treatment. The abundance of *E. onukii* in tea canopies was higher over the bare ground treatment in the first year but the opposite was observed in the second year. Our results suggest that the abundance of *A. baccarum* in a tea plantation is influenced by intercropping and it can affect its leafhopper prey, albeit, with varying levels of suppres-

sion. However, the direct interaction between *A. baccarum* and *E. onukii* is not clear.

Then, we use a predator-prey model with a generalist predator and aim to explore the dynamics of leafhopper pest *E. onukii* and predatory mite *A. baccarum* and the mechanism to inform biological control. In addition to the commonly well-presented bifurcations include saddle-node bifurcation of codimension 1 and 2, Hopf bifurcation, Bogdanov-Takens bifurcation, we also discover the nilpotent singularities of elliptic type of codimension 3 and 4 serves as organizer center to connect all the dynamics. One interesting observation is that we numerically show the existence of three limit cycles in a planar predator-prey system. It turns out that there are many different co-existence states and the co-existence of these two species is always possible. The system can have bistability and tristability. Moreover, the introduction of *A. baccarum* always reduces the *E. onukii* abundance below the carrying capacity and may be beneficial to pest control. When the carrying capacity of the predatory mite *A.baccarum* is high enough, the pest-free equilibrium is locally stable. Although eradication is possible, it also depends on the initial conditions of the *A. baccarum* and *E. onukii* populations. When the carrying capacity of *A.baccarum* is high, the coexistence equilibrium still exists. If the initial abundance of pests is high, we may not eradicate the pest. Using the generalist predator to control the pest is much difficult. We may need to understand their dynamics, then to better use this kind of natural enemy to control the tea pest.

Finally, we incorporate the stage structure of prey into our generalist predator prey

model and analyze the higher codimension bifurcations in higher dimension nonlinear systems. Also, we compare our generalist predator prey model with and without stage structure and the performance of the model with stage structure is aligned with the model without stage structure if the incubation time of *E. onukii* is extremely short. The model has complex dynamics as we noticed in the model without stage structure. Moreover, the successful hatching rate of *E. onukii* eggs has great impacts on the *E. onukii* and *A. baccarum* populations. The change of successful hatching rate can result in the periodic oscillation of *E. onukii* and *A. baccarum* populations, which is not observed in previous ordinary differential equation models. Also, with the decrease of successful hatching rate, the amplitude of the system's limit cycle may decrease, which indicates that extending the incubation time of *E. onukii* eggs can be beneficial to control of *E. onukii*.

In this work, we are focusing on the pest control effect of biological methods, especially by improving the influence of natural enemies on pest population through conservation biological control method, like the cover crop in the tea plantations. We find that the intercropping may increase the abundance of the *A. baccurum* significantly. From a mathematical point of view, we can control the bifurcation parameters that we mentioned in our work, like the K_1, the carrying capacity of *E.onukii*, K_2, the carrying capacity of *A. baccarum*, r_1, the growth rate of *E.onukii*, r_2, the growth rate of *A. baccarum*, α, the successful hatching rate of *E.onukii* eggs in the field practice. We can choose to decrease α by plucking and pruning. Also, increasing the r_2 and K_2 through the intercropping.

Hence, regular pruning and plucking are recommended, as it can take away the egg of *E. onukii*, which are crucial to pest control. Light traps and sticky traps are also helpful to reduce the carrying capacity of the pest *E.onukii*. But the growth rate and carrying capacity mainly depend on the environmental factors or biological factors. If we plant the cover crop in the tea plantations, we may increase the r_2 and K_2, but the r_1 and K_1 may also increase. These parameters are correlated in the reality. We need carefully to increase those parameters.

In conclusion, the generalist predator *A. baccarum* can be helpful to control the *E. onukii*. However, the many different co-existence states also indicate that pest control is not easy. There is the situation that *A. baccarum* and *E. onukii* are in battle forever, which the pest *E. onukii* can not be eradicated even if the number of predator are plenty. Increasing the birth rate of *A. baccarum*, increasing the carrying capacity of *A. baccarum*, like providing suitable habitat for *A. baccarum*, and extending the incubation time of *E. onukii* eggs can help to the control of *E. onukii*.

5.2 Future work

The oviposition, mortality rate of *E. onukii* can be influenced by the agricultural operations (like pruning, picking), the environmental factors (like temperature, precipitation), and the biological factors (predators, parasitoids, pathogens, viruses, and fungus). Agricultural operations, especially picking and pruning, will not only take away a large num-

ber of small *E. onukii* eggs [150], but also reduce the food for the *E. onukii* nymphs and adults, which is currently very important prevention and control measure for *E. onukii*. Also, the oviposition rate of adult *E. onukii* may be reduced due to the lack of young shoots. It will have a great impact on *E. onukii* growth and reproduction.

In future work, from the perspective of biology, we may consider the environmental factors (like the temperature, precipitation) into the model and to investigate its impact on the the *E. onukii* and *A. baccarum* population dynamics. Also, the behaviors of the insect, the fear effect or the resistant of the prey *E. onukii* can be included in the model.

Moreover, from the perspective of mathematics, we can extend our work to higher dimension nonlinear systems. To better model the reality, the stage structure for the predator, the cannibalism, different functional response can also be considered.

In addition, the population dynamics of different species in the tea plantation are complicated. In the dissertation, we only consider the two species, generalist predator, predatory mite *A. baccarum* and prey leafhopper pest *E. onukii*. In future work, we can consider more species into the model, like including the tea leaves growth, which may affect the growth of *A. baccarum* and *E. onukii*.

Bibliography

[1] D. Bolton. "Tea Consumption Second Only to Packaged Water". In: *World tea news* (2018). URL: https://worldteanews.com/tea-industry-news-and-features/tea-consumption-second-only-to-packaged-water.

[2] *FAOSTAT database*. Tech. rep. Food and Agriculture Organization of United Nations, 2018. URL: http://www.fao.org/faostat/en/#data.

[3] L.K. Hazarika, M. Bhuyan, and B.N. Hazarika. "Insect pests of tea and their management". In: *Annual Review of Entomology* 54 (2009), pp. 267–284.

[4] G.Y. Ye et al. "Tea: biological control of insect and mite pests in China". In: *Biological Control* 68 (2014), pp. 73–91.

[5] Q.C. Shi et al. "Advances on prevention and control technology of *Empoasca vitis* (Göethe) in tea garden". In: *Journal of Agriculture* 5 (2015), pp. 20–24.

[6] Q. Wei et al. “Susceptibility of *Empoasca vitis* (Hemiptera: Cicadellidae) populations from the main tea-growing regions of China to thirteen insecticides”. In: *Crop Protection* 96 (2017), pp. 204–210.

[7] G. Zehnder et al. “Arthropod pest management in organic crops”. In: *Annu. Rev. Entomol.* 52 (2007), pp. 57–80.

[8] G.M. Gurr et al. “Habitat management to suppress pest populations: progress and prospects”. In: *Annual Review of Entomology* 62 (2017), pp. 91–109.

[9] M.G. Feng et al. “Field trials of an oil-based emulsifiable formulation of Beauveria bassiana conidia and low application rates of imidacloprid for control of false-eye leafhopper *Empoasca vitis* on tea in southern China”. In: *Crop Protection* 23.6 (2004), pp. 489–496.

[10] X.Y. Pu, M.G. Feng, and C.H. Shi. “Impact of three application methods on the field efficacy of a Beauveria bassiana-based mycoinsecticide against the false-eye leafhopper, *Empoasca vitis* (Homoptera: Cicadellidae) in the tea canopy”. In: *Crop Protection* 24.2 (2005), pp. 167–175.

[11] S. Jin et al. “Characterization of EPG waveforms for the tea green leafhopper, *Empoasca vitis* Göthe (Hemiptera: Cicadellidae), on tea plants and their correlation with stylet activities”. In: *Journal of Insect Physiology* 58.9 (2012), pp. 1235–1244.

[12] Z.Q. Zhang and Z.M. Chen. “Non-host plant essential oil volatiles with potential for a ’push-pull’ strategy to control the tea green leafhopper, *Empoasca vitis*”. In: *Entomologia Experimentalis et Applicata* 156.1 (2015), pp. 77–87.

[13] F. Pavan and P. Picotti. “Influence of grapevine cultivars on the leafhopper *Empoasca vitis* and its egg parasitoids”. In: *BioControl* 54.1 (2009), pp. 55–63.

[14] D. Fornasiero et al. “Effects of irrigation on the seasonal abundance of *Empoasca vitis* in North-Italian vineyards”. In: *Journal of Economic Entomology* 105.1 (2012), pp. 176–185.

[15] D. Fornasiero et al. “Relative infestation level and sensitivity of grapevine cultivars to the leafhopper *Empoasca vitis* (Hemiptera: Cicadellidae)”. In: *Journal of Economic Entomology* 109.1 (2015), pp. 416–425.

[16] X.Y. Li and Q.G. Shi. “Research Progress on Prevention and Control Technology of *Empoasca vitis* Göthe in Tea Garden.” In: *Plant Diseases & Pests* 6.6 (2015).

[17] L.Q. Shi et al. “Adult tea green leafhoppers, *Empoasca onukii* (Matsuda), change behaviors under varying light conditions”. In: *PloS One* 12.1 (2017), e0168439.

[18] W. Zhang, M. Lin, and H. Zhang. “Relationship between temperature and development of *Empoasca vitis* Göthe (Lepidoptera: Cicadelidae)”. In: *Journal of Anhui Agricultural College* 24.4 (1997), pp. 332–335.

[19] E.A. Backus, M.S. Serrano, and C.M. Ranger. “Mechanisms of hopperburn: an overview of insect taxonomy, behavior, and physiology”. In: *Annu. Rev. Entomol.* 50 (2005), pp. 125–151.

[20] K.L. Song T.Q.and Wang et al. “Ecological effects of intercropping white clover on tea plantation in a subtropical hilly region”. In: *Acta Ecol Sin* 26.11 (2006), pp. 3647–3655.

[21] H.X. Ye et al. “Effect of intercropping tea with citrus, waxberry, or snake gourd on population density and spatial distribution of the tea green leafhopper and araneids”. In: *Acta Ecol Sinica* 30 (2010), pp. 6019–6026.

[22] Y.G. Wang et al. “Investigation on population dynamics of *Empoasca vitis* (Göthe) of different planting patterns.” In: *Southwest China Journal of Agricultural Sciences* 23.2 (2010), pp. 413–415.

[23] Q.S. Wang, D.F. Wang, and G.Y. Wu. “Research advances on *Empoasca vitis* (Göthe) in tea trees in China”. In: *Fujian Journal of Agricultural Sciences* 6 (2013), p. 021.

[24] W.J. Gao et al. “Rinsing tea before brewing decreases pesticide residues in tea infusion”. In: *Journal of Agricultural and Food Chemistry* 67.19 (2018), pp. 5384–5393.

[25] A.G.S. Cuthbertson and A.K. Murchie. “Ecological benefits of *Anystis baccarum* in an orchard ecosystem and the need for its conservation”. In: *International Journal of Environmental Science & Technology* 7.4 (2010), pp. 807–813.

[26] A.G.S. Cuthbertson, B.L. Qiu, and A.K. Murchie. “*Anystis baccarum*: an important generalist predatory mite to be considered in apple orchard pest management strategies”. In: *Insects* 5.3 (2014), pp. 615–628.

[27] H.J. Wu. “Preliminary studies on *Anystis baccarum* (Linnaeus) (Acari: Anystidae)”. In: *Natural Enemies of Insects* 3.16 (1994), pp. 101–106.

[28] Cuthbertson A.G.S. and M.K. Archie. “*Anystis baccarum*-a predatory mite in UK apple orchards”. In: *Research Journal of Chemistry and Environment* 16.3 (2012), pp. 18–21.

[29] A.G.S. Cuthbertson and A.K. Murchie. “The phenology, oviposition and feeding rate of *Anystis baccarum*, a predatory mite in Bramley apple orchards in Northern Ireland”. In: *Experimental & Applied Acarology* 34.3 (2004), pp. 367–373.

[30] Z.H. Zeng et al. “Toxicity of five insecticides on predatory mite (*Anystis baccarum* L.) and their effects on predation to tea leafhopper (Empoasca vitis Göthe)”. In: *Journal of Tea Science* 27.2 (2007), pp. 147–152.

[31] D.Q. Liao, G.E. Liang, and Y.J. Cen. “Effects of the predation of big red mite *Anystis baccarum* on tea red mite Oligonychus coffeae.” In: *Journal of Fu-*

jian Agriculture and Forestry University (Natural Science Edition) 39.2 (2010), pp. 117–122.

[32] I.J. Geary et al. "Predation of nymphal tomato potato psyllid, Bactericera cockerelli (Šulc)(Hemiptera: Triozidae), by the predatory mite, *Anystis baccarum* L.(Trombidiformes: Anystidae)". In: *New Zealand Entomologist* 39.2 (2016), pp. 110–116.

[33] Z.H. Zeng et al. "Toxicity of five insecticides on predatory mite (*Anystis baccarum* L.) and their effects on predation to tea leafhopper (Empoasca vitis Göthe)". In: *Journal of Tea Science* 27.2 (2007), pp. 147–152.

[34] P. Hong, S.H. You, and R.Z. Wang. "The dynamic regularity and control technology of *Emposca vitis* Göthe of the organic tea garden". In: *J Guizhou Tea* 42 (2014), pp. 18–20.

[35] S.D. Liu. "Effect of different interplanting modes on population dynamics of Empoasca pirisuga Matumura and its natural enemy in collar pruning tea garden". In: *Chinese Horticulture Abstracts* 28 (2012), pp. 32–36.

[36] D.Q. Liao, G.W. Liang, and Y.J. Cen. "Effects of the predation of big red mite *Anystis baccarum* on tea red mite Oligonychus coffeae." In: *Journal of Fujian Agriculture and Forestry University (Natural Science Edition)* 39.2 (2010), pp. 117–122.

[37] A.G.S. Cuthbertson and A.K. Murchie. “Environmental monitoring of *Archips podana* (fruit tree tortrix moth) in Bramley apple orchards in Northern Ireland”. In: *International Journal of Environmental Science & Technology* 2.2 (2005), pp. 101–104.

[38] R.T. Baker. “Predation of leafroller larvae by spiders and mites”. In: *Weta* 6 (1983), pp. 22–23.

[39] A.G.S. Cuthbertson, C.C. Fleming, and A.K. Murchie. “Detection of *Rhopalosiphum insertum* (apple-grass aphid) predation by the predatory mite *Anystis baccarum* using molecular gut analysis”. In: *Agricultural and Forest Entomology* 5.3 (2003), pp. 219–225.

[40] A.G.S. Cuthbertson and A.K. Murchie. “Techniques for environmental monitoring of predatory fauna on branches of Bramley apple trees in Northern Ireland”. In: *International Journal of Environmental Science & Technology* 2.1 (2005), pp. 1–6.

[41] C.A. Paull et al. “Escape from parasitoids leave larvae vulnerable to predators and has unexpected outcomes for pest suppression”. In: *Basic and Applied Ecology* 13.6 (2012), pp. 542–550.

[42] L.M. Qiu, Z.X. Zhan, and W. Wu. “Population dynamics of *Anystis baccarum* Linnaeus and its control effect on Cornegenapsylla sinica Yang et Li”. In: *J. Environ. Entomol* 33.4 (2011), pp. 529–533.

[43] Z.H. Xiong et al. “Predatory function of *Anystis baccarum* L. to *Lipaphis erysimi* (Kaltenbach) and its sensitivity to five acaricides”. In: *Jiangxi Plant Prot* 34 (2011), pp. 67–70.

[44] X.J. Jiang et al. “Predation function response of *Anystis baccarum* Linnaeus to pests on mulberry tree”. In: *Journal of Environmental Entomology* 39 (2017), pp. 1356–1362.

[45] S. Ülgentürk et al. “Predators of *Marchalina hellenica* (Hemiptera: Marchalinidae) on pine forests in Turkey”. In: *Phytoparasitica* 41.5 (2013), pp. 529–537.

[46] W.J. Wu. “Studies on predation behavior of the predaceous mite, *Anystis baccarum* L. (Acariformes: Anystidae)”. In: *T Ecol Soc Chinese Youth* 1 (1991), pp. 254–258.

[47] W.J. Ming and H.Y. Ge Q.G.and Zheng. “Studies of some major predaceous natural enemies of Matsucoccus matsumurae (Kuwana)”. In: *Journal of Nanjing Forestry University* 3 (1983).

[48] R.M. May. *Stability and Complexity in Model Ecosystems*. Princeton University Press, 1973.

[49] A.D. Bazykin. *Nonlinear Dynamics of Interacting Populations*. World Scientific, 1998.

[50] A.A Berryman. "The orgins and evolution of predator-prey theory". In: *Ecology* 73.5 (1992), pp. 1530–1535.

[51] A.J. Lotka. *Elements of Physical Biology*. Williams & Wilkins, 1925.

[52] V. Volterra. "Variations and fluctuations of the number of individuals in animal species living together". In: *ICES Journal of Marine Science* 3.1 (1928), pp. 3–51.

[53] P.H. Leslie. "Some further notes on the use of matrices in population mathematics". In: *Biometrika* 35.3/4 (1948), pp. 213–245.

[54] C.S. Holling. "Some characteristics of simple types of predation and parasitism1". In: *The Canadian Entomologist* 91.7 (1959), pp. 385–398.

[55] X.K. Sun, H.F. Huo, and C.C. Ma. "Hopf bifurcation and stability in predator–prey model with a stage-structure for prey". In: *Applied Mathematics and Computation* 219.20 (2013), pp. 10313–10324.

[56] R.Q. Shi and L.S. Chen. "Staged-structured Lotka–Volterra predator–prey models for pest management". In: *Applied Mathematics and Computation* 203.1 (2008), pp. 258–265.

[57] X.A. Zhang, L.S. Chen, and A.U. Neumann. “The stage-structured predator–prey model and optimal harvesting policy”. In: *Mathematical Biosciences* 168.2 (2000), pp. 201–210.

[58] R. Xu. “Global dynamics of a predator–prey model with time delay and stage structure for the prey”. In: *Nonlinear Analysis: Real World Applications* 12.4 (2011), pp. 2151–2162.

[59] F. Li and H.W. Li. “Hopf bifurcation of a predator–prey model with time delay and stage structure for the prey”. In: *Mathematical and Computer Modelling* 55.3-4 (2012), pp. 672–679.

[60] H.P. Zhu, S.A. Campbell, and G.S.K. Wolkowicz. “Bifurcation analysis of a predator-prey system with nonmonotonic functional response”. In: *SIAM Journal on Applied Mathematics* 63.2 (2003), pp. 636–682.

[61] W.S. Yang, X.P. Li, and Z.J. Bai. “Permanence of periodic Holling type-IV predator–prey system with stage structure for prey”. In: *Mathematical and Computer Modelling* 48.5-6 (2008), pp. 677–684.

[62] D.P. Hu et al. “Stability and Hopf bifurcation for a delayed predator–prey model with stage structure for prey and Ivlev-type functional response”. In: *Nonlinear Dynamics* 99.4 (2020), pp. 3323–3350.

[63] F.Y. Wei and Q.Y. Fu. “Hopf bifurcation and stability for predator–prey systems with Beddington–DeAngelis type functional response and stage structure for prey incorporating refuge”. In: *Applied Mathematical Modelling* 40.1 (2016), pp. 126–134.

[64] F.D. Chen and M.S. You. “Permanence, extinction and periodic solution of the predator–prey system with Beddington–DeAngelis functional response and stage structure for prey”. In: *Nonlinear Analysis: Real World Applications* 9.2 (2008), pp. 207–221.

[65] S.B. Hsu, T.W. Hwang, and Y. Kuang. “Global dynamics of a predator-prey model with Hassell-Varley type functional response”. In: *Discrete Contin. Dyn. Syst. Ser. B* 10.4 (2008), pp. 857–871.

[66] X.Y. Meng et al. “Stability in a predator–prey model with Crowley–Martin function and stage structure for prey”. In: *Applied Mathematics and Computation* 232 (2014), pp. 810–819.

[67] X.Y. Song, L.M. Cai, and U. Neumann. “Ratio-dependent predator-prey system with stage structure for prey”. In: *Discrete & Continuous Dynamical Systems-B* 4.3 (2004), p. 747.

[68] A.D. Bazykin, F.S. Berezovskaya, and S.L. Zudin. *Bifurcation approach to the predator-prey population models (Version of the computer book)*. Tech. rep. International Centre for Theoretical Physics, 1993.

[69] G.S.K. Wolkowicz. "Bifurcation analysis of a predator-prey system involving group defence". In: *SIAM Journal on Applied Mathematics* 48.3 (1988), pp. 592–606.

[70] D.M. Xiao and H.P. Zhu. "Multiple focus and Hopf bifurcations in a predator-prey system with nonmonotonic functional response". In: *SIAM Journal on Applied Mathematics* 66.3 (2006), pp. 802–819.

[71] L.K. Beay et al. "Hopf bifurcation and stability analysis of the Rosenzweig-MacArthur predator-prey model with stage-structure in prey". In: *Mathematical Biosciences and Engineering* 17.4 (2020), pp. 4080–4097.

[72] W.O.C. Symondson, K.D. Sunderland, and M.H. Greenstone. "Can generalist predators be effective biocontrol agents?" In: *Annual Review of Entomology* 47.1 (2002), pp. 561–594.

[73] M.P. Hassell and R.M. May. "Generalist and specialist natural enemies in insect predator-prey interactions". In: *The Journal of Animal Ecology* (1986), pp. 923–940.

[74] W.W. Murdoch. “Switching in general predators: experiments on predator specificity and stability of prey populations”. In: *Ecological Monographs* 39.4 (1969), pp. 335–354.

[75] I. Hanski, L. Hansson, and H. Henttonen. “Specialist predators, generalist predators, and the microtine rodent cycle”. In: *The Journal of Animal Ecology* (1991), pp. 353–367.

[76] A. Erbach, F. Lutscher, and G. Seo. “Bistability and limit cycles in generalist predator–prey dynamics”. In: *Ecological Complexity* 14 (2013), pp. 48–55.

[77] C. Magal et al. “Control of invasive hosts by generalist parasitoids”. In: *Mathematical Medicine and Biology: a journal of the IMA* 25.1 (2008), pp. 1–20.

[78] G. Seo and G.S.K. Wolkowicz. “Pest control by generalist parasitoids: a bifurcation theory approach”. In: *Discrete & Continuous Dynamical Systems-S* 13.11 (2020), p. 3157.

[79] C. Xiang et al. “Bifurcation analysis in a host-generalist parasitoid model with Holling II functional response”. In: *Journal of Differential Equations* 268.8 (2020), pp. 4618–4662.

[80] K.E.F. Watt. “Mathematical models for use in insect pest control”. In: *The Memoirs of the Entomological Society of Canada* 93.S19 (1961), pp. 5–62.

[81] A. Satake et al. “Modeling population dynamics of a tea pest with temperature-dependent development: predicting emergence timing and potential damage”. In: *Ecological Research* 21.1 (2006), pp. 107–116.

[82] T. Yamanaka et al. “Generation separation in simple structured life cycles: Models and 48 years of field data on a tea tortrix moth”. In: *The American Naturalist* 179.1 (2012), pp. 95–109.

[83] H. Kettle, C. Sann, and G. Marion. “Quantifying parasitoid and predator controls on rice hopper eggs using a dynamic stage-structured model and field data”. In: *Journal of Applied Ecology* 56.11 (2019), pp. 2536–2550.

[84] F. Chen. “Permanence of periodic Holling type predator–prey system with stage structure for prey”. In: *Applied Mathematics and Computation* 182.2 (2006), pp. 1849–1860.

[85] K. Chakraborty, S. Das, and T.K. Kar. “Optimal control of effort of a stage structured prey–predator fishery model with harvesting”. In: *Nonlinear Analysis: Real World Applications* 12.6 (2011), pp. 3452–3467.

[86] X. Tian and R. Xu. “Global dynamics of a predator-prey system with Holling type II functional response”. In: *Lithuanian Association of Nonlinear Analysts (LANA)* 16.2 (2011), pp. 242–253.

[87] S. Khajanchi. “Modeling the dynamics of stage-structure predator-prey system with Monod–Haldane type response function”. In: *Applied Mathematics and Computation* 302 (2017), pp. 122–143.

[88] R. Xu. “Global stability and Hopf bifurcation of a predator-prey model with stage structure and delayed predator response”. In: *Nonlinear Dynamics* 67.2 (2012), pp. 1683–1693.

[89] L.S. Wang, R. Xu, and G.H. Feng. “Global dynamics of a delayed predator–prey model with stage structure and holling type II functional response”. In: *Journal of Applied Mathematics and Computing* 47.1-2 (2015), pp. 73–89.

[90] L.S. Wang and G.H. Feng. “Global dynamics of a delayed predator–prey model with stage structure for the predator and the prey”. In: *Mathematical Methods in the Applied Sciences* 38.17 (2015), pp. 3937–3949.

[91] Y. Lin et al. “Convergences of a stage-structured predator-prey model with modified Leslie-Gower and Holling-type II schemes”. In: *Advances in Difference Equations* 2016.1 (2016), p. 181.

[92] Z.H. Zhao et al. “Approaches and mechanisms for ecologically based pest management across multiple scales”. In: *Agriculture, Ecosystems & Environment* 230 (2016), pp. 199–209.

[93] Z. Hossain et al. “Habitat manipulation in lucerne Medicago sativa: arthropod population dynamics in harvested and ‘refuge’crop strips”. In: *Journal of Applied Ecology* 39.3 (2002), pp. 445–454.

[94] Z.Q. Zhang et al. “Dual action of Catsia tora in tea plantations: repellent volatiles and augmented natural enemy population provide control of tea green leafhopper”. In: *Phytoparasitica* 42.5 (2014), pp. 595–607.

[95] M.J. Costello and K.M. Daane. “Spider and leafhopper (Erythroneura spp.) response to vineyard ground cover”. In: *Environmental Entomology* 32.5 (2003), pp. 1085–1098.

[96] Y.G. Chen. “Study on diversity retaining of arthropod and sustainable controlling of insect pests in tea orchards”. In: *South China Agricultural University, Guangzhou* (2002), p. 68.

[97] D.J. Jiang, L.Y. Xu, and Z.P. Cheng. “Effects of green manure intercropping on parasitoids and *Empoasca vitis* (Göthe) in tea plantations”. In: *Wuyi Sci. J* 30 (2014), pp. 154–161.

[98] C.I. Nicholls, M.P. Parrella, and M.A. Altieri. “Reducing the abundance of leafhoppers and thrips in a northern California organic vineyard through maintenance of full season floral diversity with summer cover crops”. In: *Agricultural and Forest Entomology* 2.2 (2000), pp. 107–113.

[99] G. English-Loeb et al. “Influence of flowering cover crops on Anagrus parasitoids (Hymenoptera: Mymaridae) and Erythroneura leafhoppers (Homoptera: Cicadellidae) in New York vineyards”. In: *Agricultural and Forest Entomology* 5.2 (2003), pp. 173–181.

[100] D.F. Huang et al. “Effects of inter-planting forage with tea on yield and soil fertility”. In: *Zhongguo Shengtai Nongye Xuebao/Chinese Journal of Eco-Agriculture* 22.11 (2014), pp. 1289–1293.

[101] G.Z. Lin. “Study on the Soil Conservation & Soil Improvement Effects by Planting the Paspalum notatum in the Slope Orchard [J]”. In: *Subtropical Soil and Water Conservation* 3 (2012).

[102] X.H. Luo et al. “Effects of intercropping Chamaecrista rotundifolia in tea plantation on weed diversity”. In: *Chin J Trop Crops* 34 (2013), pp. 2503–2507.

[103] H.L. Li, H. Zhang, and M.S. Zeng. “Regulating effect on *Empoasca flavescens* (Homoptera: Cicadellidae) by intercropping tea bushes with Chamaecrista rotundifolia”. In: *Acta Tea Sin* 57 (2016), pp. 205–208.

[104] H.L. Li et al. “Effects on small green leafhopper and its natural enemy mymarid in tea plantations with intercropping of green manure plants.” In: *Chinese Journal of Biological Control* 32.1 (2016), pp. 50–54.

[105] J. Zhan et al. “Preliminary variations in the environment of tea gardens and tea growth on the tea-grass interaction mode”. In: *Pratacultural Sci* 35 (2018), pp. 2694–2703.

[106] A.G.S. Cuthbertson and A.K. Murchie. “A review of the predatory mite *Anystis baccarum* and its role in apple orchard pest management schemes in Northern Ireland”. In: *J. Entomol* 4.4 (2007), pp. 275–278.

[107] J.T. Sorensen et al. “Biology of the mite, *Anystis agilis* (Acari: Anystidae): A California vineyard predator”. In: *Annals of the Entomological Society of America* 69.5 (1976), pp. 905–910.

[108] M.MK.P Smith and E.A. Ueckermann. “A taxonomic study of some Anystidae (Acari: Prostigmata)”. In: *Entomology Memoir (Pretoria)* 68 (1987), pp. 1–37.

[109] J.L. Li et al. “Population dynamic and the spatial distribution of *Anystis baccarum* (Linnaeus) in tea garden”. In: *Guangdong Agricultural Sciences* 18 (2011), pp. 47–48.

[110] A.G.S. Cuthbertson, A.C. Bell, and A.K. Murchie. “Impact of the predatory mite *Anystis baccarum* (Prostigmata: Anystidae) on apple rust mite *Aculus schlechtendali* (Prostigmata: Eriophyidae) populations in Northern Ireland Bramley orchards”. In: *Annals of Applied Biology* 142.1 (2003), pp. 107–114.

[111] L.L. Chen, M.S. You, and S.B. Chen. “Effects of cover crops on spider communities in tea plantations”. In: *Biological Control* 59.3 (2011), pp. 326–335.

[112] L.L. Chen. “Effects of Tea Intercropped with Ground Cover on the Composition and Sturcture of Arthropods and Other Related Animals”. PhD thesis. Fujian Agriculture and Forestry University, Apr. 2011.

[113] D.B. Hall. “Zero-inflated Poisson and binomial regression with random effects: a case study”. In: *Biometrics* 56.4 (2000), pp. 1030–1039.

[114] M.E. Brooks et al. “glmmTMB balances speed and flexibility among packages for zero-inflated generalized linear mixed modeling”. In: *The R journal* 9.2 (2017), pp. 378–400.

[115] R Core Team. *R: A Language and Environment for Statistical Computing*. R Foundation for Statistical Computing. Vienna, Austria, 2020. URL: https://www.R-project.org/.

[116] S.D. Liu. “Effect of different interplanting modes on population dynamics of *Empoasca pirisuga* Matumura and its natural enemy in collar pruning tea garden”. In: *Chinese Horticulture Abstracts* (2012).

[117] A.B. Lange, E.M. Drozdovskii, and L.M. Bushkovskaya. “Anystid mites-effective predators of small phytophagous pests”. In: *Zashchita Rastenii* 1.1 (1974), pp. 26–28.

[118] E. Aguilar-Fenollosa et al. “Effect of ground-cover management on spider mites and their phytoseiid natural enemies in clementine mandarin orchards (I): bottom-up regulation mechanisms”. In: *Biological Control* 59.2 (2011), pp. 158–170.

[119] E. Aguilar-Fenollosa et al. “Effect of ground-cover management on spider mites and their phytoseiid natural enemies in clementine mandarin orchards (II):top-down regulation mechanisms”. In: *Biological Control* 59.2 (2011), pp. 171–179.

[120] H.J. Cai, Z.S. Li, and M.S. You. “Impact of habitat diversification on arthropod communities: a study in the fields of Chinese cabbage, Brassica chinensis”. In: *Insect Science* 14.3 (2007), pp. 241–249.

[121] L.L. Chen et al. “Cover crops enhance natural enemies while help suppressing pests in a tea plantation”. In: *Annals of the Entomological Society of America* 112.4 (2019), pp. 348–355.

[122] L.L. Chen et al. “The impact of cover crops on the predatory mite *Anystis baccarum* (Acari, Anystidae) and the leafhopper pest *Empoasca onukii* (Hemiptera, Cicadellidae) in a tea plantation”. In: *Pest Management Science* 75.12 (2019), pp. 3371–3380.

[123] L. Bian, X.L. Sun, and Z.M. Chen. “Studies on daily flight activity and adult flight capacity of *Empoasca vitis* Göthe.” In: *Journal of Tea Science* 34.3 (2014), pp. 248–252.

[124] M.L. Zeeman. “Hopf bifurcations in competitive three-dimensional Lotka–Volterra systems”. In: *Dynamics and Stability of Systems* 8.3 (1993), pp. 189–216.

[125] V.V. Alekseev. “Effect of saturation factor on dynamics of predator prey system”. In: *Biofizika* 18 (1973), pp. 922–926.

[126] A.D. Bazykin. “Volterra system and Michaelis-Menten equation”. In: *Voprosy matematicheskoi genetiki, Novosibirsk* (1974), pp. 103–143.

[127] F. Dumortier et al. *Bifurcations of planar vector fields: Nilpotent Singularities and Abelian Integrals*. Springer, 1991.

[128] H.P. Zhu and C. Rousseau. “Finite cyclicity of graphics with a nilpotent singularity of saddle or elliptic type”. In: *Journal of Differential Equations* 178.2 (2002), pp. 325–436.

[129] G. Dangelmayr and J. Guckenheimer. “On a four parameter family of planar vector fields”. In: *Archive for Rational Mechanics and Analysis* 97.4 (1987), pp. 321–352.

[130] A.I. Khibnik, B. Krauskopf, and C. Rousseau. “Global study of a family of cubic Liénard equations”. In: *Nonlinearity* 11.6 (1998), p. 1505.

[131] H.B. Chen and H.P. Zhu. “Global bifurcation studies of a cubic Liénard system”. In: *Journal of Mathematical Analysis and Applications* 496.2 (2021), p. 124810.

[132] Maple. *Maplesoft, a division of Waterloo Maple Inc.* Version 2019. Waterloo, Ontario, 2019. URL: https://hadoop.apache.org.

[133] MATLAB (R2020a). *The MathWorks Inc.* Natick, Massachusetts, 2020.

[134] S.J. Fan. “A new extracting formula and a new distinguishing means on the one variable cubic equation”. In: *Nat. Sci. J. Hainan Teach. Coll* 2.2 (1989), pp. 91–98.

[135] C.Z. Li and H.P. Zhu. “Canard cycles for predator–prey systems with Holling types of functional response”. In: *Journal of Differential Equations* 254.2 (2013), pp. 879–910.

[136] C.H. Shan and H.P. Zhu. “Bifurcations and complex dynamics of an SIR model with the impact of the number of hospital beds”. In: *Journal of Differential Equations* 257.5 (2014), pp. 1662–1688.

[137] C.H. Shan, Y.F. Yi, and H.P. Zhu. “Nilpotent singularities and dynamics in an SIR type of compartmental model with hospital resources”. In: *Journal of Differential Equations* 260.5 (2016), pp. 4339–4365.

[138] J.B. Collings and D.J. Wollkind. “A global analysis of a temperature-dependent model system for a mite predator-prey interaction”. In: *SIAM Journal on Applied Mathematics* 50.5 (1990), pp. 1348–1372.

[139] L.Q. Shi et al. “Identification of *Empoasca onukii* (Hemiptera: Cicadellidae) and monitoring of its populations in the tea plantations of south China”. In: *Journal of economic entomology* 108.3 (2015), pp. 1025–1033.

[140] J.A. Cui and X.Y. Song. “Permanence of predator-prey system with stage structure”. In: *Discrete & Continuous Dynamical Systems-B* 4.3 (2004), p. 547.

[141] F.D. Chen. “Permanence of periodic Holling type predator–prey system with stage structure for prey”. In: *Applied Mathematics and Computation* 182.2 (2006), pp. 1849–1860.

[142] J. A. Cui and Y. Takeuchi. “A predator–prey system with a stage structure for the prey”. In: *Mathematical and Computer Modelling* 44.11-12 (2006), pp. 1126–1132.

[143] S.Q. Liu and J.H. Zhang. “Coexistence and stability of predator–prey model with Beddington–DeAngelis functional response and stage structure”. In: *Journal of Mathematical Analysis and Applications* 342.1 (2008), pp. 446–460.

[144] Y. Song, W. Xiao, and X.Y. Qi. “Stability and Hopf bifurcation of a predator–prey model with stage structure and time delay for the prey”. In: *Nonlinear Dynamics* 83.3 (2016), pp. 1409–1418.

[145] X.Y. Meng, H.F. Huo, and X.B. Zhang. “Stability and global Hopf bifurcation in a Leslie–Gower predator-prey model with stage structure for prey”. In: *Journal of Applied Mathematics and Computing* 60.1 (2019), pp. 1–25.

[146] B. Dubey and A. Kumar. “Dynamics of prey–predator model with stage structure in prey including maturation and gestation delays”. In: *Nonlinear Dynamics* 96.4 (2019), pp. 2653–2679.

[147] G. Fan and G.S.K Wolkowicz. “Chaotic dynamics in a simple predator-prey model with discrete delay”. In: *Discrete and Continuous Dynamical Systems Series B* 26.1 (2021), pp. 191–216.

[148] F. Dumortier, R. Roussarie, and J. Sotomayor. “Generic 3-parameter families of vector fields on the plane, unfolding a singularity with nilpotent linear part. The cusp case of codimension 3”. In: *Ergodic theory and dynamical systems* 7.3 (1987), pp. 375–413.

[149] H.G. Zhang and J.C. Tan. “Tea pests in China and their contaminant-free management”. In: *Anhui Scientific and Technical Publishers, Hefei* (2004), pp. 1–389.

[150] B.H. Hou et al. “Susceptibility of Selected Tea Shoots to Oviposition by *Empoasca onukii* (Hemiptera: Cicadellidae) and Feasibility of Egg Removal with Harvesting”. In: *Insects* 11.6 (2020), p. 338.